



ZOOTAXA

4467

**A molecular phylogenetic hypothesis for the Asian agamid lizard
genus *Phrynocephalus* reveals discrete biogeographic clades
implicated by plate tectonics**

J. ROBERT MACEY^{1,8,9}, JAMES A. SCHULTE II², NATALIA B. ANANJEVA³,
ERIK T. VAN DYKE¹, YUEZHAO WANG⁴, NIKOLAI ORLOV³, SOHEILA SHAFIEI⁵,
MICHAEL D. ROBINSON⁶, TATJANA DUJSEBAYEVA⁷, GABRIEL S. FREUND¹,
CLAYTON M. FISCHER¹, DAVID LIU¹ & THEODORE J. PAPENFUSS⁸

¹Genomics, Department of Biosciences, Merritt College, 12500 Campus Drive, Oakland, CA 94619, USA

²Department of Biology, 700 College Street, Center for the Sciences 338, Beloit College, Beloit, WI 53511, USA

³Zoological Institute, Russian Academy of Sciences, St. Petersburg 199034, Russia

⁴Chengdu Institute of Biology, PO Box 416, Chengdu, Sichuan, China

⁵Department of Biology, Faculty of Science, Shahid Bahonar University of Kerman, PO Box 76169-133, Kerman, Iran

⁶Department of Biology, Sultan Qaboos University, PO Box 36, Al Khoud, PC 123, Muscat, Oman

⁷Institute of Zoology, Ministry of Education and Sciences, al-Farabi Av., 93, Academgoradok, Almaty, 050060, Kazakhstan

⁸Museum of Vertebrate Zoology, University of California, Berkeley, CA 94720, USA

⁹Corresponding author. E-mail: jrobertmacey@gmail.com



Magnolia Press
Auckland, New Zealand

J. ROBERT MACEY, JAMES A. SCHULTE II, NATALIA B. ANANJEVA, ERIK T. VAN DYKE,
YUEZHAO WANG, NIKOLAI ORLOV, SOHEILA SHAFIEI, MICHAEL D. ROBINSON, TATJANA
DUJSEBAYEVA, GABRIEL S. FREUND, CLAYTON M. FISCHER, DAVID LIU & THEODORE J.
PAPENFUSS

A molecular phylogenetic hypothesis for the Asian agamid lizard genus *Phrynocephalus* reveals discrete biogeographic clades implicated by plate tectonics

(*Zootaxa* 4467)

81 pp.; 30 cm.

3 Sept. 2018

ISBN 978-1-77670-444-6 (paperback)

ISBN 978-1-77670-445-3 (Online edition)

FIRST PUBLISHED IN 2018 BY

Magnolia Press

P.O. Box 41-383

Auckland 1346

New Zealand

e-mail: magnolia@mapress.com

<http://www.mapress.com/j/zt>

© 2018 Magnolia Press

All rights reserved.

No part of this publication may be reproduced, stored, transmitted or disseminated, in any form, or by any means, without prior written permission from the publisher, to whom all requests to reproduce copyright material should be directed in writing.

This authorization does not extend to any other kind of copying, by any means, in any form, and for any purpose other than private research use.

ISSN 1175-5326 (Print edition)

ISSN 1175-5334 (Online edition)

Table of contents

Abstract	3
Introduction	3
Materials and methods	7
A. Taxon Sampling	7
B. Data Collection	8
C. Mitochondrial DNA Structural Shifts from Standard Vertebrates	8
D. DNA Alignment	10
E. Phylogenetic Tree Reconstruction	10
F. Linear Dating with Pairwise Sequence Divergence of Mitochondrial DNA	11
G. Statistical Evaluation of Alternative Hypotheses	11
H. Evaluation of Habitat Evolution in <i>Phrynocephalus</i>	12
Results	12
A. Phylogenetic Hypotheses	12
B. Estimated Dates based on Pairwise Sequence Divergence of Mitochondrial DNA Compared to Geologic Events	30
C. Statistical Evaluation of Taxon Placement with Mitochondrial DNA and Combined Data	31
Discussion	34
A. <i>Phrynocephalus</i> Taxonomic Recommendations	34
B. Geologic Activity and <i>Phrynocephalus</i> Cladogenesis	38
C. Glacial History and the Root of <i>Phrynocephalus</i>	44
D. Habitat Evolution Among <i>Phrynocephalus</i>	45
E. <i>Phrynocephalus</i> Size Diversity	48
F. <i>Phrynocephalus</i> Species Diversity as Related to Geology, Habitat and Size	51
Acknowledgments	60
References	60
APPENDIX 1	65
APPENDIX 2	68
APPENDIX 3	76
APPENDIX 4	79
APPENDIX 5	80

Abstract

Phylogenetic relationships of the agamid lizard genus *Phrynocephalus* are described in the context of plate tectonics. A near comprehensive taxon sampling reports three data sets: (1) mitochondrial DNA from ND1 to COI (3' end of ND1, tRNA^{Gln}, tRNA^{Ile}, tRNA^{Met}, ND2, tRNA^{Trp}, tRNA^{Ala}, tRNA^{Asn}, tRNA^{Cys}, tRNA^{Tyr}, and the 5' end of COI) with 1761 aligned positional sites (1595 included, 839 informative), (2) nuclear RAG-1 DNA with 2760 aligned positional sites (342 informative), and (3) 25 informative allozyme loci with 213 alleles (107 informative when coded as presence/absence). It is hypothesized that *Phrynocephalus* phyletic patterns and speciation reflect fault lines of ancient plates now in Asia rejuvenated by the more recent Indian and Arabian plate collisions. Molecular estimates of lineage splits are highly congruent with geologic dates from the literature. A southern origin for the genus in Southwest Asia is resolved in phylogenetic estimates and a northern origin is statistically rejected. On the basis of monophyly and molecular evidence several taxa previously recognized as subspecies are recognized as species: *P. hongyuanensis*, *P. sogdianus*, and *P. strauchi* as “Current Status”; *Phrynocephalus bannikovi*, *Phrynocephalus longicaudatus*, *Phrynocephalus turcomanus*, and *Phrynocephalus vindumi* are formally “New Status”. Phylogenetic evaluation indicates a soft substrate habitat of sand for the shared ancestor of modern *Phrynocephalus*. Size diversity maximally overlaps in the Caspian Basin and northwestern Iranian Plateau. The greatest species numbers of six in sympatry and regional allopatry are found in the southern Caspian Basin and southern Helmand Basin, both from numerous phylogenetic lineages in close proximity attributed to tectonic induced events.

Key words: Reptilia, Squamata, Agamidae, *Phrynocephalus*, Asia, biogeography, evolution, phylogenetics, tectonics, mitochondrial DNA, RAG-1, allozyme

Introduction

The Asian agamid lizard genus *Phrynocephalus* Kaup, 1825, with the first species described as *Lacerta helioscopia* by Pallas in 1771, shows intriguingly complex morphological and ecological patterns. This has led to difficulty in

understanding phyletic patterns regionally and throughout arid Asia where *Phrynocephalus* is endemic. In addition, taxonomic confusion has persisted since extensive Russian exploration by Przewalsky, Roborowsky, and Zarudny in the 1800s and early 1900s covering the Caspian Basin, western China including northern Tibet, Iran, and Afghanistan (for review see Barabanov & Ananjeva 2007; Leviton & Anderson 2010, 2013; Wagner *et al.* 2016). After centuries of study many questions still remain unanswered, with phylogenetic relationships being paramount.

Phrynocephalus species occur in all major desert regions of Asia (Fig. 1), with the exception of the Thar Desert in India having *Bufoinceps laungwalaensis*, which was originally described as a *Phrynocephalus* species (Sharma 1978) and is the sister taxon to *Trapelus* (Macey *et al.* 2006). Previous molecular phylogenetic studies have concentrated on regional diversity such as the Tibetan Plateau (Jin *et al.* 2008), Chinese taxa (Pang *et al.* 2003; Jin & Brown 2013), and the northern Caspian Basin (Melville *et al.* 2009), or taxonomic units such as the *P. versicolor* species complex (Wang & Fu 2004), and the *P. helioscopus* superspecies complex (Solovyeva *et al.* 2011). A previous report included a more comprehensive taxon sampling, but their data is limited to four mitochondrial protein coding genes [cytochrome c oxidase subunit I (COI), NADH dehydrogenase subunits II and IV (ND2, ND4), and cytochrome b (Cyt b)] (Solovyeva *et al.* 2014).

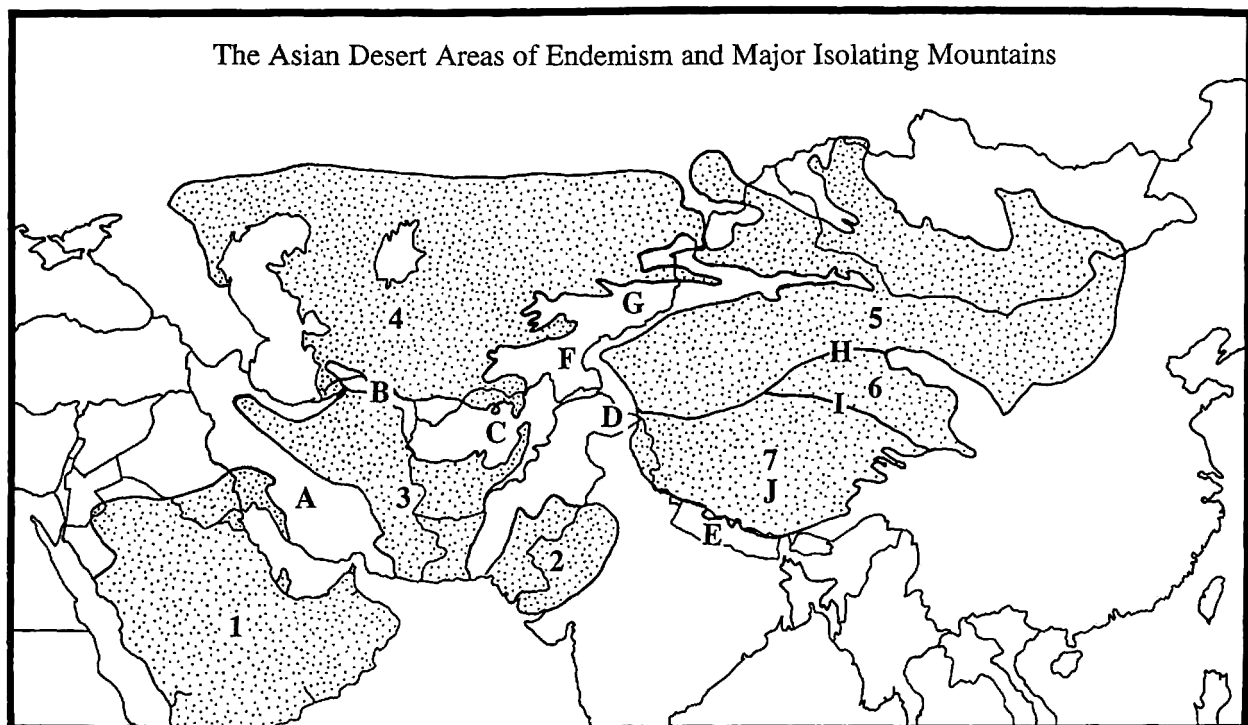


FIGURE 1. The major deserts of Asia and intervening mountain belts. Major deserts are labeled 1–7 which are: (1) Arabian, (2) Thar, (3) Southwest Asian, (4) Caspian Basin, (5) Gobi-Taklimakan, (6) Qaidam-Qinghai, and (7) High Elevation Tibetan. Intervening mountain belts are labeled A–J which are: (A) Zagros, (B) Kopet-Dagh, (C) Hindu Kush, (D) Karakorum, (E) Himalaya, (F) Pamir, (G) Tien Shan, (H) Arjin-Qilan, (I) Kunlun, and (J) Tangula Shan. *Phrynocephalus* species occur in all major desert regions of Asia, with the exception of the Thar Desert in India having *Bufoinceps laungwalaensis*, which was originally described as a *Phrynocephalus* species (Sharma 1978) and is the sister taxon to *Trapelus* (Macey *et al.* 2006).

The molecular data presented here concentrates on a near comprehensive sampling of the genus *Phrynocephalus*, which includes *Bufoinceps laungwalaensis*. A detailed description of sampling is found in the Materials and Methods section, as well as appendix 1 (Fig. 2). This includes new DNA sequences reported from taxa collected in (1) Afghanistan, (2) China including Tibet, (3) India, (4) Iran, (5) Kazakhstan, (6) Oman, (7) Pakistan, (8) Russia, (9) Saudi Arabia, (10) Turkmenistan, and (11) Uzbekistan.

Described are results from three molecular data sets. (1) Mitochondrial DNA of an 11 genic segment consisting of the 3' end of ND1 (NADH dehydrogenase subunit I), tRNA^{Gln}, tRNA^{Ile}, tRNA^{Met}, ND2 (NADH

dehydrogenase subunit II), tRNA^{Trp}, tRNA^{Ala}, tRNA^{Asn}, tRNA^{Cys}, tRNA^{Tyr}, and the 5' end of COI (cytochrome c oxidase subunit I). The reported DNA sequences contain 1761 aligned positions (1595 included, 839 parsimony informative). (2) Nuclear recombination activating gene 1 (RAG-1) DNA, which contain 2760 aligned bases (342 parsimony informative). (3) Twenty-five presumptive allozyme loci sampled using starch electrophoresis discovering a total of 213 alleles (107 parsimony informative when coded as presence/absence). This molecular systematic research started with fieldwork in 1986, allozyme lab work from 1989–1992, and DNA sequencing initiating in 1993.

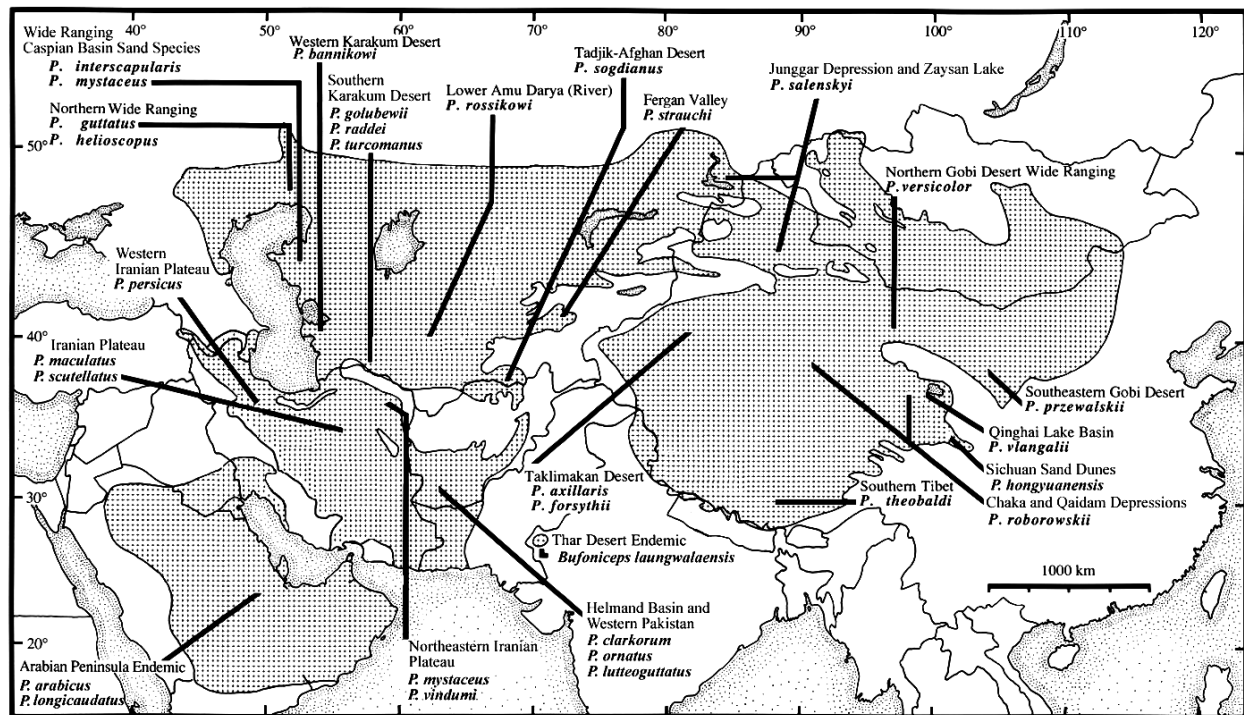


FIGURE 2. The approximate distribution of *Phrynocephalus* and *Bufoniceps laungwalaensis*. The 29 *Phrynocephalus* species sampled are indicated with general geographic distribution. Multiple populations were sampled from 10 species which are: *P. arabicus*, *P. forsythii*, *P. luteoguttatus*, *P. maculatus*, *P. mystaceus*, *P. przewalskii*, *P. roborowskii*, *P. salenskyi*, *P. scutellatus*, and *P. vlangalii*. Two populations are included from all of the above except for *P. przewalskii* which is four populations, and *P. vlangalii* which is three populations. In some cases these are depicted on the map. See appendix 1 for exact localities of samples.

The biogeographic history of *Phrynocephalus* lies in the ancient set-up of tectonic plates now deep in internal Asia.

Prior to formation of the present Eurasian continent, an extremely complex history of microcontinental plate accretions occurred. These early plate accretions created sutures that were later reactivated as strike-slip faults in the Tertiary by the Indian and Arabian collisions, and the continued movement of Southeast Asian plates. The positioning of these sutures created a setting for future fault movements that shaped the topography of the Asian interior and influenced *Phrynocephalus* cladogenesis. These plates are: (1) Junggar Block, (2) Tarim Block, (3) Kunlun Block, (4) Qiangtang Block, (5) South Tibet Block, (6) Farah Block, (7) Helmand Block, (8) Lut Block, (9) Makran uplift region, (10) Arabian Plate, (11) Indian Plate and (12) conglomerated Southeast Asian Plates. See figure 3 for a simplified map of the major plates within present day Asia. We review the pre-Eocene and subsequent Tertiary events that helped shape the present Asian topography. Dates are presented as millions of years before present (MYBP).

Approximately 300 MYBP, the Tarim Plate (Taklimakan Desert) collided with the Siberian and Kazakhstan blocks of Laurasia (Feng *et al.* 1989; Kwon *et al.* 1989) forming the paleo-Tien Shan (mountains) in the vicinity of what is now the western Chinese—Kazakhstan border (Fig. 3). Next there were successive accretions of blocks to the southern margin of Eurasia. These blocks, termed the “Cimmerian Continent”, broke off of Gondwana in the late Permian (250 MYBP) and migrated northward across the Tethys Sea, fragmenting along the way. The individual blocks collided with Eurasia, most of which completed suturing from late Triassic to middle Jurassic

(225-175 MYBP; for details see Sengör, 1984; Sengör *et al.* 1988). These blocks are now situated from Turkey through Iran, Afghanistan, Tibet and Southeast Asia. Figure 3 shows their current positions.

These events produced the geological conditions necessary for further changes in the Eocene and later are directly related to the phylogenetic history of *Phrynocephalus* under investigation. Extant agamid lizard clades are predicted to have arrived in Asia with some of the more recent microcontinental collisions (for review see Macey *et al.* 2000b): (1) Southeast Asian Blocks which connected with Asia in three main accretionary events (1a) 120 MYBP (Indochina Block; Richter & Fuller 1996), (1b) 65 MYBP (small terranes to the south of Indochina; Metcalfe 1996) and (1c) 10 MYBP (small island terranes as far north as Sulawesi; Hall, 1996); (2) India 50 MYBP (Dewey *et al.* 1989; Molnar *et al.* 1987; Royden *et al.* 2008; Windley 1988); and (3) Arabia 18 MYBP (Dercourt *et al.* 1986; Steininger & Rogl 1984). As these more recent microcontinental plates carrying agamid lizards began impinging into conglomerated Asian blocks, paleo-sutures of older accreted tectonic plates situated deep in Asia were reactivated as strike-slip faults, like bumper cars at an amusement park, with micro-plates being shuffled around within internal Asia. Mountain building occurred along these faults as far inland as Mongolia.

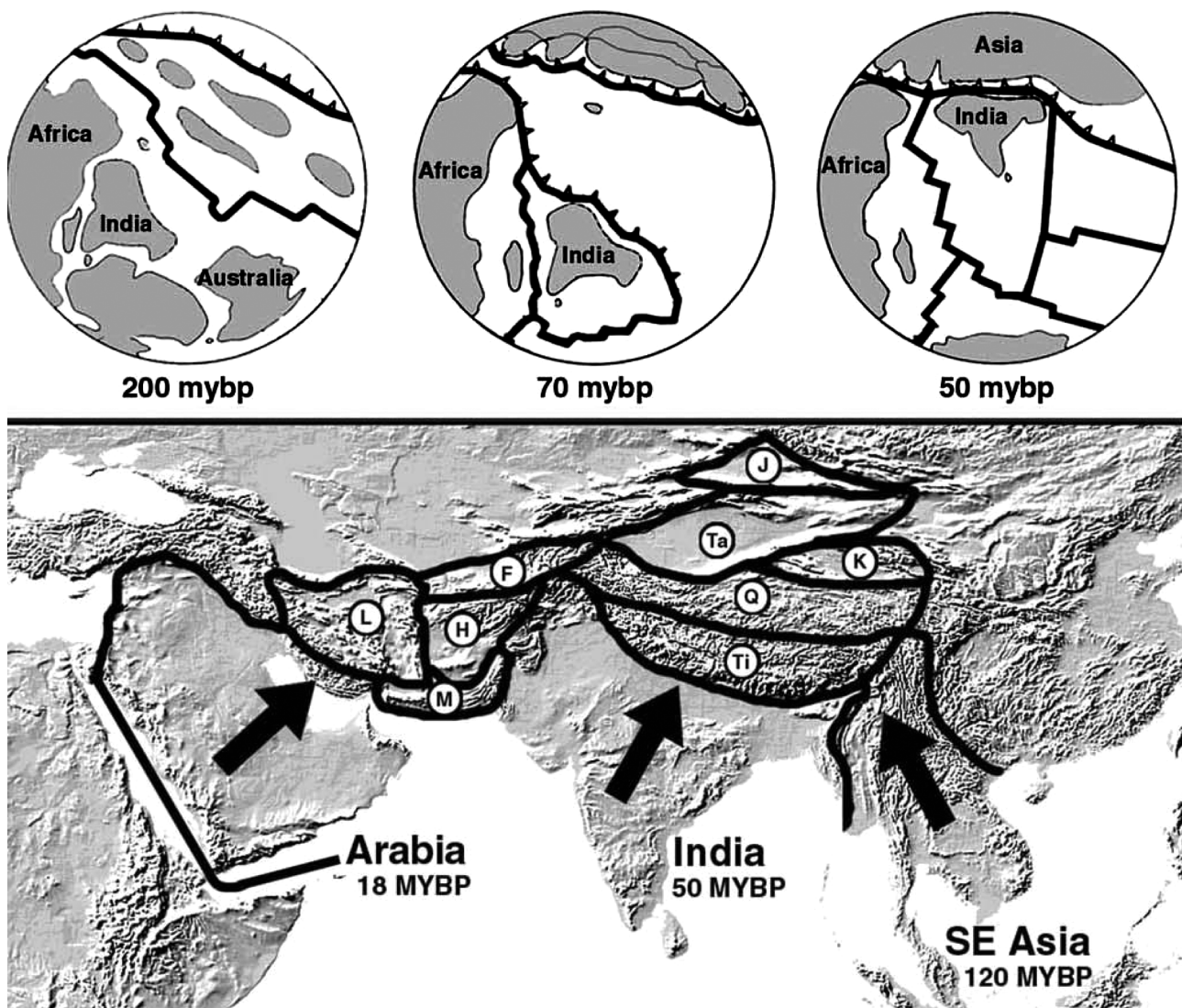


FIGURE 3. A simplified tectonic map of Asia's associated tectonic plates. Top: The tectonic history of Asia including the break up of Gondwana, trans-Tethys migration of microplates, the isolation of the Indian plate, and subsequent docking of India with Asia (after Tapponier *et al.* 1981). Bottom: Major plates and suture zones of Asia: low elevations plates of China, J= Junggar and Ta= Tarim; high elevation plates of Tibet, K= Kunlun, Q= Qiangtang and Ti= South Tibet; Southwest Asian plates, F= Farah, H= Helmand, L= Lut, and M= Makran which is an uplift from the Gulf of Oman. Note the complex shifting of plates deep in Asia by Arabia, India, and SE Asia.

The agamid lizard genus *Phrynocephalus* is part of the Afro-Asian clade, taxonomically termed the subfamily Agaminae (Macey *et al.* 2000b). The origin of the Agaminae is most likely Afro-Arabia, but an Indian origin could not be rejected (Macey *et al.* 2000b).

This study provides a comprehensive taxon sampling that includes species from all major Asian deserts and tectonic regions where *Phrynocephalus* occurs to elucidate a better understanding of phyletic patterns across biogeographic history. The three data sets take a multi-locus approach to provide molecular phylogenetic characters derived from mitochondrial DNA, nuclear DNA, and nuclear encoded protein data to give a combined picture of phyletic relationships. This project, which spans three decades of sample collection and molecular character acquisition, is intended to assist further research on *Phrynocephalus* embarking on a genomic revolution. By providing an outline of taxon sampling, estimates of phylogenetic relationships and offering an interpretation of data based on a geologic setting, this study can be of assistance to future genomic-scale studies applying techniques such as: (1) gene capture of exons using RNA probes known as “baits” to acquire thousands of exons per sample and (2) total genome sequencing using nanochip technology that can perform single DNA reads ranging from tens of thousands of bases to hundreds of thousands bases.

Materials and methods

A. Taxon Sampling

Three data sets were collected: (1) mitochondrial DNA, (2) nuclear RAG-1 DNA, and (3) allozymic data from 25 presumptive loci.

All operational taxonomic units (OTUs) were sampled in the mitochondrial DNA data set. This included sequence data from 46 individuals representing 29 *Phrynocephalus* species [note: *Phrynocephalus* taxonomy is in flux so we defer to further studies to stabilize the number of species in the group; i.e., Barabanov & Ananjeva (2007), Kamali & Anderson (2015), Melnikov *et al.* (2015); see Appendix 1]. For 10 species sample collection is from individuals representing multiple localities that are numbered in appendix 1. Population 2 of *P. arabicus* from Oman is recognized as a distinct species *P. sakoi* by Melnikov *et al.* (2015). Four recognized outgroup species (*Laudakia caucasia*, *Bufoinceps laungwalaensis*, *Trapelus persicus*, and *T. sanguinolentus*) were included based on results of Macey *et al.* (2000b, 2006). We refrain from recognizing *Paralaudakia* (Baig *et al.* 2012) at this time and consider *Laudakia** a metataxon denoted with an asterisk, in which monophyly has not been demonstrated or rejected (see Schulte *et al.* 1998). Of these taxa the mitochondrial DNA segment sequenced has been previously reported for *P. interscapularis* (AF128517; Macey *et al.* 2000b), *P. mystaceus* population 1 (AF128518; Macey *et al.* 2000b), *P. raddei* (U82691; Macey *et al.* 1997c), *Laudakia caucasia* (AF028685, Macey *et al.* 1998a), *Bufoinceps laungwalaensis* (DQ008214, Macey *et al.* 2006), *Trapelus persicus* (AF128510, Macey *et al.* 2000b), and *T. sanguinolentus* (AF128511, Macey *et al.* 2000b). Two sequences collected for mitochondrial DNA contain missing data. Of the 1761 aligned DNA bases, *P. luteoguttatus* population 2 was not sequenced for the last 15 bases corresponding to amino acid positions 7–11 of COI; and *P. mystaceus* population 2 was not sequenced for the last 955 bases corresponding to the 3' half of ND2, tRNA^{Trp}, tRNA^{Ala}, tRNA^{Asn}, tRNA^{Cys}, tRNA^{Tyr}, and the 5' end of COI.

The nuclear RAG-1 gene was sequenced for most species and populations sampled in the mitochondrial DNA data set except: *P. arabicus* population 1, *P. clarkorum*, *P. ornatus*, *P. strauchi*, and *T. sanguinolentus*. One sequence was previously reported for *P. raddei* (AY662586 positions 26–2785; Townsend *et al.* 2004), and the overlapping area independently re-sequenced here completely matches. Three sequences collected for nuclear RAG-1 DNA contain missing data. Of the 2670 aligned DNA bases, *P. luteoguttatus* population 1 was not sequenced for the last 1110 bases; *P. vindumi* for 23 bases corresponding to positions 724–746; and *P. rossikowi* for 74 bases corresponding to positions 723–796.

Allozymic data was further collected from a subset of 26 taxa and populations represented in the mitochondrial data set. In some cases samples were added from nearby localities to boost population sizes. The outgroup population used for *Laudakia caucasia* is different than that used in the DNA data sets. Details of our sampling are outlined in appendix 1.

All sequences generated in this study are deposited in GenBank (mitochondrial DNA KJ195906–KJ195944; nuclear RAG-1 DNA KJ195945–KJ195984; see Appendix 1).

B. Data Collection

1). **Mitochondrial DNA**—Genomic DNA was extracted from liver or muscle using the Qiagen QIAamp tissue kit. Amplification of genomic DNA was conducted using a denaturation at 94°C for 35 sec, annealing at 50°C for 35 sec, and extension at 70°C for 150 sec with 4 sec added to the extension per cycle, for 30 cycles. Negative controls were run for all amplifications. Amplified products were purified on 2.5% Nusieve GTG agarose gels and reamplified under similar conditions. Reamplified double-stranded products were purified on 2.5% acrylamide gels (Maniatis *et al.* 1982). Template DNA was eluted from acrylamide passively over three days with Maniatis elution buffer (Maniatis *et al.* 1982). Cycle-sequencing reactions were run using the Promega fmol DNA-sequencing system with a denaturation at 95°C for 35 sec, annealing at 45–60°C for 35 sec, and extension at 70°C for 1 min for 30 cycles. Sequencing reactions were run on either Long Ranger sequencing gels for 5–12 hours at 38–40°C or sent to Beckman Coulter Genomics Company (Danvers, MA) for purification and DNA sequencing. Amplification and sequencing primers are summarized in Macey *et al.* (1997a, 1997c, 2000b).

2). **Nuclear RAG-1 DNA**—Amplification of the RAG-1 gene from genomic DNA was performed with Phusion™ High Fidelity DNA Polymerase (Finnzymes Oy) in a DNA Engine™ (PTC-200™) Peltier Thermal Cycler or MyCycler (MJ Research) using an initial denaturation at 98°C for 120 sec, 35 cycles of denaturation at 98°C for 10 sec, annealing between 60–64°C for 20 sec, and extension at 72°C for 120 sec. Successful PCR products were sent to Beckman Coulter Genomics Company (Danvers, MA) for purification and DNA sequencing.

Amplification of the RAG-1 gene was acquired using:

R13f (5'-TCTGAATGGAAATTCAAGCTGTT-3') and

JRAG1r.8 (5'-GACTCATTTCCTCACTTGCCCAAG-3') or

JRAG1f.1 (5'-CAAAGTGAGACSACTTGGAAAGCC-3') and JRAG1r.8.

Sequencing primers are summarized in Townsend *et al.* (2004).

3). **Allozyme Data**—Tissues were taken in the field and immediately frozen in liquid nitrogen. At a later date the tissues were transferred to an ultra-cold freezer and maintained at -76°C to -80°C. Liver tissue was homogenized completely independent of any other tissue that it had been previously stored with. Horizontal starch gel electrophoresis was employed to differentiate presumed alleles in 25 loci. Only loci that displayed scorable staining for all taxa and individuals were recorded. The 25 loci and eight buffer conditions utilized to resolve them are presented in Table 1. Allozymes were stained using standard methods (Harris & Hopkinson 1976; Murphy *et al.* 1990; Richardson *et al.* 1986; Selander *et al.* 1971). The carboxylic ester hydrolase (EST) scored was monomeric. Alcohol dehydrogenase (ADH) was resolved using Trans-2-Hexen-1-ol as the substrate, Peptidase B (PEP-B) using L-leucylglycylglycine as the substrate, and Peptidase D (PEP-D) with the use of L-phenylalanyl-L-proline as the substrate. The isozymes, and loci if more than one, were labeled according to their migration from anode to cathode.

C. Mitochondrial DNA Structural Shifts from Standard Vertebrates

The mitochondrial DNA segment sequenced encompasses the ND1 to COI region; 3' end of ND1 (NADH dehydrogenase subunit I), tRNA^{Gln}, tRNA^{Ile}, tRNA^{Met}, ND2 (NADH dehydrogenase subunit II), tRNA^{Trp}, tRNA^{Ala}, tRNA^{Asn}, tRNA^{Cys}, tRNA^{Tyr}, and the 5' end of COI (cytochrome c oxidase subunit I). It should be noted that there are three differences in this region from the standard vertebrate mitochondrial genome.

1). **Gene Order**—All acrodont lizards (Agamidae and Chamaeleonidae) have a unique gene rearrangement where tRNA^{Ile} is switched in order with tRNA^{Gln} relative to the standard vertebrate arrangement (Macey *et al.* 1997a). Because the mitochondrial genome is transcribed on two strands and subsequently cleaved, genes that overlap must be on opposite strands except bi-cistronically encoded protein genes, such as ATP 6 & 8 and ND4L & ND4. An interesting molecular evolutionary twist is that when the light-strand tRNA^{Gln} gene is placed after the heavy-strand encoding ND1, stop codons are placed inside the encoding AA-stem of the tRNA^{Gln} gene, and in frame. Most *Phrynocephalus* and outgroups use “TAG” as a stop codon for the ND1 gene, while some *Phrynocephalus* use “AGA” because of a base deletion. Those taxa are: *P. clarkorum* (MVZ:Herp:236888), *P.*

longicaudatus (CAS:Herp:251100), *P. persicus* (MVZ:Herp:236928), and *P. vlangalii* populations 1–3 (MVZ:Herp:211536, MVZ:Herp:272842, KIZ 020262, respectively); see appendix 1.

2). Light-Strand Replication Origin—All acrodont lizards lack a recognizable replication origin for the light strand O_L between the genes encoding tRNA^{Asn} and tRNA^{Cys}. While *Phrynocephalus* taxa do have sequences between these two tRNA genes, there are no obvious stem-and-loop structures. It has been shown that even when stem-and-loop structures exist, they are highly variable between clades of acrodont lizards (Macey *et al.* 1997a; 1997c; 2000a).

3). Transfer RNA Secondary Structure—The cysteine transfer RNA gene lacks a D-stem in all acrodont lizards, as well as parallel losses in other reptiles, and instead contains a D-arm replacement loop (Macey *et al.* 1997b; 2000a).

These unique characteristics have been accommodated in DNA alignments as described below.

TABLE 1. The 25 allozyme loci scored and the eight electrophoretic conditions within which they were resolved.

Enzyme or Blood Protein	Abbreviation	E.C. No.	Electrophoretic Conditions ¹
1. Serum albumin	AB	-	3
2. Aconitase hydratase	ACON	4.2.1.3	1
3. Alcohol dehydrogenase	ADH	1.1.1.1	5
4. Aspartate aminotransferase	AAT	2.6.1.1	2
5. Carboxylic ester hydrolase	EST ²	3.1.1.-	7
6. Carboxylic ester hydrolase	EST-D ²	3.1.1.-	3
7. Fructose-bisphosphate aldolase	FBA	4.1.2.13	4
8. Glucose-6-phosphate isomerase	GPI	5.3.1.9	2
9. Glycerol-3-phosphate dehydrogenase	GAPDH	1.2.1.12	3
10. D-2-Hydroxy-acid dehydrogenase	HADH	1.1.99.6	4
11. L-Iditol dehydrogenase	IDDH	1.1.1.14	4
12. Isocitrate dehydrogenase	IDH-1	1.1.1.42	1
13. Isocitrate dehydrogenase	IDH-2	1.1.1.42	1
14. L-Lactate dehydrogenase	LDH-1	1.1.1.27	5
15. L-Lactate dehydrogenase	LDH-2	1.1.1.27	5
16. Malate dehydrogenase	MDH-1	1.1.1.37	6
17. Malate dehydrogenase	MDH-2	1.1.1.37	6
18. Mannose-6-phosphate isomerase	MPI	5.3.1.8	6
19. Peptidase B	PEP-B	3.4.11.4	3
20. Peptidase D	PEP-D	3.4.13.9	7
21. Phosphoglucomutase	PGM	5.4.2.2	8
22. Phosphogluconate dehydrogenase	PGDH	1.1.1.44	6
23. Purine-nucleoside phosphorylase	PNP	2.4.2.1	7
24. Pyruvate kinase	PK	2.7.1.40	8
25. Superoxide dismutase	SOD	1.15.1.1	2

¹Electrophoretic conditions: (1) Amine-citrate (Morpholine) pH 6.0, 250 v for 6 h or 300 v for 5 h (Clayton & Tretiak 1972); (2) Histidine-citrate pH 7.8, 150 v for 8 h (Harris & Hopkinson 1976); (3) Lithium-borate/Tris-citrate pH 8.2, 250 v for 6 h or 300 v for 5 h; (4) Phosphate-citrate pH 7.0, 120 v for 7 h; (5) Tris-citrate/borate pH 8.7, 250 v for 5 h; (6) Tris-citrate II pH 8.0, 130 v for 8 h; (7) Tris-HCL pH 8.5, 250 v for 4 1/2 h; (8) Tris-maleate-EDTA pH 7.4, 100 v for 10 h (3-8, Selander *et al.* 1971).

²EST = Monomeric Esterase, EST-D = Dimeric Esterase

D. DNA Alignment

Alignment of protein coding and tRNA gene sequences were performed manually using amino-acid sequence translations for protein-coding genes and secondary-structural models for tRNA genes. Transfer-RNA secondary structure was determined manually using the criteria of Kumazawa & Nishida (1993) to ensure proper alignment (Macey & Verma 1997). Protein-coding sequences were translated to amino acids using MacClade version 4.0 (Maddison & Maddison 2000) and MacVector (North Carolina, versions 8–12) for confirmation of alignment.

The mitochondrial DNA alignment contains 1761 DNA positions of which we deemed 166 unalignable, resulting in 1595 included nucleotide sites. The 166 positions that were excluded from the mitochondrial DNA data set are from the following encoded gene regions or non-coding regions as identified: The D-loop of tRNA^{Gln} (DNA positions 138–146), the non-coding region between tRNA^{Gln} and tRNA^{Ile} (DNA positions 160–167), tRNA^{Ile} D-loop (DNA positions 181–187), tRNA^{Ile} T-loop (DNA positions 219–224), tRNA^{Met} T-loop (DNA positions 289–293), ND2 amino acid positions 2–11 (DNA positions 311–340), ND2 amino acid positions 325–329 (DNA positions 1280–1294), tRNA^{Trp} D-loop (DNA positions 1358–1369), tRNA^{Trp} T-loop (DNA positions 1401–1408), tRNA^{Ala} T-loop (DNA positions 1436–1442), non-coding region between tRNA^{Ala} and tRNA^{Cys} (DNA positions 1567–1593), tRNA^{Cys} T-loop (DNA positions 1607–1615), tRNA^{Cys} D-arm replacement loop (DNA positions 1643–1653), tRNA^{Tyr} T-loop (DNA positions 1673–1678), and tRNA^{Tyr} D-loop (DNA positions 1710–1715).

The nuclear RAG-1 sequence alignment was straightforward. All taxa have the same length except two outgroup taxa: *Bufoniceps laungwalaensis* and *Trapelus persicus*. These two have a deletion of two amino acids at amino acid positions 203–204 in the sampled sequence, which corresponds to DNA positions 607–612 in the DNA alignment.

The data alignment files of all DNA sequences used in this study have been deposited in GenBank [Note from GenBank: Please note that the alignments will not receive their own ID number. However, once your records are released, each set will get an ID number to be retrieved in the PopSet database].

E. Phylogenetic Tree Reconstruction

Five parsimony analyses were performed using the program PAUP* version 4.0 (Swofford 2002) with heuristic searches applying random-addition replicates and TBR branch swapping. All analyses gave equal weight to all character changes. In calculating decay indices, constraint trees were generated in MacClade version 4.0 (Maddison & Maddison 2000) and analyzed in PAUP* version 4.0 (Swofford 2002) as indicated below.

1). Mitochondrial DNA Analysis Methods—The mitochondrial DNA data set applied 500 random-addition replicates to discover shortest trees. Bootstrapping was done with 500 bootstrap replicates each applying 100 random-additions per replicate. Decay indices were calculated by searches for suboptimal trees that did not contain each node using constraint trees with 500 random-additions.

2). Nuclear RAG-1 DNA Analysis Methods—The nuclear RAG-1 DNA data set applied 500 random-addition replicates to discover shortest trees. Bootstrapping was done with 250 bootstrap replicates each applying 25 random-additions per replicate. Decay indices were calculated by searches for suboptimal trees that did not contain each node using constraint trees with 25 random-additions.

3). Allozyme Data Analyses Methods—Allozymic data (sections a and b below) were analyzed in two ways with parsimony. Although presence/absence coding of alleles has received considerable criticism for a lack of independence of alleles and the possibility of no allele being reconstructed for an ancestral node, it remains the method that provides the greatest amount of resolution. Alternatively, combinations of alleles for a particular locus may be coded as discrete character states (Buth 1984). If step matrices are used to connect character states, a greater amount of information can be retained (Mabee & Humphries 1993). In our analysis, step matrices were constructed on the basis of gains and losses of alleles. For example, a fixed difference between two alleles was counted as two steps, one allele lost and another gained. If a two-allele polymorphism in one population, which shares one allele with another monomorphic population, a single gain or loss was counted as one step. Additional polymorphisms were counted in the same manner. The 25 locus codes and step matrices are provided in appendix 2.

a). The allele presence/absence data set applied 500 random-addition replicates to discover the shortest trees. Bootstrapping was done with 500 bootstrap replicates each applying 25 random-additions per replicate. Decay

indices were calculated by searches for suboptimal trees that did not contain each node using constraint trees with 25 random-additions.

b). The locus coding of allele combinations with step matrices data set applied 250 random-addition replicates to discover the shortest trees. Bootstrapping was done with 250 bootstrap replicates each applying 25 random-additions per replicate. Decay indices were calculated by searches for suboptimal trees that did not contain each node using constraint trees with 25 random-additions.

4). Combined Data Analysis Methods—A further parsimony analysis was conducted on a combined data set of the mitochondrial DNA, nuclear RAG-1 DNA, and the allele presence/absence data. Allele presence/absence was treated the same as a nucleotide change. This data set applied 500 random-addition replicates to discover the shortest trees. Bootstrapping was done with 500 bootstrap replicates each applying 100 random-additions per replicate. Decay indices were calculated by searches for suboptimal trees that did not contain each node using constraint trees with 500 random-additions.

5). Maximum-likelihood Analyses Methods—Maximum-likelihood analyses were performed with RAxML v. 7.4.2 (Stamatakis *et al.* 2008) in the CIPRES portal (Miller *et al.* 2010) on two datasets, mitochondrial DNA alone and RAG-1 DNA alone. Evolutionary models to analyze allozyme data are not available in current software preventing a combined analysis. For each dataset, PartitionFinder (Lanfear *et al.* 2012) was used to determine the best-fit model of molecular evolution and partitioning scheme with four independent runs. This program selects the best-fit partitioning scheme and DNA sequence models based on pre-defined data blocks and using alternative information criteria. This program combines the analyses of ModelTest with comparisons of alternative a priori partitions into one analysis. A priori partitions compared in PartitionFinder were each codon position (1st, 2nd, 3rd) for each protein coding gene (ND1, ND2, COI, and RAG-1) plus one partition for all tRNA genes and noncoding mitochondrial DNA positions (10 partitions in mitochondrial DNA only dataset; 3 partitions in RAG-1 DNA only dataset). Model parameter values were estimated from the data. Optimal partitioning schemes and a GTR + Gamma model (see Appendix 3) for each dataset were implemented in RAxML with bootstrap resampling applying 250 replicates and parameter values estimated for each replicate. To provide an easy comparison with parsimony analyses of the same data set comparative parsimony decay indices are calculated (Macey 2005). Branches that appear in parsimony analyses have the parsimony decay index plotted. Branches with no parsimony cost but are not present in strict consensus trees are listed as a "0" decay value. Branches that conflict with the parsimony analysis have a negative decay value representing the number of parsimony steps cost to obtain the maximum-likelihood branch on a particular tree.

F. Linear Dating with Pairwise Sequence Divergence of Mitochondrial DNA

The region of mitochondrial DNA sequenced has been found to evolve with an approximately consistent rate of change per lineage per million years among a wide range of vertebrates [fish 0.65% (Bermingham *et al.* 1997); hynobiid salamanders 0.64% (unpublished analysis of data presented in Weisrock *et al.* 2013); frogs of the genus *Bufo* 0.69% (Macey *et al.* 1998b); lizards of the genus *Laudakia* 0.65% (Macey *et al.* 1998a); lizards of the genus *Teratoscincus* 0.57% (Macey *et al.* 1999)]. The calibrations derived from hynobiid salamanders and *Laudakia* lizards are each based on four geologic dates and are therefore the most reliable calibrations, suggesting a pairwise rate of change of 1.3% sequence divergence per million years. This value is within the range of rates (0.5–1.0% change per lineage per million years) tentatively accepted by Moritz *et al.* (1987) for the mitochondrial genome in primates. Mitochondrial DNA has been shown to saturate beyond a period of 10 MYBP and is not anticipated to show a linear relationship between nucleotide substitution and divergence times (Moritz *et al.* 1987), therefore dates estimated from nucleotide substitutional data beyond 10 MYBP are expected to be an underestimate of the actual date of divergence.

G. Statistical Evaluation of Alternative Hypotheses

Wilcoxon signed-ranks tests (Felsenstein 1985; Templeton 1983) were used to examine statistical significance of the shortest tree(s) relative to alternative hypotheses. This test asks whether the most parsimonious tree is

significantly shorter than an alternative or whether their differences in length can be attributed to chance alone (Larson 1998). Wilcoxon signed-ranks tests were conducted both as one- and two-tailed tests. Felsenstein (1985) showed that one-tailed probabilities are close to the exact probabilities for this test but not always conservative, whereas the two-tailed test is always conservative. Tests were conducted using PAUP* version 4.0 (Swofford 2002), which incorporates a correction for tied ranks. Alternative phylogenetic hypotheses were tested using the most parsimonious phylogenetic topologies compatible with them. To find the most parsimonious tree(s) compatible with a particular phylogenetic hypothesis, phylogenetic topologies were constructed using MacClade version 4.0 (Maddison & Maddison 2000) and analyzed as constraints using PAUP* version 4.0 (Swofford 2002) with heuristic searches using 100 random additions of sequences. Tests were conducted using the mitochondrial DNA alone and combined mitochondrial DNA, RAG-1, and allele presence/absence allozyme data but not on the RAG-1 DNA data alone because of the unforgivingly large number of equally parsimonious trees required to be evaluated. Taxon sampling for allozyme data is not extensive enough to adequately test hypotheses under question and tests applying allozyme data alone were not conducted.

H. Evaluation of Habitat Evolution in *Phrynocephalus*

Discrete taxon habitats are described pertaining to taxa under study. The outgroup *Laudakia caucasia* occupies mountain areas that are not inhabited by *Phrynocephalus* and is treated as a separated category: “Rock” habitat defined as a large rock boulder area. Habitats occupied by *Phrynocephalus* and additional outgroup species in the genera *Bufo* and *Trapelus* are categorized in the following ways. Hard substrates are: (1) “Gravel” defined as complex soils that tend to be isolated with unique gravel covers, or gravel from alluvial fans draining mountain regions; (2) “Clay” defined as hard clay soil, which does not have gravel; and (3) “Dry Lakebed” habitats defined as flat desert dry lakebeds that often have salt deposits. Soft substrates are: (1) “Small Sand Dune” defined as light sand, small sand dunes or edge of large shifting sand dunes; and (2) “Large Sand Dune” defined as large shifting sand dunes. Hard and soft substrates were plotted on the most parsimonious phylogenetic results of the combined data analysis using mitochondrial DNA, nuclear RAG-1 DNA, and allozyme data with the program MacClade version 4.0 (Maddison & Maddison 2000).

Note that *P. forsythii* lives in gravel habitats, but uses mounds of sand around bushes to make burrows. We have not separated this unique life history trait from other gravel species. *P. raddei* is considered to be of gravel habitat because it lives in recessive sinks of small size with hard soil among large sand dune systems. The habitat of *B. laungwalaensis* is after Sharma (1978), and the habitat of *T. persicus* is after Anderson (1999). The habitat of *P. arabicus* from Saudi Arabia (population 1) was determined via google earth. The authors of this manuscript made all other habitat designations based on personal collection experiences.

Results

A. Phylogenetic Hypotheses

Phylogenetic analyses of the three different data sets collected for the genus *Phrynocephalus* are reported, which are (1) approximately 11% of the mitochondrial genome that includes portions or all of 11 encoded genes, (2) the nuclear encoded RAG-1 gene, and (3) 25 nuclear encoded allozyme loci.

1). Parsimony Analysis of Mitochondrial DNA Data—The mitochondrial DNA data set encompasses the following genic regions, ND1 (subunit one of NADH dehydrogenase), tRNA^{Gln}, tRNA^{Ile}, tRNA^{Met}, ND2 (subunit two of NADH dehydrogenase), tRNA^{Trp}, tRNA^{Ala}, tRNA^{Asn}, tRNA^{Cys}, tRNA^{Tyr}, and COI (subunit I of cytochrome c oxidase) containing 1761 aligned character positions, of which 166 are excluded due to ambiguous alignment. Of the included characters, 181 are non-informative variable positions with 839 of these being parsimony informative positions. Parsimony analysis of the total data set produces three equally parsimonious trees of 4425 steps in length. The strict consensus of these three trees is presented in figure 4.

The genus *Phrynocephalus* is monophyletic receiving high support (bootstrap 100%, decay index 53). Within the outgroups, monophyly of *Bufo laungwalaensis* and *Trapelus* species is well supported with a bootstrap of

100% and a decay index of 66 (as previously reported by Macey *et. al.* 2006), and monophyly of both *Trapelus* species receiving support from a bootstrap of 99% and a decay index of 19.

Identified are 13 reasonably well-supported clades and lineages within the genus *Phrynocephalus* that are labeled A through M in figure 4. Beyond the four outgroups listed above, sampling consists of 42 *Phrynocephalus* species and populations, of which 29 are species, with 13 additional populations for multiple sampling within species.

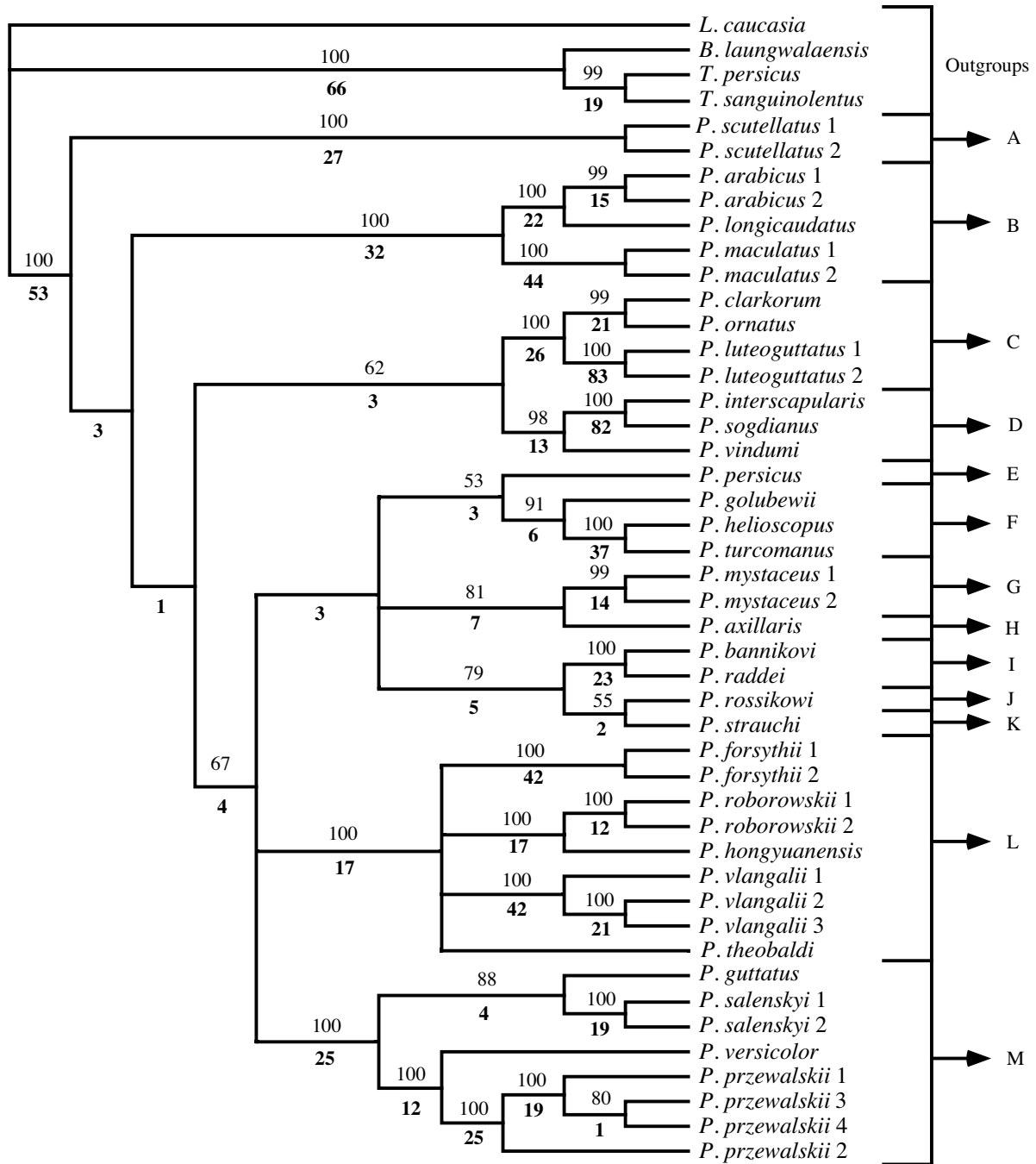


FIGURE 4. Strict consensus of three equally parsimonious trees of 4425 steps from the 1595 included (839 informative) aligned mitochondrial DNA positions. Bootstrap values are presented above branches and decay indices are presented below branches in bold. Outgroups (*Laudakia*, *Bufoniceps*, and *Trapelus*), and well-supported *Phrynocephalus* clades and lineages are identified to the right as A–M.

Clade A consists of *P. scutellatus* populations from the southern and eastern Iranian Plateau inhabiting gravel areas (bootstrap of 100%, decay index 27).

Clade B consists of *P. arabicus* populations, *P. longicaudatus*, and *P. maculatus* populations, which are from the Arabian Peninsula and the Iranian Plateau, receiving high support (bootstrap 100%, decay index 32). The Arabian subgroup consists of *P. arabicus* populations and *P. longicaudatus* forming a well-supported clade (bootstrap 100%, decay index 22). *P. arabicus* population 1 from the Saudi Arabian Empty Quarter and *P. arabicus* population 2 from Oman are monophyletic with high support (bootstrap 99%, decay index 15). The second subgroup contains the two populations of *P. maculatus* from the Iranian Plateau, which additionally receives high support (bootstrap 100%, decay index 44).

Clade C contains *P. clarkorum*, *P. ornatus*, and *P. luteoguttatus* populations from the Helmand Basin in Afghanistan and adjacent Pakistani Baluchistan, receiving high support (bootstrap 100%, decay index 26). Within this clade two well-supported groups appear, *P. clarkorum* and *P. ornatus* (bootstrap 99%, decay index 21), and both *P. luteoguttatus* populations (bootstrap 100%, decay index 83).

Clade D consists of *P. interscapularis*, *P. sogdianus*, and *P. vindumi* (bootstrap 98%, decay index 13) with *P. vindumi* from the northeastern Iranian Plateau sister to *P. interscapularis* and *P. sogdianus* from the Caspian Basin with support of a bootstrap of 100% and a decay index of 82. Clades C and D are small species that live in sandy substrates and receive minimal support as a clade (bootstrap 62%, decay index 3).

Lineage E is a single taxon *P. persicus* from the northwestern Iranian Plateau, and groups with Clade F with weak support (bootstrap 53%, decay index 3). Clade F consists of *P. golubewii*, *P. helioscopus*, and *P. turcomanus* receiving reasonably high support (bootstrap 91%, decay index 6), with *P. golubewii* from the southern Caspian Basin, sister to a well supported clade containing *P. helioscopus* from the northern Caspian Basin and *P. turcomanus* from the southern Caspian Basin (bootstrap 100%, decay index 37). Note all taxa in lineage E and Clade F live in gravel habitats except *P. golubewii*, which lives in a single dry lakebed in Turkmenistan.

Clade G consists of *P. mystaceus* populations north and south of the Kopet-Dagh (mountains) from the Caspian Basin and the northeastern Iranian Plateau living in large sand dunes (bootstrap 99%, decay index 14).

Lineage H is *P. axillaris* living in hard soil habitats from the Taklimakan Desert of northwestern China, which is sister to the two *P. mystaceus* populations in Clade G together receiving moderate support (bootstrap 81%, decay index 7).

Clade I consists of *P. bannikovi* and *P. raddei* receiving high support (bootstrap 100%, decay index 23). Lineage J is *P. rossikowi* and lineage K is *P. strauchi*, which group with low support (bootstrap 55%, decay index 2). Clades and lineages I, J, and K are relatively small species that inhabit gravel habitats all in the southern Caspian Basin, which form a moderately supported clade (bootstrap 79%, decay index 5). Clades and lineages E-K all group together but receive no bootstrap support and only a decay index of 3.

Clade L is a viviparous group from high elevation Tibet and the adjacent low elevation Taklimakan Desert in northwestern China, containing *P. forsythii* populations, *P. roborowskii* populations, *P. hongyuanensis*, *P. vlangalii* populations and *P. theobaldi* (bootstrap 100%, decay index 17). The low elevation Taklimakan Desert *P. forsythii* populations group with high support (bootstrap 100%, decay index 42). *P. roborowskii* populations from the Chaka Basin and Qaidam Depression on the western side of the northeastern Tibetan Plateau, and *P. hongyuanensis* from the far eastern side of the northeastern Tibetan Plateau in Sichuan Province China group with high support (bootstrap 100%, decay index 17). The two *P. roborowskii* populations form a well-supported clade (bootstrap 100%, decay index 12). All *P. vlangalii* populations in the vicinity of Qinghai Lake in a central region of the northeastern Tibetan Plateau appear monophyletic (bootstrap 100%, decay index 42) with population 1 (more western, Heimaha) being sister to population 2 (more eastern, east side of Qinghai Lake) and population 3 (more southern, Maqên), (bootstrap 100%, decay index 21). Relationships between *P. theobaldi* from southern Tibet, and the other viviparous groups described from northern Tibet and adjacent low elevation Taklimakan Desert are unresolved.

Clade M consists of low elevation northern species in China, Kazakhstan and Russia: *P. guttatus*, two *P. salenskyi* populations, *P. versicolor*, and four *P. przewalskii* populations (bootstrap 100%, decay index 25). *P. guttatus* from the European side of the Caspian Sea, and *P. salenskyi* populations from the Junggar Depression of China and Zaysan Depression in adjacent Kazakhstan form a monophyletic group with moderate support (bootstrap 88%, decay index 4). *P. guttatus* is sister to *P. salenskyi* populations with high support (bootstrap 100%, decay index 19). The sister clade to that group contains the Gobi Desert samples from *P. versicolor* and four *P. przewalskii* populations (bootstrap 100% decay index 12), with monophyly of all *P. przewalskii* populations

receiving high support (bootstrap 100%, decay index 25). *P. przewalskii* population 2 from the south shore of the Yellow River across from Shapotou Ningxia Autonomous Region in China is sister to the clade containing populations 1, 3, and 4 with high support (bootstrap 100%, decay index 19). Population 1 from Wujiachuan Gansu Province China is sister to the clade containing population 3 from the north shore of the Yellow River in Shapotou Ningxia Autonomous Region China and population 4 from Wuwei Gansu Province China, though by a slim margin indicated by the decay index of 1 (bootstrap 80%, decay index 1).

Relationships between clades A, B, C, and D do not bootstrap and are supported by either a decay index of 3 or 1. Clades E through M are supported by a low bootstrap of 67% and a decay index of 4.

All clades identified in the parsimony analysis of the mitochondrial DNA data A through M are recovered in the maximum-likelihood (ML) tree (see Appendix 3). The consensus tree of the three most parsimonious trees from the mitochondrial DNA dataset only differs in topology with the maximum-likelihood tree in two weakly supported areas. In the maximum-likelihood analysis, clades A through D appear monophyletic with no ML bootstrap support and a cost of four parsimony steps (negative decay index 4). In addition, the sister relationship of *P. rossikowi* and *P. strauchi* recovered in the parsimony analysis is broken in the maximum-likelihood analysis with *P. rossikowi* in a basal position to a clade containing *P. strauchi* and the grouping of *P. bannikovi* with *P. raddei* receiving a ML bootstrap of 51% and a parsimony cost of 2 steps (negative decay index 2). The three polytomies resulting from the consensus tree of the three most parsimonious trees are resolved in the maximum-likelihood analysis. Grouping of E/F with H/G is topologically recovered in the maximum likelihood analysis with no bootstrap support and no parsimony cost. Clades E–K group in both the parsimony and maximum-likelihood analyses, and is resolved as grouping with Clade M in the maximum-likelihood analysis with ML bootstrap support of 65% and no parsimony cost. In the viviparous group of Clade L, the grouping of *P. forsythii* populations, *P. theobaldi*, *P. hongyuanensis*, and *P. roborowskii* populations is resolved with ML bootstrap support of 67% and no parsimony cost; the grouping of *P. theobaldi*, *P. hongyuanensis*, and *P. roborowskii* populations is resolved with ML bootstrap support of 87% and no parsimony cost. All differences between results of the parsimony and maximum-likelihood analyses revolve around weak areas in tree topologies, with the maximum-likelihood analysis simply choosing a fully resolved topology 12 steps longer than the shortest parsimony solutions (ML tree 4437 parsimony steps). Hence, differing results of the maximum-likelihood analysis should be treated with caution.

2). Parsimony Analysis of RAG-1 DNA Data—Parsimony analysis of the nuclear RAG-1 data set contains 2760 aligned character positions. Of the 2760 included characters, 209 are parsimony uninformative variable positions with 342 of these being parsimony informative positions. Parsimony analysis of the total data set produces 62 equally parsimonious trees 831 steps in length. The strict consensus of these trees is presented in figure 5. Beyond the three outgroups listed below, sampling consists of 38 *Phrynocephalus* species and populations, of which 26 are species, with 12 additional populations for multiple sampling within species.

The genus *Phrynocephalus* is monophyletic receiving high support (bootstrap 100%, decay index 48). Within outgroups, monophyly of *Bufoniceps laungwalaensis* and *Trapelus persicus* is well supported with a bootstrap of 100% and a decay index of 104 (as previously reported by Macey *et. al.* 2006).

In the nuclear RAG-1 DNA phylogenetic estimate, all except for one of the clades and lineages A through M appear monophyletic, as recognized by the mitochondrial DNA analysis; Clade F appears in a non-monophyletic grouping (labeled F-1 and F-2 in Fig. 5). Clades recovered are:

Clade A consists of the two *P. scutellatus* populations from the Iranian Plateau with high support (bootstrap 100%, decay index 20), matching the mitochondrial DNA analysis.

Clade B consists of *P. arabicus* population 2, *P. longicaudatus*, both from the Arabian Peninsula, and the two *P. maculatus* populations from the Iranian Plateau (bootstrap 100%, decay index 13). *P. arabicus* population 2 groups with *P. longicaudatus* with high support (bootstrap 100%, decay index 7), and the two *P. maculatus* populations group with low support (bootstrap 72%, decay index 1). All relationships in this clade match the mitochondrial DNA analysis.

Clade D is comprised of *P. interscapularis*, *P. sogdianus*, and *P. vindumi* with high support (bootstrap 98%, decay index 6). The Caspian Basin species *P. interscapularis* and *P. sogdianus* group with high support (bootstrap 100%, decay index 14), with *P. vindumi* from the northeastern Iranian Plateau in a sister position. All relationships in this clade match the mitochondrial DNA analysis.

Clade C consists of the two *P. luteoguttatus* populations from the Helmand Basin of Afghanistan and adjacent Baluchistan in Pakistan, which receive high support (bootstrap 100%, decay index 11), matching the mitochondrial DNA analysis.

100%, decay index 10), while Clade I consisting of *P. bannikovi* and *P. raddei* receives moderate support (bootstrap 91%, decay index 3). With other relationships among clades and lineages E, F-1, F-2, J and I not well supported (decay index 1).

TABLE 2. Allele frequency data for the 24 species and populations of *Phrynocephalus* and two outgroup taxa. Sample sizes (N) are provided following taxon names. Where multiple populations of a species are reported a number follows the species name: *P. przewalskii* population 1 is from Wujiachuan and Baiyin, population 2 from across the Yellow River from Shapotou, population 3 from Shapotou and north of Shapotou, population 4 from Wuwei; *P. salenskyi* population 1 from Jimsar and Wujiaqu, population 2 from Zaysan Lake; *P. forsythii* population 1 from Yengisar, population 2 from Tikanlik; *P. roborowskii* population 1 from Chaka; population 2 from Magnai and Ruoqiang. See Appendix 1 for full locality information and museum numbers.

	Size	AB	ACON	ADH	AAT	EST	EST-D	FBA
1. <i>P. przewalskii</i> -1 (Wujiachuan, Baiyin)	N=10	c 1.000	b 0.100 c 0.900	f 0.650 j 0.250 l 0.100	e 1.000	c 1.000	d 1.000	d 0.650 e 0.350
2. <i>P. przewalskii</i> -2 (Across Shapotou)	N=6	c 1.000	c 1.000	c 0.083 f 0.584 j 0.250 n 0.083	e 1.000	c 1.000	d 1.000	d 1.000
3. <i>P. przewalskii</i> -3 (Shapotou, N. Shapotou)	N=6	c 1.000	c 1.000	c 0.083 f 0.500 j 0.334 m 0.083	e 1.000	c 1.000	d 1.000	d 1.000
4. <i>P. przewalskii</i> -4 (Wuwei)	N=8	c 1.000	c 1.000	f 0.500 l 0.125 n 0.3125 o 0.0625	e 1.000	c 1.000	d 1.000	d 1.000
5. <i>P. versicolor</i>	N=10	c 1.000	c 1.000	c 0.050 f 0.850 j 0.100	e 1.000	c 1.000	d 0.900 i 0.050 k 0.050	d 1.000
6. <i>P. salenskyi</i> -1 (Jimsar, Wujiaqu)	N=10	c 1.000	c 1.000	a 0.050 c 0.050 f 0.750 j 0.050 o 0.100	b 1.000	c 0.750 e 0.250	a 0.100 d 0.800 g 0.100	c 0.1000 d 0.900
7. <i>P. salenskyi</i> -2 (Zaysan Lake)	N=5	c 1.000	c 1.000	f 0.200 j 0.800	b 0.700 c 0.300	c 1.000	d 1.000	b 0.400 d 0.600
8. <i>P. guttatus</i>	N=10	c 1.000	c 1.000	f 0.200 j 0.650 m 0.150	b 0.750 c 0.250	c 1.000	d 1.000	d 0.950 e 0.050
9. <i>P. axillaris</i>	N=10	c 1.000	c 1.000	b 0.100 f 0.750 j 0.150	b 1.000	c 1.000	c 0.050 d 0.950	a 0.100 d 0.900
10. <i>P. forsythii</i> -1 (Yengisar)	N=4	c 1.000	c 1.000	h 1.000	b 1.000	f 1.000	b 0.125 d 0.750 g 0.125	d 1.000

.....continued on the next page

TABLE 2. (Continued)

	Size	AB	ACON	ADH	AAT	EST	EST-D	FBA
11. <i>P. forsythii</i> -2 (Tikanlik)	N=4	c 1.000	c 1.000	h 1.000	b 1.000	f 1.000	b 0.125 d 0.875	d 1.000
12. <i>P. vlangalii</i> -1 (Heimahe)	N=10	c 1.000	c 1.000	n 1.000	b 1.000	c 1.000	d 0.950 i 0.050	d 1.000
13. <i>P. roborowskii</i> -1 (Chaka)	N=9	c 1.000	c 1.000	n 1.000	b 0.889 d 0.111	c 1.000	d 1.000	d 1.000
14. <i>P. roborowskii</i> -2 (Mangai, Ruoqiang)	N=8	c 1.000	c 1.000	n 1.000	b 1.000	c 1.000	a 0.125 d 0.875	d 1.000
15. <i>P. theobaldi</i>	N=10	c 1.000	c 0.900 e 0.100	n 1.000	a 1.000	c 1.000	d 1.000	d 1.000
16. <i>P. helioscopus</i>	N=9	c 1.000	c 1.000	f 1.000	c 1.000	c 1.000	d 1.000	b 0.778 d 0.222
17. <i>P. turcomanus</i>	N=10	c 1.000	c 1.000	b 0.150 f 0.700 g 0.100 j 0.050	c 1.000	c 1.000	d 0.750 g 0.250	b 0.100 d 0.850 e 0.050
18. <i>P. golubewii</i>	N=4	c 1.000	e 1.000	f 1.000	b 0.750 c 0.250	c 1.000	d 1.000	d 1.000
19. <i>P. bannikovi</i>	N=10	c 1.000	c 1.000	c 0.200 e 0.300 i 0.500	b 0.450 c 0.550	c 1.000	d 1.000	d 1.000
20. <i>P. raddei</i>	N=10	c 1.000	c 1.000	c 0.950 f 0.050	b 1.000	f 1.000	d 0.450 g 0.550	d 1.000
21. <i>P. rossikowi</i>	N=10	c 1.000	a 1.000	f 0.900 i 0.050 j 0.050	b 1.000	d 1.000	d 1.000	d 1.000
22. <i>P. mystaceus</i> -1 (N. Ashkabad)	N=10	c 1.000	c 1.000	c 0.050 g 0.550 n 0.400	b 1.000	c 1.000	d 0.900 g 0.100	d 0.950 f 0.050
23. <i>P. interscapularis</i>	N=10	b 1.000	e 1.000	d 0.100 f 0.900	b 1.000	a 0.300 c 0.700	b 0.050 d 0.900 f 0.050	d 1.000
24. <i>P. sogdianus</i>	N=7	b 1.000	e 1.000	f 0.929 k 0.071	b 1.000	b 1.000	d 0.857 h 0.143	d 1.000
25. <i>T. sanguinolentus</i>	N=10	a 1.000	d 1.000	g 1.000	b 1.000	g 1.000	e 0.950 k 0.050	d 1.000
26. <i>L. caucasia</i>	N=10	d 1.000	b 1.000	b 0.050 c 0.800 f 0.150	b 1.000	g 1.000	j 0.450 k 0.500 l 0.050	d 1.000
	Size	GPI	GAPDH	HADH	IDDH	IDH-1	IDH-2	LDH-1
1. <i>P. przewalskii</i> -1	N=10	b 0.050	f 1.000	a 0.150	i 1.000	a 0.300	f 1.000	b 1.000

.....continued on the next page

TABLE 2. (Continued)

	Size	GPI	GAPDH	HADH	IDDH	IDH-1	IDH-2	LDH-1
(Wujiachuan, Baiyin)		g 0.950		b 0.150 c 0.050 f 0.650		d 0.650 g 0.050		
2. <i>P. przewalskii</i> -2 (Across Shapotou)	N=6	g 1.000	f 1.000	b 0.167 f 0.666 g 0.167	c 0.167 i 0.833	a 0.500 d 0.500	f 0.917 h 0.083	b 1.000
3. <i>P. przewalskii</i> -3 (Shapotou, N. Shapotou)	N=6	g 1.000	f 1.000	b 0.167 c 0.167 f 0.666	i 1.000	a 0.167 d 0.833	f 1.000	b 1.000
4. <i>P. przewalskii</i> -4 (Wuwei)	N=8	g 1.000	f 1.000	b 0.250 e 0.125 f 0.625	c 0.125 i 0.875	a 0.1875 d 0.8125	f 1.000	b 1.000
5. <i>P. versicolor</i>	N=10	g 1.000	f 1.000	f 0.900 i 0.100	i 1.000	a 0.200 d 0.750 h 0.050	f 0.800 g 0.200	b 0.400 d 0.600
6. <i>P. salenskyi</i> -1 (Jimsar, Wujiaqu)	N=10	g 1.000	f 0.900 h 0.100	b 0.400 e 0.050 f 0.300 i 0.250	i 1.000	d 0.100 g 0.900	a 0.050 f 0.950	d 1.000
7. <i>P. salenskyi</i> -2 (Zaysan Lake)	N=5	g 1.000	f 1.000	b 0.500 f 0.500	f 0.200 i 0.800	d 0.800 g 0.200	f 1.000	d 1.000
8. <i>P. guttatus</i>	N=10	g 1.000	e 0.400 f 0.600	b 0.700 i 0.300	i 1.000	a 0.400 d 0.600	f 1.000	d 1.000
9. <i>P. axillaris</i>	N=10	c 0.300 g 0.700	f 0.800 i 0.200	b 0.400 f 0.600	e 0.400 i 0.600	a 1.000	a 0.100 f 0.900	d 1.000
10. <i>P. forsythii</i> -1 (Yengisar)	N=4	g 1.000	f 1.000	c 0.125 f 0.625 i 0.125 j 0.125	i 1.000	d 1.000	f 1.000	d 1.000
11. <i>P. forsythii</i> -2 (Tikanlik)	N=4	g 1.000	f 1.000	d 0.125 f 0.500 j 0.375	d 0.250 i 0.750	a 0.125 d 0.875	f 1.000	d 1.000
12. <i>P. vlangalii</i> -1 (Heimahe)	N=10	d 1.000	j 1.000	f 1.000	c 1.000	d 1.000	f 1.000	d 1.000
13. <i>P. roborowskii</i> -1 (Chaka)	N=9	d 1.000	a 0.111 f 0.889	f 0.055 h 0.278 j 0.667	d 0.833 i 0.167	d 1.000	f 1.000	c 0.056 d 0.944
14. <i>P. roborowskii</i> -2 (Mangai, Ruoqiang)	N=8	e 0.875 h 0.125	f 0.750 g 0.125 k 0.125	g 1.000	d 1.000	d 1.000	f 1.000	d 1.000
15. <i>P. theobaldi</i>	N=10	a 1.000	c 1.000	g 1.000	a 1.000	d 1.000	c 1.000	d 1.000

.....continued on the next page

TABLE 2. (Continued)

	Size	GPI	GAPDH	HADH	IDDH	IDH-1	IDH-2	LDH-1
16. <i>P. helioscopus</i>	N=9	g 1.000	f 1.000	i 1.000	j 1.000	h 1.000	f 1.000	b 1.000
17. <i>P. turcomanus</i>	N=10	g 1.000	f 1.000	i 1.000	j 1.000	h 1.000	f 1.000	b 1.000
18. <i>P. golubewii</i>	N=4	i 1.000	d 0.875 f 0.125	f 1.000	i 1.000	d 1.000	f 1.000	b 1.000
19. <i>P. bannikovi</i>	N=10	g 1.000	f 1.000	d 0.100 f 0.900	i 1.000	b 0.100 d 0.900	f 1.000	a 1.000
20. <i>P. raddei</i>	N=10	g 1.000	f 1.000	f 0.700 g 0.300	i 1.000	d 0.650 g 0.350	a 0.600 f 0.400	b 1.000
21. <i>P. rossikowi</i>	N=10	i 1.000	f 0.900 i 0.100	f 1.000	e 1.000	c 0.100 d 0.900	a 0.100 f 0.900	a 1.000
22. <i>P. mystaceus</i> -1 (N. Ashkabad)	N=10	a 1.000	a 0.100 f 0.900	b 0.900 f 0.100	h 0.100 i 0.600 k 0.300	d 0.950 f 0.050	f 1.000	b 1.000
23. <i>P. interscapularis</i>	N=10	e 1.000	f 1.000	b 0.200 f 0.700 i 0.100	c 0.650 i 0.350	c 1.000	f 1.000	b 1.000
24. <i>P. sogdianus</i>	N=7	e 1.000	f 1.000	f 1.000	a 0.357 c 0.643	c 1.000	b 0.143 e 0.143 f 0.714	b 1.000
25. <i>T. sanguinolentus</i>	N=10	g 0.150 k 0.850	b 1.000	b 1.000	b 1.000	a 1.000	d 1.000	b 1.000
26. <i>L. caucasica</i>	N=10	j 1.000	f 1.000	k 1.000	g 0.200 i 0.800	e 1.000	f 1.000	a 1.000
	Size	LDH-2	MDH-1	MDH-2	MPI	PEP-B	PEP-D	PGM
1. <i>P. przewalskii</i> -1 (Wujiachuan, Baiyin)	N=10	d 1.000	e 1.000	b 1.000	g 1.000	f 1.000	c 1.000	d 1.000
2. <i>P. przewalskii</i> -2 (Across Shapotou)	N=6	c 0.167 d 0.833	e 1.000	b 1.000	g 1.000	c 0.083 f 0.917	c 1.000	d 1.000
3. <i>P. przewalskii</i> -3 (Shapotou, N. Shapotou)	N=6	d 1.000	e 1.000	b 1.000	g 1.000	b 0.083 f 0.834 j 0.083	c 1.000	d 1.000
4. <i>P. przewalskii</i> -4 (Wuwei)	N=8	d 1.000	e 1.000	b 1.000	g 1.000	c 0.125 f 0.875	c 1.000	d 1.000
5. <i>P. versicolor</i>	N=10	a 0.700 c 0.300	b 0.300 c 0.600 e 0.100	b 1.000	g 1.000	e 0.400 f 0.500 h 0.100	c 1.000	d 1.000
6. <i>P. salenskyi</i> -1 (Jimsar, Wujiaqu)	N=10	a 0.900 d 0.100	b 1.000	b 1.000	g 1.000	f 1.000	c 1.000	d 1.000
7. <i>P. salenskyi</i> -2 (Zaysan Lake)	N=5	a 1.000	b 1.000	b 1.000	g 1.000	f 1.000	c 1.000	d 1.000

.....continued on the next page

TABLE 2. (Continued)

	Size	LDH-2	MDH-1	MDH-2	MPI	PEP-B	PEP-D	PGM
8. <i>P. guttatus</i>	N=10	a 1.000	b 1.000	b 1.000	g 0.950 l 0.050	f 1.000	c 1.000	d 1.000
9. <i>P. axillaris</i>	N=10	a 1.000	b 1.000	a 1.000	a 0.100 c 0.900	e 0.100 f 0.900	c 1.000	d 1.000
10. <i>P. forsythii</i> -1 (Yengisar)	N=4	d 1.000	b 1.000	b 1.000	g 0.750 j 0.250	f 0.125 j 0.875	c 1.000	d 1.000
11. <i>P. forsythii</i> -2 (Tikanlik)	N=4	d 1.000	b 1.000	b 0.875 c 0.125	g 0.875 j 0.125	d 0.125 f 0.125 i 0.375 j 0.375	c 1.000	c 0.125 d 0.875
12. <i>P. vlangalii</i> -1 (Heimahe)	N=10	d 1.000	b 1.000	b 1.000	j 0.500 m 0.500	f 1.000	e 1.000	a 0.050 b 0.250 d 0.300 e 0.400
13. <i>P. roborowskii</i> -1 (Chaka)	N=9	d 1.000	b 1.000	b 1.000	b 0.056 g 0.944	c 0.056 f 0.944	e 1.000	d 1.000
14. <i>P. roborowskii</i> -2 (Mangai, Ruoqiang)	N=8	d 1.000	b 1.000	b 1.000	g 1.000	c 0.250 f 0.750	e 1.000	d 1.000
15. <i>P. theobaldi</i>	N=10	d 1.000	b 1.000	b 1.000	d 1.000	d 1.000	e 1.000	d 1.000
16. <i>P. helioscopus</i>	N=9	a 1.000	b 1.000	b 1.000	g 1.000	f 1.000	f 1.000	d 1.000
17. <i>P. turcomanus</i>	N=10	a 1.000	b 1.000	b 1.000	g 1.000	f 1.000	f 1.000	d 0.950 e 0.050
18. <i>P. golubewii</i>	N=4	a 1.000	b 1.000	b 1.000	g 1.000	f 1.000	f 1.000	d 1.000
19. <i>P. bannikovi</i>	N=10	a 0.950 b 0.050	b 1.000	b 1.000	f 0.200 g 0.350 h 0.300 k 0.050 m 0.100	f 1.000	b 1.000	d 1.000
20. <i>P. raddei</i>	N=10	a 1.000	b 1.000	b 1.000	l 1.000	j 0.400 l 0.600	f 1.000	d 1.000
21. <i>P. rossikowi</i>	N=10	a 1.000	d 1.000	b 1.000	g 1.000	b 0.400 f 0.600	c 0.850 g 0.150	d 0.950 e 0.050
22. <i>P. mystaceus</i> -1 (N. Ashkabad)	N=10	d 0.950 e 0.050	a 0.950 b 0.050	b 1.000	g 0.350 i 0.050 j 0.550 m 0.050	f 1.000	c 1.000	d 1.000
23. <i>P. interscapularis</i>	N=10	d 1.000	b 1.000	d 1.000	g 0.850 j 0.150	b 0.950 f 0.050	d 1.000	d 1.000
24. <i>P. sogdianus</i>	N=7	d 1.000	b 0.429 d 0.571	d 1.000	g 1.000	a 0.071 b 0.929	d 1.000	b 0.070 d 0.860 e 0.070
25. <i>T. sanguinolentus</i>	N=10	d 1.000	b 1.000	b 1.000	e 1.000	i 0.100	a 1.000	b 0.150

.....continued on the next page

TABLE 2. (Continued)

	Size	LDH-2	MDH-1	MDH-2	MPI	PEP-B	PEP-D	PGM
						k 0.800		d 0.850
						l 0.100		
26. <i>L. caucasia</i>	N=10	d 1.000	f 1.000	b 1.000	i 1.000	g 0.900	a 1.000	d 1.000
						l 0.100		
	Size	PGDH	PNP	PK	SOD			
1. <i>P. przewalskii</i> -1 (Wujiachuan, Baiyin)	N=10	m 0.900 r 0.050 s 0.050	f 1.000	b 1.000	e 1.000			
2. <i>P. przewalskii</i> -2 (Across Shapotou)	N=6	m 0.750 s 0.250	f 0.917 i 0.083	b 1.000	e 1.000			
3. <i>P. przewalskii</i> -3 (Shapotou, N. Shapotou)	N=6	m 0.917 q 0.083	f 1.000	b 1.000	e 1.000			
4. <i>P. przewalskii</i> -4 (Wuwei)	N=8	e 0.1875 m 0.750 s 0.0625	f 1.000	b 1.000	e 1.000			
5. <i>P. versicolor</i>	N=10	e 0.100 k 0.050 m 0.750 t 0.100	f 1.000	b 1.000	e 1.000			
6. <i>P. salenskyi</i> -1 (Jimsar, Wujiaqu)	N=10	h 0.100 j 0.050 m 0.850	f 0.900 i 0.100	b 1.000	b 0.050 e 0.900 g 0.050			
7. <i>P. salenskyi</i> -2 (Zaysan Lake)	N=5	d 0.100 m 0.800 o 0.100	f 0.800 i 0.200	b 1.000	e 1.000			
8. <i>P. guttatus</i>	N=10	m 1.000	d 1.000	b 1.000	e 1.000			
9. <i>P. axillaris</i>	N=10	m 1.000	d 1.000	c 1.000	c 1.000			
10. <i>P. forsythii</i> -1 (Yengisar)	N=4	g 0.375 i 0.625	d 1.000	b 1.000	d 1.000			
11. <i>P. forsythii</i> -2 (Tikanlik)	N=4	e 0.750 i 0.125 m 0.125	d 1.000	b 1.000	d 1.000			
12. <i>P. vlangalii</i> -1 (Heimahe)	N=10	i 0.550 j 0.050 m 0.150 n 0.150 p 0.100	d 1.000	a 1.000	f 1.000			
13. <i>P. roborowskii</i> -1 (Chaka)	N=9	e 1.000	d 1.000	a 1.000	f 1.000			
14. <i>P. roborowskii</i> -2 (Mangai, Ruoqiang)	N=8	e 1.000	d 0.875 e 0.125	a 1.000	f 1.000			

.....continued on the next page

TABLE 2. (Continued)

	Size	PGDH	PNP	PK	SOD
15. <i>P. theobaldi</i>	N=10	e 1.000	d 1.000	a 1.000	f 1.000
16. <i>P. helioscopus</i>	N=9	e 1.000	a 0.110 b 0.445 c 0.445	a 0.556 d 0.444	e 1.000
17. <i>P. turcomanus</i>	N=10	c 0.100 e 0.900	c 1.000	a 1.000	e 1.000
18. <i>P. golubewii</i>	N=4	f 1.000	c 1.000	a 1.000	e 1.000
19. <i>P. bannikovi</i>	N=10	e 1.000	d 1.000	a 1.000	h 1.000
20. <i>P. raddei</i>	N=10	e 1.000	b 0.150 d 0.850	a 1.000	h 1.000
21. <i>P. rossikowi</i>	N=10	a 0.100 c 0.100 e 0.800	d 0.800 h 0.200	a 1.000	h 1.000
22. <i>P. mystaceus</i> -1 (N. Ashkabad)	N=10	c 0.950 e 0.050	d 1.000	a 1.000	a 1.000
23. <i>P. interscapularis</i>	N=10	b 0.100 c 0.900	d 1.000	b 1.000	h 1.000
24. <i>P. sogdianus</i>	N=7	c 0.857 e 0.143	c 0.500 d 0.500	b 1.000	h 1.000
25. <i>T. sanguinolentus</i>	N=10	l 1.000	d 0.800 f 0.200	a 1.000	j 1.000
26. <i>L. caucasia</i>	N=10	q 1.000	d 0.550 g 0.450	a 1.000	i 1.000

Lineage H consists of *P. axillaris* from the low elevation Taklimakan Desert in northwestern China which appears as the sister taxon to all species in Clade M from the northern Chinese deserts and the northern Caspian Basin (*P. guttatus*, *P. salenskyi* populations, *P. versicolor*, and *P. przewalskii* populations), and together forms a clade with minor support (bootstrap 92%, decay index 2). Species and population relationships in Clade M are unresolved, but monophyly matches the mitochondrial DNA analysis (bootstrap 98%, decay index 4).

Clade L consists of all viviparous species from high elevation Tibet and adjacent low elevation Taklimakan Desert in northwestern China receiving high support (bootstrap 100%, decay index 15) as recovered from the mitochondrial DNA analysis. *P. forsythii* populations receive strong support (bootstrap 100%, decay index 4). Relationships between *P. forsythii* populations as a clade and *P. roborowskii* populations, *P. hongyuanensis*, *P. vlangalii* populations and *P. theobaldi* all collapse with one positional change (decay index 1) and are regarded as not well-supported.

The RAG-1 DNA analysis recovers different phyletic arrangements from the mitochondrial DNA analysis regarding deep-positions of groups and lineages A through M. A dichotomous arrangement appears in the RAG-1 DNA analysis that is not represented in the mitochondrial DNA analysis. Some of these relationships receive considerable support.

Clades A, B, D, C, and G group (bootstrap 53%, decay index 1), with clades A, B, D, and C further containing a subgroup (bootstrap 95%, decay index 6). Clades A and B are grouped (bootstrap 79%, decay index 2), and clades D and C are grouped (bootstrap 93%, decay index 3).

Clades and lineages E, F-1, F-2, J, I, H, M and L group (bootstrap 81%, decay index 3). Clades and lineages E, F-1, F-2, J, I, H, and M group (bootstrap 94%, decay index 7).

The maximum-likelihood analysis of the RAG-1 data set chooses one of the 62 equally parsimonious trees recovered as described above (see Appendix 3). All branches resolved in the maximum-likelihood analysis further

than the parsimony analysis are in Clade M, but no reliability for this arrangement is reasonable provided that the maximum-likelihood analysis just picked one of 62 parsimony trees of equal length.

3). Allozyme Allele Presence/Absence Coded Analysis—Parsimony analysis of the 25 allozyme loci (Table 1), applying the 213 alleles discovered as presence/absence characters is presented in figure 6. Allele frequency data for the 24 populations and species of *Phrynocephalus* and two outgroups, *L. caucasia* and *T. sanguinolentus*, are presented in table 2. Of the 213 allelic characters, 104 were variable parsimony uninformative, with 107 parsimony informative characters. Parsimony analysis of the total data set produces six equally parsimonious trees of 381 steps in length, with the strict consensus of these trees presented in figure 6.

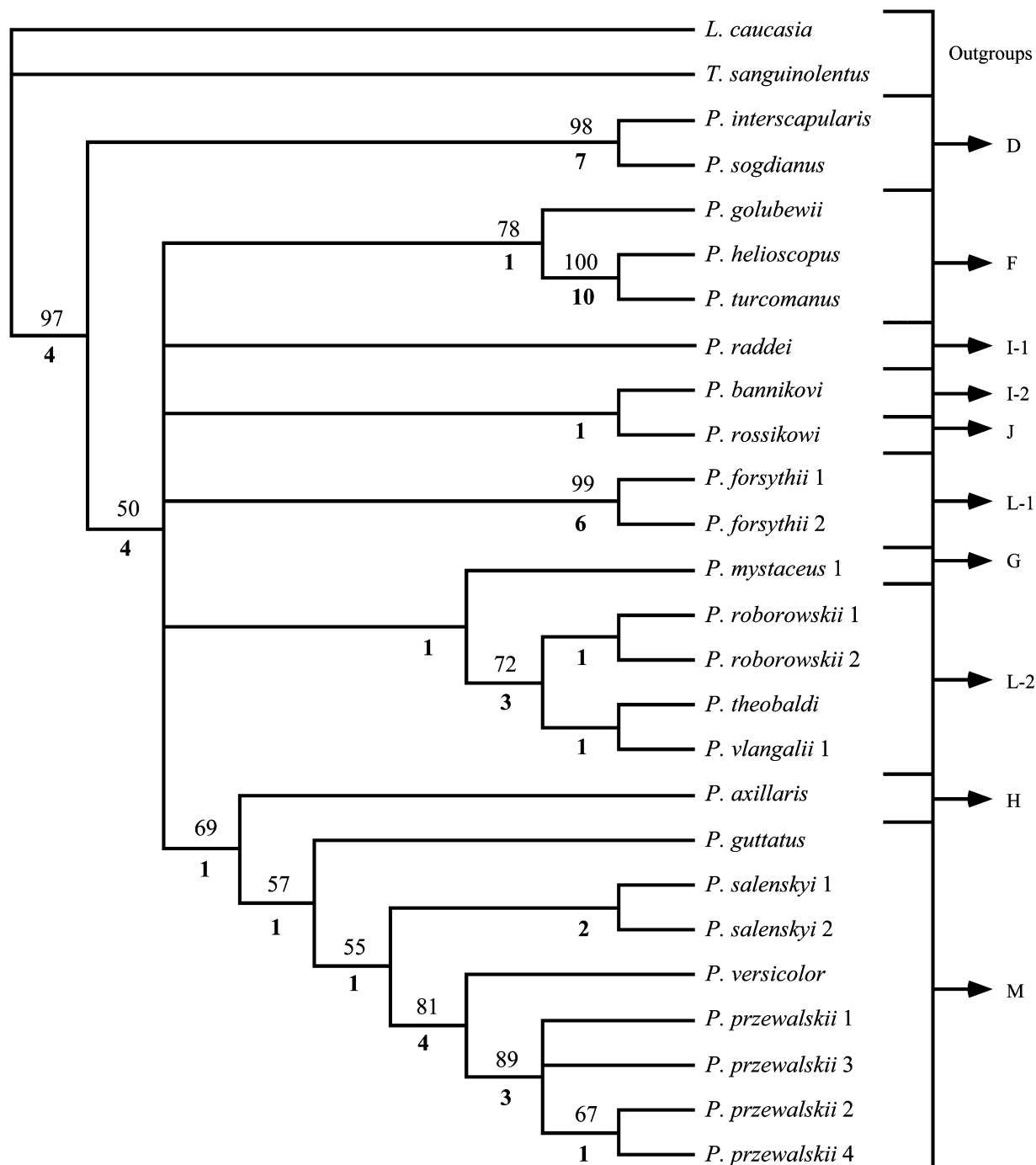


FIGURE 6. Strict consensus of six equally parsimonious trees of 381 steps from the 213 (107 informative) allozyme alleles, coded as presence/absence. Bootstrap values are presented above branches and decay indices are presented below branches in bold. Outgroups (*Laudakia*, and *Trapelus*), and well-supported *Phrynocephalus* clades and lineages discovered in the mitochondrial DNA analysis are identified to the right as D–M where sampling overlaps (clades that are broken are numbered as in Fig. 5).

The genus *Phrynocephalus* is monophyletic receiving strong support (bootstrap 97%, decay index 4).

Clade D consisting of *P. interscapularis* and *P. sogdianus* is strongly supported (bootstrap 98%, decay index 7), and placed in a sister position to all remaining *Phrynocephalus* species (clades and lineages F, I-1, I-2, J, L-1, G, L-2, H and M) with weak support (bootstrap 50%, decay index 4).

Clade F consists of *P. golubewii*, *P. helioscopus*, and *P. turcomanus* (bootstrap 78%, decay index 1) which matches the mitochondrial DNA analysis, but conflicts with the nuclear RAG-1 DNA analysis due to a series of weak 1 step decay indices.

Unlike both the mitochondrial DNA and nuclear RAG-1 DNA analyses, Clade I does not appear monophyletic. *P. raddei* (Lineage I-1) is part of a polytomy with *P. bannikovi* (Lineage I-2) in a sister position to *P. rossikowi* (Lineage J) with a decay index of 1.

Clade L consisting of viviparous species does not appear monophyletic. The two populations of *P. forsythii* from the low elevation Taklimakan Desert of northwestern China appear monophyletic (bootstrap 99%, decay index 6; Clade L-1) and is part of a polytomy. *P. mystaceus* population 1 from the Caspian Basin (Clade G) groups with Tibetan taxa (*P. roborowskii* populations, *P. theobaldi*, and *P. vlangalii* population 1; Clade L-2) with a decay index of 1. The viviparous Tibetan taxa (Clade L-2) are monophyletic (bootstrap 72%, decay index 3). Within Tibetan taxa (Clade L-2) the two populations of *P. roborowskii* appear monophyletic (decay index 1), and *P. theobaldi* is sister to *P. vlangalii* population 1 (decay index 1), being consistent with the RAG-1 DNA analysis and not in conflict with the mitochondrial DNA analysis.

Lineage H, consisting of *P. axillaris* from the low elevation Taklimakan Desert of northwestern China, groups with low elevation species from northern China and the northern Caspian Basin (*P. guttatus*, *P. salenskyi* populations, *P. versicolor*, and *P. przewalskii* populations; Clade M) with weak support (bootstrap 69%, decay index 1). This topology is consistent with the RAG-1 DNA analysis, but in conflict with the mitochondrial DNA analysis. Clade M described above appears monophyletic (bootstrap 57%, decay index 1). Within Clade M, *P. guttatus* appears sister to a clade containing *P. salenskyi* populations, *P. versicolor*, and *P. przewalskii* populations (bootstrap 55%, decay index 1). *P. salenskyi* populations appear monophyletic (decay index 2) and are sister to the grouping of *P. versicolor* and *P. przewalskii* populations receiving good support (bootstrap 81%, decay index 4). Monophyly of *P. przewalskii* populations is supported by a bootstrap of 89% and decay index of 3; among the four *P. przewalskii* populations only populations 2 and 4 group (bootstrap 67%, decay index 1). All relationships within Clade M in the nuclear RAG-1 DNA analysis are unresolved; for comparison purposes refer to the mitochondrial DNA analysis (Fig. 4). Clades F, I-1, I-2+J, L-1, G+L-2, H+M all form a polytomy, which is unresolved.

4). Allozyme Locus Coded Step Matrix Analysis—An alternative method of coding allozyme data for parsimony analysis is the utilization of step matrices to examine gains and losses of alleles while preserving the locus as the character. Parsimony analysis of the 25 allozyme loci sampled, containing 213 alleles, applying step matrices for each individual locus are presented in appendix 2. All 25 locus characters are parsimony informative. Parsimony analysis of the total data set produces 18 equally parsimonious trees of 408 steps in length. The strict consensus of these trees is presented in figure 7. Sampling of allozyme data is the same as described above.

The genus *Phrynocephalus* is monophyletic receiving good support (bootstrap 79%, decay index 3).

The clade containing *P. bannikovi*, *P. rossikowi*, *P. raddei*, *P. golubewii*, *P. helioscopus*, and *P. turcomanus* (decay index 1) is not fully resolved in the allele presence/absence analysis. Within this clade, *P. bannikovi* (Lineage I-2) and *P. rossikowi* (Lineage J) group (decay index 1) matching the allele presence/absence analysis, and is sister to a clade containing *P. raddei* (Lineage I-1) with *P. golubewii*, *P. helioscopus*, and *P. turcomanus* from Clade F (decay index 1). Clade F, containing *P. golubewii*, *P. helioscopus*, and *P. turcomanus*, is monophyletic (bootstrap 75%, decay index 2), including the strongly supported grouping of *P. helioscopus* and *P. turcomanus* (bootstrap 98%, decay index 8), all consistent with the allele presence/absence analysis.

An additional clade that matches the allele presence/absence analysis contains *P. mystaceus* population 1 (Clade G) and Tibetan Plateau taxa (Clade L-2) *P. theobaldi*, *P. vlangalii* population 1 and *P. roborowskii* populations (decay index 2). Tibetan Plateau taxa (Clade L-2) *P. theobaldi*, *P. vlangalii* population 1 and *P. roborowskii* populations are monophyletic (bootstrap 73%, decay index 3), also matching the allele presence/absence analysis. Within Tibetan Plateau taxa, *P. theobaldi* is basal to the grouping of *P. vlangalii* population 1 and *P. roborowskii* populations (decay index 1), which differs from the allele presence/absence analysis. *P. roborowskii* populations group (bootstrap 54%, decay index 1), which is consistent with previous analyses considering taxon sampling.

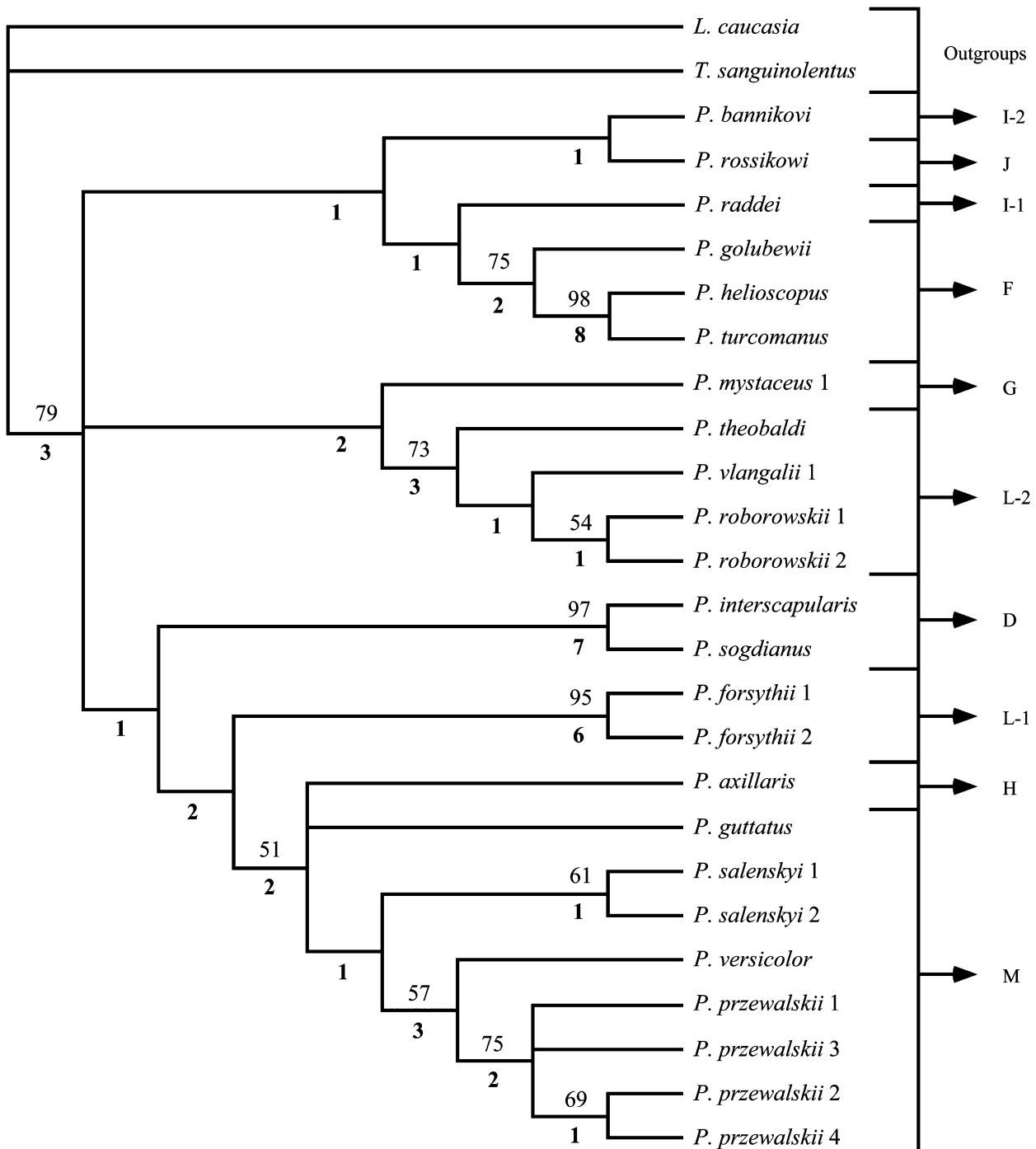


FIGURE 7. Strict consensus of 18 equally parsimonious trees of 408 steps from the 25 (all informative) allozyme loci, coded using allele combinations and analyzed with step matrices. Bootstrap values are presented above branches and decay indices are presented below branches in bold. Outgroups (*Laudakia*, and *Trapelus*), and well-supported *Phrynocephalus* clades and lineages discovered in the mitochondrial DNA analysis are identified to the right as D–M where sampling overlaps (clades that are broken are numbered as in Figs. 5 and 6).

A clade that does not match the allele presence/absence analysis contains *P. interscapularis*, *P. sogdianus* (Clade D), *P. forsythii* populations (Clade L-1), *P. axillaris* (Lineage H), *P. guttatus*, *P. salenskyi* populations, *P. versicolor*, and *P. przewalskii* populations (Clade M), which group with a decay index of 1. Consistent with the allele presence/absence analysis are the following groups: The monophyly of *P. interscapularis* and *P. sogdianus* (bootstrap 97%, decay index 7; Clade D); monophyly of *P. forsythii* populations (bootstrap 95%, decay index 6; Clade L-1); and monophyly of *P. axillaris* (Lineage H) with low elevation species from northern China and the

northern Caspian Basin (*P. guttatus*, *P. salenskyi* populations, *P. versicolor*, and *P. przewalskii* populations; Clade M) receiving a bootstrap value of 51% and a decay index of 2. This arrangement (Lineage H + Clade M) grouping with *P. forsythii* populations (Clade L-1) has a decay index of 2 and is not in conflict with the allele presence/absence analysis. The relationships between *P. axillaris* (Lineage H), *P. guttatus*, and the grouping of all other taxa in Clade M (*P. salenskyi* populations, *P. versicolor*, and *P. przewalskii* populations) are unresolved, with recognition of monophyly in the latter taxa among Clade M (decay index 1). Consistent with the allele presence/absence analysis is monophyly of *P. salenskyi* populations (bootstrap 61%, decay index 1), monophyly of *P. versicolor* and *P. przewalskii* populations (bootstrap 57%, decay index 3), monophyly of *P. przewalskii* populations (bootstrap 75%, decay index 2), and monophyly of *P. przewalskii* populations 2 and 4 (bootstrap 69%, decay index 1).

An unresolved trichotomy exists between the following three clades: (1) lineages and clades I-2, J, I-1, and F; (2) lineages and clades G and L-2; and (3) lineages and clades D, L-1, H, and M.

5). Combined Data Analysis—Results from a combined analysis of mitochondrial DNA data, nuclear RAG-1 DNA data, and allele presence/absence coding of allozyme alleles, produces an overall phylogenetic estimate of relationships based on the three different data sets presented in this study. Of the 4743 characters 166 sites are excluded. Of the 4568 included characters, 495 are variable parsimony uninformative, and 1288 are parsimony informative characters. Parsimony analysis of the total data set produces 3 equally parsimonious trees of 5683 steps in length. The strict consensus of these trees is presented in figure 8.

Consistent with all analyses: The genus *Phrynocephalus* is monophyletic receiving high support (bootstrap 100%, decay index 85). Within the outgroups, monophyly of *Bufoniceps laungwalaensis* and *Trapelus* species is well supported with a bootstrap of 100% and a decay index of 103 (as previously reported by Macey *et al.* 2006), with monophyly of both *Trapelus* species receiving support of a bootstrap of 100% and a decay index of 21.

The 13 clades and lineages identified in the mitochondrial DNA analysis within the genus *Phrynocephalus* are all recovered in the combined analysis and labeled A through M in figure 8. Beyond the four outgroups listed above, sampling consists of 42 *Phrynocephalus* species and populations, of which 29 are species, with 13 additional populations for multiple sampling within species.

Clade A consists of *P. scutellatus* populations from the southern and eastern Iranian Plateau inhabiting gravel areas (bootstrap of 100%, decay index 49), as discovered in both the mitochondrial DNA and nuclear RAG-1 DNA analyses and not sampled in the allozyme data set.

Clade B consists of *P. arabicus* populations, *P. longicaudatus*, and *P. maculatus* populations, which are from the Arabian Peninsula and the Iranian Plateau, receiving high support (bootstrap 100%, decay index 46). The Arabian subgroup consists of *P. arabicus* populations and *P. longicaudatus* forming a well-supported clade (bootstrap 100%, decay index 30). *P. arabicus* population 1 from the Saudi Arabian Empty Quarter and *P. arabicus* population 2 from Oman are monophyletic with high support (bootstrap 99%, decay index 14). The second subgroup contains the two populations of *P. maculatus* from the Iranian Plateau, which additionally receives high support (bootstrap 100%, decay index 46). All of these relationships are consistent with both the mitochondrial DNA and nuclear RAG-1 DNA analyses, and not sampled in the allozyme data set. In addition, clades A and B are grouped with little support (decay index 2), which is consistent with the nuclear RAG-1 DNA analysis, but in conflict with the mitochondrial DNA analysis, and not sampled in the allozyme data set.

Clade C contains *P. clarkorum*, *P. ornatus*, and *P. luteoguttatus* populations from the Helmand Basin in Afghanistan and adjacent Pakistani Baluchistan, receiving high support (bootstrap 100%, decay index 30). Within this clade two well-supported groups appear, *P. clarkorum* and *P. ornatus* (bootstrap 99%, decay index 19), and the two *P. luteoguttatus* populations (bootstrap 100%, decay index 84). All of these relationships are consistent with both the mitochondrial DNA and nuclear RAG-1 DNA analyses, and not sampled in the allozyme data set.

Clade D consists of *P. interscapularis*, *P. sogdianus*, and *P. vindumi* (bootstrap 99%, decay index 19) with *P. vindumi* from the northeastern Iranian Plateau sister to *P. interscapularis* and *P. sogdianus* from the Caspian Basin with support of a bootstrap of 100% and a decay index of 95. Clades C and D are small species that live in sandy substrates and receive support as a clade (bootstrap 84%, decay index 6). All of these relationships are consistent with the mitochondrial DNA, nuclear RAG-1 DNA, and allele presence/absence allozyme analyses considering sampling.

Lineage E is a single taxon *P. persicus* from the northwestern Iranian Plateau, and groups with Clade F (bootstrap 74%, decay index 5). Clade F consists of *P. golubewii*, *P. helioscopus*, and *P. turcomanus* receiving

reasonably high support (bootstrap 87%, decay index 7), with *P. golubewii* from the southern Caspian Basin, sister to a well-supported clade containing *P. helioscopus* from the northern Caspian Basin and *P. turcomanus* from the southern Caspian Basin (bootstrap 100%, decay index 53). Note all taxa in Lineage E and Clade F live in gravel habitats except *P. golubewii*, which lives in a single dry lakebed in Turkmenistan. All of these relationships are consistent with the mitochondrial DNA, allele presence/absence allozyme, locus step matrix allozyme analyses, and in conflict with the nuclear RAG-1 DNA analysis considering sampling.

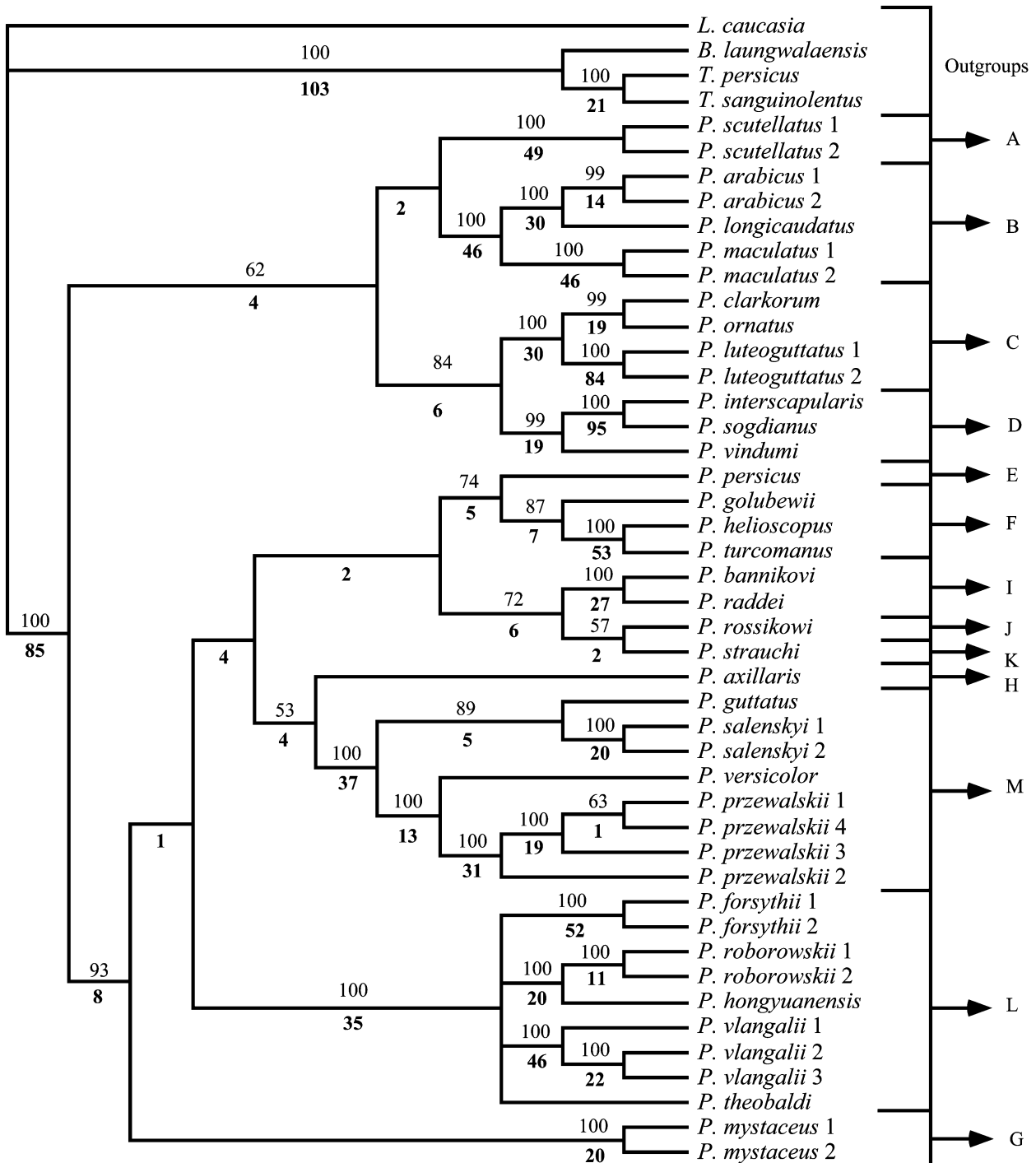


FIGURE 8. Strict consensus of three equally parsimonious trees of 5683 steps from the combined data with 4568 included (1288 informative) characters. These data consist of aligned mitochondrial DNA and nuclear RAG-1 DNA positions, as well as allozyme alleles coded as presence/absence characters. Bootstrap values are presented above branches and decay indices are presented below branches in bold. Outgroups (*Laudakia*, *Bufoniceps*, and *Trapelus*), and well-supported *Phrynocephalus* clades and lineages discovered in the mitochondrial DNA analysis are identified to the right as A–M.

Clade I consists of *P. bannikovi* and *P. raddei* receiving high support (bootstrap 100%, decay index 27). Lineage J is *P. rossikowi* and lineage K is *P. strauchi*, which group with low support (bootstrap 57%, decay index 2). Clades and lineages I, J, and K are relatively small species that inhabit gravel habitats all in the southern Caspian Basin, which form a moderately supported clade (bootstrap 72%, decay index 6). All of these relationships are consistent with the mitochondrial DNA analysis, and monophyly of Clade I is recovered in the nuclear RAG-1 DNA analysis, with alternative arrangements in the allozyme analyses; see figures 5–7 for conflicts.

Clades and lineages E, F, I, J, and K all group together but receive no bootstrap support and only a decay index of 2. Considering sampling, this arrangement does not conflict with all of the nuclear data set analyses (nuclear RAG-1 DNA, allele presence/absence allozyme, and locus step matrix allozyme analyses), but is not present in the mitochondrial DNA analysis.

Lineage H consists of *P. axillaris* from the low elevation Taklimakan Desert in northwestern China which appears as the sister taxon to all species in Clade M from the northern Chinese deserts and the northern Caspian Basin (*P. guttatus*, *P. salenskyi* populations, *P. versicolor*, and *P. przewalskii* populations), and together forms a clade with minor support (bootstrap 53%, decay index 4). This arrangement is consistent with the nuclear data set analyses (nuclear RAG-1 DNA, allele presence/absence allozyme, and locus step matrix allozyme analyses), but is not present in the mitochondrial DNA analysis.

Clade M consists of low elevation northern species in China, Kazakhstan and Russia: *P. guttatus*, two *P. salenskyi* populations, *P. versicolor*, and four *P. przewalskii* populations (bootstrap 100%, decay index 37). *P. guttatus* from the European side of the Caspian Sea, and *P. salenskyi* populations from the Junggar Depression of China and Zaysan Depression in adjacent Kazakhstan form a monophyletic group with moderate support (bootstrap 89%, decay index 5). *P. guttatus* is sister to *P. salenskyi* populations with high support (bootstrap 100%, decay index 20). The sister clade to that group contains the Gobi Desert samples from *P. versicolor* and four *P. przewalskii* populations (bootstrap 100%, decay index 13), with monophyly of all *P. przewalskii* populations receiving high support (bootstrap 100%, decay index 31). *P. przewalskii* population 2 from the south shore of the Yellow River across from Shapotou Ningxia Autonomous Region in China is sister to the clade containing populations 1, 3, and 4 with high support (bootstrap 100%, decay index 19). Population 3 from the north shore of the Yellow River in Shapotou Ningxia Autonomous Region China is sister to the clade containing population 1 from Wujiachuan Gansu Province China, and population 4 from Wuwei Gansu Province China, though by a slim margin indicated by the decay index of 1 (bootstrap 63%, decay index 1). Relationships among samples in Clade M are unresolved in the nuclear RAG-1 DNA analysis. Species relationships are consistent with the mitochondrial DNA analysis but there is a conflict in the arrangement of *P. przewalskii* populations 1, 3, and 4. Allozyme data analyses are consistent with monophyly of *P. salenskyi* populations and monophyly of *P. versicolor* with *P. przewalskii* populations.

Clade L is a viviparous group from high elevation Tibet and the adjacent low elevation Taklimakan Desert in northwestern China, containing *P. forsythii* populations, *P. roborowskii* populations, *P. hongyuanensis*, *P. vlangalii* populations and *P. theobaldi* (bootstrap 100%, decay index 35). The low elevation Taklimakan Desert *P. forsythii* populations group with high support (bootstrap 100%, decay index 52). *P. roborowskii* populations from the Chaka Basin and Qaidam Depression on the western side of the northeastern Tibetan Plateau, and *P. hongyuanensis* from the far eastern side of the northeastern Tibetan Plateau in Sichuan Province China group with high support (bootstrap 100%, decay index 20). The two *P. roborowskii* populations form a well-supported clade (bootstrap 100%, decay index 11). All *P. vlangalii* populations in the vicinity of Qinghai Lake in a central region of the northeastern Tibetan Plateau appear monophyletic (bootstrap 100%, decay index 46) with population 1 (more western, Heimaha) being sister to population 2 (more eastern, east side of Qinghai Lake) and population 3 (more southern, Maqên), (bootstrap 100%, decay index 22). Relationships between *P. theobaldi* from southern Tibet, and the other viviparous groups described from northern Tibet and adjacent low elevation Taklimakan Desert are unresolved. All relationships in the combined analysis are recovered for this clade in the mitochondrial DNA analysis, with weakly supported conflicting arrangements recovered in the nuclear RAG-1 DNA and allozyme analyses (see Figs. 5–7 for alternative sample placements among Clade L).

Clade G consists of *P. mystaceus* populations north and south of the Kopet-Dagh (mountains) from the Caspian Basin and the northeastern Iranian Plateau living in large sand dunes (bootstrap 100%, decay index 20), as discovered in both the mitochondrial DNA and nuclear RAG-1 DNA analyses, and not fully sampled in the allozyme data set.

The grouping of clades A+B with clades C+D is supported by a bootstrap of 62% and a decay index of 4; this is only consistent with the nuclear RAG-1 DNA analysis. While weakly supported this forms one of the lineages of *Phrynocephalus* species in a dichotomy of taxa restricted to Southwest Asia and the Arabian Peninsula, except for *P. interscapularis* and *P. sogdianus* from the Caspian Basin.

The other side of the *Phrynocephalus* dichotomy discovered in the combined analysis consists of clades and lineages E/F, I-K, H/M, L and G, which receive considerable support (bootstrap 93%, decay index 8). Clade G (*P. mystaceus* populations) is sister to the remaining taxa in this section of the dichotomy (clades and lineages E/F, I-K, and H/M) with only a decay index of 1 reflecting the floating position of *P. mystaceus*; this clearly is a unique placement among analyses. Clade L (viviparous taxa from the Tibetan Plateau and adjacent Taklimakan Desert) is sister to the grouping of clades and lineages E/F, I-K, and H/M with weak support (decay index 4). The overall structure of relationships between E/F, I-K, and H/M is largely consistent with the nuclear RAG-1 DNA analysis (Fig. 5) except for the breaking of Clade F into Clade F-1 and Lineage F-2; see figures 4, 6, and 7 for alternative arrangements.

B. Estimated Dates based on Pairwise Sequence Divergence of Mitochondrial DNA Compared to Geologic Events

Presented below are estimated dates from uncorrected pairwise sequence divergence of mitochondrial DNA data with an applied pairwise divergence rate of 1.3% per million years (Macey *et al.* 1998a; see Materials and Methods). *Phrynocephalus* cladogenesis crosses a series of well-established geologic events with dates derived from nucleotide substitutional data compared to geologic dates from the literature as presented in table 4.

P. guttatus and *P. salenskyi* populations are separated from *P. versicolor* and *P. przewalskii* populations by the eastern Tien Shan (mountains), which has an estimated geologic uplift time of 5 MYBP (Smit *et al.* 2013). These taxa show an average pairwise sequence divergence of 7.81%, and applying a pairwise rate of 1.3% divergence per million years, these taxa are estimated to have diverged around 6.0 MYBP, which is slightly older than the geologic estimate.

P. bannikovii is separated from *P. raddei* by the late Miocene drying of the Paratethys Sea, which is estimated to have taken place 5.5–6 MYBP (Steininger & Rogl 1984). These taxa show a pairwise sequence divergence of 8.60%, and applying a pairwise rate of 1.3% divergence per million years, these taxa are estimated to have diverged approximately 6.6 MYBP, which is slightly older than the geologic estimate.

P. golubewii is separated from *P. helioscopus* and *P. turcomanus* by the late Miocene drying of the Paratethys Sea, which took place 5.5–6 MYBP (Steininger & Rogl 1984). These taxa show an average pairwise sequence divergence of 11.60%, and applying a pairwise rate of 1.3% divergence per million years, these taxa are estimated to have diverged 8.9 MYBP, which is significantly older than the geologic estimate.

P. helioscopus is separated from *P. turcomanus* by the Pliocene inundation of the Caspian Basin, which took place 3–3.5 MYBP (Steininger & Rogl 1984). These taxa show a pairwise sequence divergence of 4.45%, and applying a pairwise rate of 1.3% divergence per million years, these taxa are estimated to have diverged approximately 3.4 MYBP, which is in the expected range of divergence.

P. mystaceus populations 1 and 2 from the Caspian Basin and northeastern Iranian Plateau are separated by the Kopet-Dagh (mountains), which has an estimated geologic uplift time of 5 MYBP (Smit *et al.* 2013). These populations show a pairwise sequence divergence of 6.77%, and applying a pairwise rate of 1.3% divergence per million years, these populations are estimated to have diverged 5.2 MYBP, which is slightly older than the geologic estimate.

P. interscapularis and *P. sogdianus* from the Caspian Basin are separated from *P. vindumi* of the northeastern Iranian Plateau by the Kopet-Dagh (mountains), which has an estimated geologic uplift time of 5 MYBP (Smit *et al.* 2013). These taxa show an average pairwise sequence divergence of 15.63%, and applying a pairwise rate of 1.3% divergence per million years, these taxa are estimated to have diverged 12.0 MYBP, which is significantly older than the geologic estimate.

P. scutellatus populations 1 and 2 are separated by the north-south Iranian Plateau compression, which took place 5–10 MYBP (Mouthereau *et al.* 2012; Smit *et al.* 2013). These populations show a pairwise sequence divergence of 10.43%, and applying a pairwise rate of 1.3% divergence per million years, these populations are estimated to have diverged 8.0 MYBP, which is within the expected range.

P. arabicus and *P. longicaudatus* are separated from *P. maculatus* by the Zagros Mountains experiencing rapid uplift from 5–10 MYBP (Mouthereau *et al.* 2012). These populations show an average pairwise sequence divergence of 11.28%, and applying a pairwise rate of 1.3% divergence per million years, these taxa are estimated to have diverged 8.7 MYBP, which is within the expected range.

All comparisons in Tibet are between northern Tibetan species and populations, and a single southern Tibetan taxa sampled, *P. theobaldi*. There are three comparisons across the Tibetan Plateau that include all Tibetan Plateau taxa because of a polytomy (listed as Tibet comparisons 1–3); the placement of *P. forsythii* with other viviparous *Phrynocephalus* from the Tibetan Plateau has an ambiguous phylogenetic placement of either in a sister position to all Tibetan samples, or nested within Tibetan samples (Figs. 4, 5, 8). If *P. forsythii* were sister to all Tibetan species sampled, it would not affect any of the comparisons described. If it is nested within Tibetan Plateau samples, it would possibly be left out of an average reported in the three comparisons, and would not significantly change the data reported. It is highly unlikely that *P. forsythii*, distributed in the Taklimakan Desert north of the Tibetan Plateau is the sister taxon to *P. theobaldi*, distributed in southern Tibet.

a). Tibet Comparison 1—*P. roborowskii* populations and *P. hongyuanensis* are separated from *P. theobaldi* north-south across Tibet, which experienced a period of rapid uplift 5 MYBP (Shackleton & Chang 1988). These taxa show an average pairwise sequence divergence of 7.64%, and applying a pairwise rate of 1.3% divergence per million years, these taxa are estimated to have diverged 5.9 MYBP, which is slightly older than the geologic estimate (Tibet Comparison 1, Table 4).

b). Tibet Comparison 2—*P. vlangalii* populations 1–3 are separated from *P. theobaldi* north-south across Tibet, which experienced a period of rapid uplift 5 MYBP (Shackleton & Chang 1988). These taxa show an average pairwise sequence divergence of 10.60%, and applying a pairwise rate of 1.3% divergence per million years, these taxa are estimated to have diverged 8.2 MYBP, which is significantly older than expected, but within the range of geologic activity (Tibet Comparison 2, Table 4).

c). Tibet Comparison 3—*P. roborowskii* populations, *P. hongyuanensis*, and *P. vlangalii* populations 1–3 are separated from *P. theobaldi* north-south across Tibet, which experienced a period of rapid uplift 5 MYBP (Shackleton & Chang 1988). These taxa show an average pairwise divergence of 9.12%, and applying a pairwise rate of 1.3% divergence per million years, these taxa are estimated to have diverged 7.0 MYBP, which is significantly older than expected, but within the range of geologic activity (Tibet Comparison 3, Table 4).

C. Statistical Evaluation of Taxon Placement with Mitochondrial DNA and Combined Data

Phylogenetic results suggest a southern root for the genus *Phrynocephalus*. To test the alternative hypothesis of a basal position for northern taxa, the Wilcoxon signed-ranks test (Felsenstein 1985; Templeton 1983) is applied (Table 3). There are two clades of *Phrynocephalus* restricted to northern regions: The northern lowland clade, restricted to low elevation deserts in China and the northern Caspian Basin consisting of *P. guttatus*, *P. salenskyi* populations, *P. versicolor*, and *P. przewalskii* populations (Clade M, Figs. 4 and 8), and viviparous/Tibetan clade which includes taxa from the high elevation Tibetan Plateau and adjacent low elevation Taklimakan Desert consisting of *P. forsythii* populations, *P. roborowskii* populations, *P. hongyuanensis*, *P. vlangalii* populations, and *P. theobaldi* (Clade L, Figs. 4 and 8). The northern lowland clade in the parsimony analysis of mitochondrial DNA data corresponds to Clade M in figure 4, whereas in the combined analysis (Fig. 8) it corresponds to Clade M and may additionally include *P. axillaris* of Lineage H; the viviparous/Tibetan clade corresponds to Clade L in figures 4 and 8. All constrained analyses produce a single most parsimonious tree, and are compared with the three most parsimonious trees overall either from the mitochondrial DNA (mt-DNA) analysis or the combined data analysis as presented in figures 4 and 8 respectively. Combined data throughout refers to the mitochondrial DNA data, nuclear RAG-1 data, and allele presence/absence coding of allozyme data as a single data set. See table 3 for statistical information and appendix 3 for tree topologies used in all tests.

1). Test of a basal position for northern lowland taxa (Clade M) applying mt-DNA data among Phrynocephalus—The strict consensus of the three most parsimonious trees from analysis of the mt-DNA data places the northern lowland clade as nested within the genus *Phrynocephalus*. When the three shortest trees overall (A1–3 in Appendix 4) showing a nested position for the northern lowland clade are compared to the alternative single most parsimonious tree constraining the northern lowland clade as basal, the alternative (C1 in Appendix 4)

is rejected in favor of the overall shortest trees by either the one-tailed or the two-tailed test (test 1 in Table 3). **This result suggests that the mt-DNA data does not support a basal position for the northern lowland clade among *Phrynocephalus*.**

TABLE 3. Wilcoxon signed-ranks tests for basal placement of northern taxa. Overall shortest trees are A1-3 for mitochondrial DNA (mt-DNA) and B1-3 for combined data (Comb). All shortest alternative trees (Alt) found using constraint trees are one per comparison (C1-J1). See appendix 4 for all trees used and Materials and Methods for definitions of clades with ax representing *P. axillaris* below.

	N ¹	Z ²	P ³
1a). A1 mt-DNA vs C1 Lowland Alt	77	1.9373	<0.026**
1b). A2 mt-DNA vs C1 Lowland Alt	73	1.9897	<0.023**
1c). A3 mt-DNA vs C1 Lowland Alt	88	1.7821	<0.037*
2a). A1 mt-DNA vs D1 Viviparous/Tibet Alt	66	2.2156	<0.013**
2b). A2 mt-DNA vs D1 Viviparous/Tibet Alt	52	2.4962	<0.006**
2c). A3 mt-DNA vs D1 Viviparous/Tibet Alt	97	1.8	<0.036*
3a). A1 mt-DNA vs E1 Lowland & V/Tibet Alt	44	1.8091	<0.035*
3b). A2 mt-DNA vs E1 Lowland & V/Tibet Alt	54	1.633	<0.051
3c). A3 mt-DNA vs E1 Lowland & V/Tibet Alt	97	1.2	<0.115
4a). B1 Comb vs F1 Lowland no ax Alt	107	2.3650	<0.009**
4b). B2 Comb vs F1 Lowland no ax Alt	124	2.2906	<0.011**
4c). B3 Comb vs F1 Lowland no ax Alt	125	2.3160	<0.010**
5a). B1 Comb vs G1 Lowland w/ax Alt	89	2.6930	<0.004**
5b). B2 Comb vs G1 Lowland w/ax Alt	109	2.4602	<0.007**
5c). B3 Comb vs G1 Lowland w/ax Alt	73	2.9352	<0.002**
6a). B1 Comb vs H1 Viviparous/Tibet Alt	81	2.1111	<0.017**
6b). B2 Comb vs H1 Viviparous/Tibet Alt	59	2.4736	<0.007**
6c). B3 Comb vs H1 Viviparous/Tibet Alt	97	1.9292	<0.027*
7a). B1 Comb vs I1 Lowland no ax & V/Tibet Alt	120	2.2075	<0.014**
7b). B2 Comb vs I1 Lowland no ax & V/Tibet Alt	132	2.1388	<0.016**
7c). B3 Comb vs I1 Lowland no ax & V/Tibet Alt	120	2.2075	<0.014**
8a). B1 Comb vs J1 Lowland w/ax & V/Tibet Alt	89	3.1767	<0.001**
8b). B2 Comb vs J1 Lowland w/ax & V/Tibet Alt	115	2.8158	<0.002**
8c). B3 Comb vs J1 Lowland w/ax & V/Tibet Alt	71	3.5269	<0.001**

¹N = number of characters that differ in minimum number of evolutionary steps between compared trees.

²Z = normal approximation from Wilcoxon signed-ranks tests.

³P = Probabilities are presented as one-tailed. Two-tailed values are double. One asterisk indicates significance with the one-tailed test, while two asterisks indicates significance with the two-tailed test.

2). Test of a basal position for viviparous/Tibetan taxa (Clade L) applying mt-DNA data among *Phrynocephalus*—The strict consensus of the three most parsimonious trees from analysis of the mt-DNA data places the viviparous/Tibetan clade as nested within the genus *Phrynocephalus*. When the three shortest trees overall (A1–3 in Appendix 4) showing a nested position for the viviparous/Tibetan clade are compared to the alternative single most parsimonious tree constraining the viviparous/Tibetan clade as basal, the alternative (D1 in Appendix 4) is rejected in favor of the overall shortest trees by either the one-tailed or the two-tailed test (test 2 in Table 3). **This result suggests that the mt-DNA data does not support a basal position for the viviparous/Tibetan clade among *Phrynocephalus*.**

3). Test of a basal position for northern lowland and viviparous/Tibetan taxa (clades L and M) applying mt-DNA data among *Phrynocephalus*—The strict consensus of the three most parsimonious trees from analysis of the mt-DNA data places the northern lowland and viviparous/Tibetan clades as nested within the genus

Phrynocephalus. When the three shortest trees overall (A1–3 in Appendix 4) showing a nested position for the northern lowland and viviparous/Tibetan clades are compared to the alternative single most parsimonious tree constraining the northern lowland and viviparous/Tibetan clades as basal, the alternative (E1 in Appendix 4) is either rejected or close to significant with the one-tailed test (test 3 in Table 3). **This test is inconclusive, but leans towards rejecting a basal position for the northern lowland and viviparous/Tibetan clades together among *Phrynocephalus*.**

4). Test of a basal position for northern lowland taxa not including *P. axillaris* (Clade M) applying the combined data among *Phrynocephalus*—The strict consensus of the three most parsimonious trees from analysis of the combined data places the northern lowland clade as nested within the genus *Phrynocephalus*. When the three shortest trees overall (B1–3 in Appendix 4) showing a nested position for the northern lowland clade are compared to the alternative single most parsimonious tree constraining the northern lowland clade as basal, the alternative (F1 in Appendix 4) is rejected in favor of the overall shortest trees by the two-tailed test (test 4 in Table 3). **This result suggests that the combined data does not support a basal position for the northern lowland clade among *Phrynocephalus*.**

5). Test of a basal position for northern lowland taxa including *P. axillaris* (clades H and M) applying the combined data among *Phrynocephalus*—The strict consensus of the three most parsimonious trees from analysis of the combined data places the northern lowland clade including *P. axillaris* as nested within the genus *Phrynocephalus*. When the three shortest trees overall (B1–3 in Appendix 4) showing a nested position for the northern lowland clade including *P. axillaris* are compared to the alternative single most parsimonious tree constraining the northern lowland clade as basal, the alternative (G1 in Appendix 4) is rejected in favor of the overall shortest trees by the two-tailed test (test 5 in Table 3). **This result suggests that the combined data does not support a basal position for the northern lowland clade including *P. axillaris* among *Phrynocephalus*.**

6). Test of a basal position for viviparous/Tibetan taxa (Clade L) applying the combined data among *Phrynocephalus*—The strict consensus of the three most parsimonious trees from analysis of the combined data places the viviparous/Tibetan clade as nested within the genus *Phrynocephalus*. When the three shortest trees overall (B1–3 in Appendix 4) showing a nested position for the viviparous/Tibetan clade are compared to the alternative single most parsimonious tree constraining the viviparous/Tibetan clade as basal, the alternative (H1 in Appendix 4) is rejected in favor of the overall shortest trees by either the one-tailed test or the two-tailed test (test 6 in Table 3). **This result suggests that the combined data does not support a basal position for the viviparous/Tibetan among *Phrynocephalus*.**

7). Test of a basal position for northern lowland taxa not including *P. axillaris* and viviparous/Tibetan taxa (clades L and M) applying the combined data among *Phrynocephalus*—The strict consensus of the three most parsimonious trees from analysis of the combined data places the northern lowland and viviparous/Tibetan clades as nested within the genus *Phrynocephalus*. When the three shortest trees overall (B1–3 in Appendix 4) showing a nested position for the northern lowland and viviparous/Tibetan clades are compared to the alternative single most parsimonious tree constraining the northern lowland and viviparous/Tibetan clades as basal, the alternative (I1 in Appendix 4) is rejected in favor of the overall shortest trees by the two-tailed test (test 7 in Table 3). **This result suggests that the combined data does not support a basal position for the northern lowland and viviparous/Tibetan clades together among *Phrynocephalus*.**

8). Test of a basal position for northern lowland taxa including *P. axillaris* and viviparous/Tibetan taxa (clades H, L and M) applying the combined data among *Phrynocephalus*—The strict consensus of the three most parsimonious trees from analysis of the combined data places the northern lowland clade including *P. axillaris* and the viviparous/Tibetan clade as nested within the genus *Phrynocephalus*. When the three shortest trees overall (B1–3 in Appendix 4) showing a nested position for the northern lowland clade including *P. axillaris* and the viviparous/Tibetan clade are compared to the alternative single most parsimonious tree constraining the northern lowland clade including *P. axillaris* and the viviparous/Tibetan clade as basal, the alternative (J1 in Appendix 4) is rejected in favor of the overall shortest trees by the two-tailed test (test 8 in Table 3). **This result suggests that the combined data does not support a basal position for the northern lowland clade including *P. axillaris* and the viviparous/Tibetan clade together among *Phrynocephalus*.**

Discussion

A. *Phrynocephalus* Taxonomic Recommendations

Based on phylogenetic analyses, a few taxonomic changes are proposed. The following taxonomic changes are based on the principle of monophyly as well as genetic and geographic differences. In each case, the reason a change is suggested is provided, whether data are genetic, distributional or phylogenetic (ie. non-monophyly).

1). *Phrynocephalus maculatus* Complex as Previously Recognized

Based on complete regional sampling, this study recognizes all previous subspecies of *P. maculatus* as distinct species on the minim-basis of non-monophyly. *Phrynocephalus maculatus* was described from the Iranian Plateau (Anderson 1872) with the type locality of “Awada, Shiraz, Persia”; corrected to “Abadeh [31° 10' N, 52° 37' E; Fars Province, Iran], north of Shiraz” by Blanford (1876). *Phrynocephalus maculatus longicaudatus* was described by Haas (1957), with a type locality of “Doha Dhalum, Saudi Arabia”. The sole known population of *P. maculatus* from Turkmenistan was reported by Bogdanov *et al.* (1974), and subsequently described as a distinct species, *Phrynocephalus golubewii* with the type locality of “vicinity of the Bami rail-road station” [= 7 km N railway station Bamy], (Shenbrot & Semenov 1990). It is recommended to recognize *P. golubewii*, *P. longicaudatus*, and *P. maculatus* as distinct species based on phylogenetic results:

a). While *Phrynocephalus golubewii* (Shenbrot & Semenov 1990) may look like *P. maculatus* living in salt-bed dry lakes, it is directly-related to the clade containing *P. turcomanus* and *P. helioscopus* (mt-DNA, bootstrap 91%, decay index 6; combined data, bootstrap 87%, decay index 7; allozyme presence/absence, bootstrap 78%, decay index 1; allozyme step matrix, bootstrap 75%, decay index 2; non-monophyly in RAG-1); in fact *P. turcomanus* occurs within meters of *P. golubewii* and may overlap in distribution.

b). *Phrynocephalus maculatus* (Anderson 1872) is restricted to salt-bed dry lakes on the Iranian Plateau where its type locality is located, and adjacent Baluchistan Plateau including the base of the Sulaiman Range of southern Pakistan. *P. maculatus* is related, yet outside and sister to a clade containing *P. arabicus* and *P. longicaudatus* (see below) based on both mitochondrial and nuclear RAG-1 DNA evidence (mt-DNA, bootstrap 100%, decay index 32; RAG-1, bootstrap 100%, decay index 13; combined data, bootstrap 100%, decay index 46; all of these taxa were not sampled for allozyme data).

c). *Phrynocephalus longicaudatus* (Haas 1957) **New Status** is restricted to the Arabian Peninsula. It is the sister taxon to *P. arabicus* which is also endemic to the Arabian Plate and supported by mitochondrial and nuclear RAG-1 DNA evidence (mt-DNA, bootstrap 100%, decay index 22; RAG-1, bootstrap 100%, decay index 7; combined data, bootstrap 100%, decay index 30; these taxa were not sampled for allozyme data).

These taxa in any combination do not form a monophyletic group.

2). Small Sand Dune Species of Southwest Asia and Caspian Basin

Phrynocephalus interscapularis interscapularis (Lichtenstien 1856; type locality “Bucharei” = Uzbekistan) and *Phrynocephalus interscapularis sogdianus* (Chernov 1948; type locality “Tadjikistan, vicinity of the Pjandzh village”, approximately 37° 14' N, 69° 05' E) are recognized here as full species *P. interscapularis* and *P. sogdianus* based on allozyme and DNA differences. The mt-DNA pair-wise uncorrected sequence distance between *P. interscapularis* and *P. sogdianus* is 3.2% and these taxa show one fixed allozyme difference at the carboxylic ester hydrolase locus (EST; Table 2).

Phrynocephalus ornatus vindumi [Golubev, 1998; type locality “Iran, Khorasan Prov., 35 km. N of Gonabad on road to Torbat-E. Heydariyeh (ca. 34° 49' N, 58° 47' E), 850 m. elevation”; sampling here within ten kilometers of the type locality, see appendix 1] is elevated to species status as *Phrynocephalus vindumi* **New Status**. *Phrynocephalus ornatus* (Boulenger 1887; type locality “between Nushki and Helmand, Baluchistan”) and *P. vindumi* appear in a non-monophyletic arrangement as *P. vindumi* occurring on the northeastern portion of the Iranian Plateau is separated from *P. ornatus* that occurs south of the Hindu Kush in Afghanistan and southwestern Pakistan. In fact, *P. vindumi* is related to small sand dune species in the Caspian Basin to the north: *P. interscapularis* and *P. sogdianus*. In the mt-DNA parsimony analysis, *P. vindumi* appears in a sister position to the clade containing *P. interscapularis* and *P. sogdianus*, with those three taxa grouping with high support (bootstrap 98%, decay index 13). Alternatively, *P. ornatus* is sister to *P. clarkourum* (bootstrap 99%, decay index 21), and those two taxa are included in a clade with the two *P. luteoguttatus* samples that also receive high support (bootstrap 100%, decay index 26). Allozyme and RAG-1 DNA data did not sample appropriately to test this question.

3). Gravel Dwelling *Phrynocephalus* Species in the Caspian Basin

Previously, *P. reticulatus*, *P. bannikovi*, and *P. strauchi* were all considered subspecies of *P. reticulatus* (Eichwald 1831): The nominal subspecies *Phrynocephalus reticulatus reticulatus* [Eichwald 1831; type locality "Hab. ad Oxum, pristinum amnem, in caspii maris litore orietali", corrected to the Amu-Darja River by Golubev (1991)] and two additional distinct subspecies, *Phrynocephalus reticulatus strauchi* [Nikolsky 1899; restricted type locality "Khodzhent, 40° 17' N, 69° 37' E, northern Tajikistan" by lectotype designated by Dunayev (1995)] and *Phrynocephalus reticulatus bannikovi* (Darevsky, Rustamov & Shammakov 1976; type locality "Tuarkyr Mountains, northwestern Turkmenistan"), (see Bannikov *et al.* 1977; although *P. reticulatus* and *P. strauchi* were originally described as species). Here these gravel ecotypes are recognized as distinct species based on genetic difference and lack of monophyly.

In our sampling, *P. bannikovi* and *P. strauchi* do not appear monophyletic with *P. strauchi* and *P. rossikowi* grouping with light support (mt-DNA, bootstrap 55%, decay Index 2). *P. reticulatus* from central Uzbekistan was not sampled in our study or the study of Solovyeva *et al.* (2014). If *P. bannikovi* and *P. rossikowi* were removed from the parsimony analysis performed on the mt-DNA data, the topology of the trees in this study and that of Solovyeva *et al.* (2014) would be congruent. Based on incomplete sampling, it is recommended that members of the *P. reticulatus* complex be recognized as separate species *Phrynocephalus bannikovi* (Darevsky, Rustamov & Shammakov 1976) **New Status**, *P. reticulatus*, and *P. strauchi*. Solovyeva *et al.* (2014) appear to have not sampled any species from Turkmenistan, which includes *P. raddei raddei* and *P. rossikowi*, and in our phylogenetic analyses are related to the *P. reticulatus* complex. The inclusion of *P. raddei raddei* and *P. rossikowi* in the sampling presented here indicates the traditional *P. reticulatus* complex is not monophyletic, deserving species recognition for the three former subspecies. In common with this study, Solovyeva *et al.* (2014) only sampled *P. strauchi* from the *P. reticulatus* complex.

In the sampling of this study, *P. bannikovi* and *P. raddei* are geographically oriented disjunctive-adjacent to each other in eastern and west-central Turkmenistan, respectively, and are sister taxa receiving high support from mt-DNA (bootstrap 100%, decay index 23), nuclear RAG-1 DNA (bootstrap 91%, decay index 3), and combined data analyses (bootstrap 100%, decay index 27). Solovyeva *et al.* (2014) did not sample *P. bannikovi*, *P. rossikowi*, or *P. raddei raddei* from Turkmenistan. However, Solovyeva *et al.* (2014) and this study did sample *P. strauchi* from the Fergan Valley of eastern Uzbekistan or northern Tadjikistan. Sampling between this study and Solovyeva *et al.* (2014) differs in the subspecies of *P. raddei*: This study uses *P. raddei raddei*, (Boettger 1888: type locality "Perewalnaja an der transcaspischen Bahn", = Perevalnaja railroad station, southwestern Turkmenistan; near where this study's sample originated from), whereas Solovyeva *et al.* (2014) uses *P. raddei boettgeri* (Nikolsky 1905; type locality "Schirabad, Buchara orient" = Sherabad, approximately 37° 42' N, 67° 04' E, southern Uzbekistan) with a vague locality provided as "Turan Depression" [= Caspian Basin]; but occurs in extreme southern Uzbekistan and southern Tajikistan along the Afghanistan border (Bannikov *et al.* 1977). Until a single study samples both subspecies of *P. raddei*, it will be unclear how they relate to *P. bannikovi*, *P. reticulatus*, *P. strauchi*, and *P. rossikowi*.

In Solovyeva *et al.* (2014) no detailed locality information is available, nor is an appendix with this information provided. All GenBank entries do not include locality data, so this information is not archival with NIH GenBank. The Zoological Museum of Moscow University (ZMMU) (<http://zmmu.msu.ru/en/about-muzeum/fonds/amphibians-&-reptiles-collections>) in which specimens reported in Solovyeva *et al.* (2014) are housed, does not offer an obvious means of searching by voucher number on their website. Additionally, this institution does not currently participate in global databases which compile data from institutions across the globe and allow free public access to museum collections involving voucher number relating to locality information. VertNet, a global organization whose participants include 64 institutions spanning 13 countries including Russia, is one prominent database to organize museum collections around the world. The Global Information Biodiversity Facility (GBIF) also offers a forum for researchers to access information on specimens collected in select countries on every continent, which is an added resource. The Zoological Museum of Moscow University is not currently participating in any of these databases, and localities in the manuscript of Solovyeva *et al.* (2014) are very vague, crossing large geographic regions, and not informative for the difficulties of dealing with *Phrynocephalus* taxonomy and sampling. Solovyeva *et al.* (2014) present GenBank sequences as common courtesy in the scientific community, but in those sequences, no locality information is provided so comparing Solovyeva *et al.* (2014) results with this study is difficult across all issues, starting with taxonomy. Published localities in Solovyeva *et al.*



(2014) such as Central and Middle Asia are not informative, as in the Russian style geography, Middle Asia refers to the Caspian Basin, and Central Asia refers to Tibet, Mongolia and western China. Localities of such gross generality do not provide any information for a study of this detail.

4). *Phrynocephalus helioscopus* Complex in the Caspian Basin

Phrynocephalus helioscopus turcomanus [Dunayev, Solovyeva & Poyarkov 2012 (in Solovyeva *et al.* 2012); type locality 40° 01' 00" N 52° 58' 00" E, current name Turkmenbashi, Turkmenistan] is recognized as a distinct species *Phrynocephalus turcomanus* [Dunayev, Solovyeva & Poyarkov 2012 (in Solovyeva *et al.* 2012)] **New Status** from *P. helioscopus* based on a north-south distributional disjunction in the Caspian Basin with significant mt-DNA differences. *P. helioscopus* [Pallas (1771) listed the type locality as "in deserti australioris collibus ardentissimis"; restricted (with no lectotype) to the "Inderskija Gory, Gebiet des unteren Uralfusses" by Mertens & Müller (1928), now Inderskije (Inder) Mountains, Atyrau Region, northwestern Kazakhstan] here is sampled from the northern Aral Sea region of Kazakhstan, and *P. turcomanus* from southwestern Turkmenistan (Appendix 1). While no fixed allozyme differences are detected between populations sampled, there is a high mt-DNA difference. The mt-DNA pairwise uncorrected sequence distance between *P. helioscopus* and *P. turcomanus* is 4.5%; therefore significantly diverged and in the range of sister species divergence for this segment of the mitochondrial genome among amphibians and reptiles (for summary see table 6 in Weisrock *et al.* 2001).

5). Use of Names in the Low Elevation Chinese Desert—Northern Caspian Basin Clade

a). *Phrynocephalus salenskyi*

The name *P. salenskyi* Bedriaga 1907 is applied here for populations sampled from the Junggar Depression of northwestern China, and the Zaysan Depression of northeastern Kazakhstan. *P. salenskyi* is the oldest name available by date and page number for *Phrynocephalus* populations of the low elevation Chinese desert – northern Caspian Basin clade in this geographic region, see below:

Phrynocephalus Salenskyi Bedriaga 1907: 141, 213.—Restricted type locality: "Urungu Fluss" [= Ulungur River, Xinjiang Uygur Autonomous Region, China].

Phrynocephalus Isseli Bedriaga 1907: 229.—Type locality: Desert in vicinity of Mt. Ssalburty (in Saur Mountains of the Tarbagatay Range, Xinjiang Uygur Autonomous Region, China).

Phrynocephalus Haeckeli Bedriaga 1907: 237.—Type locality: Desert in vicinity of Mt. Ssalburty (in Saur Mountains of the Tarbagatay Range), in the Tarbagataï (= Tacheng County) district, northern Xinjiang Uygur Autonomous Region, China.

Phrynocephalus Arcellazzii Bedriaga 1907: 307.—Type locality: "Gaschun, in der Nähe von Gutschen in der Dschungarei" [= Qitai (44° 00' N, 89° 50' E), Junggar Depression, Xinjiang Uygur Autonomous Region, China].

Phrynocephalus Grum-Grzmailoi Bedriaga 1909: 420.—Restricted type locality: "Gutschen" [= Qitai (44° 00' N, 89° 50' E), Junggar Depression, Xinjiang Uygur Autonomous Region, China].

Phrynocephalus bedriaga Tsarevsky 1926: 214.—Restricted type locality: Zaisan Lake region, eastern Kazakhstan.

Phrynocephalus albolineatus K. Zhao 1979: 113.—Type locality: "45 kilometers south of Tacheng County, Xinjiang Uygur Autonomous Region, China; 584 m elevation".

The Irtysh River flows out of Zaysan Lake linking the Junggar Depression with the Zaysan Depression, which makes a compelling case for sampling presented in this study representing *P. salenskyi* populations.

b). *Phrynocephalus przewalskii* Complex in the Gobi Desert

Phrynocephalus Przewalskii Strauch 1876: 10.—Type locality: "deserto Alaschanico" [= Tengger Desert, Nei Mongol Autonomous Region, China]; corrected to eastern Tengger Desert west from 106° E, southwest Nei Mongol Autonomous Region, China in Barabanov & Ananjeva (2007). This taxon is generally a sand dwelling ecotype.

P. frontalis Strauch 1876: 15.—Type locality: locality "Ordos dicta" [= Ordos Desert, Nei Mongol Autonomous Region, China]. This taxon is generally thought of as a gravel dwelling ecotype, and here considered a synonym of *P. przewalskii* (see below).

A lack of genetic diversity between populations from these taxa (two populations each), confirm that only the name *P. przewalskii* is valid, whereas *P. frontalis* is a synonym of *P. przewalskii* (following Gozdzik & Fu 2009). This is supported by nuclear encoded allozyme data, and mt-DNA data. Alternative names exist as reviewed in Barabanov & Ananjeva (2007), but without detailed sampling of type localities, the validity of alternate names cannot be addressed.

Across the 25 allozyme loci sampled here, we detected no fixed differences among the four populations of *P.*

przewalskii, indicating a fair amount of gene flow between the populations. The average mt-DNA pair-wise uncorrected sequence distances between population 2 and the clade containing populations 1, 3, and 4 is 3.64% (range 3.41–3.79%). The average pair-wise comparison within the clade containing populations 1, 3 and 4 is 0.57% (range 0.51–0.63%). These results match the phylogenetic topology discovered in the mt-DNA parsimony analysis, with population 2 placed in a sister position to the clade containing populations 1, 3 and 4 (bootstrap 100%, decay index 19). No resolution was discovered among the four *P. przewalskii* populations in the RAG-1 DNA parsimony analysis.

Urquhart *et al.* (2009) suggests a vicariant break among *P. przewalskii* populations roughly corresponding to the Helan Shan (mountains). Data reported here do not corroborate that hypothesis. Sampled are a single population east of the Yellow River and three populations west of the Yellow River, which flows north to south in this region. Population 2 is sampled on the east side of the river, and population 3 is sampled on the west side of the river, on banks directly across from each other in Shapotou, Ningxia Autonomous Region, China. Population 2, the only population on the east side of the Yellow River is the most divergent, with populations 1, 3 and 4 on the west side of the river nearly identical in our sampling. Population 1 (Wujiachuan, Gansu Province, China) is west of the Yellow River and further south than sampling conducted in Urquhart *et al.* (2009) and Wang & Fu (2004), yet nearly identical to other populations sampled west of the Yellow River. In our sampling, only population 4 lies west of the Helan Shan (Wuwei, Gansu Province, China) in the Tengger Desert, the type locality of *P. przewalskii*. Sampling in this study suggests the Yellow River could be responsible for a genetic break in *P. przewalskii* populations, and not the Helan Shan, though more detailed, fine-scale sampling and analysis will need to be done to confirm this hypothesis. In the Zhongwei region of Ningxia Autonomous Region, there is an indication that east and west haplotypes as described above occur in the same locality, which could indicate a point of hybridization, but further detailed work is needed (Wang & Fu 2004). Sampling conducted in similar areas in Wang & Fu (2004) and Urquhart *et al.* (2009) did not completely overlap, making conclusions between these studies and this study very difficult for comparative interpretation, further indicating additional work is needed.

In sampling of the *P. przewalskii* complex in Jin & Brown (2013), populations to the east are grouped, and are referred to as *P. frontalis*, with populations to the west grouping and referred to as *P. przewalskii*, not conflicting with results reported here.

6. Use of Names in the Northern Tibetan Plateau

Species distributed on the northern side of the Tibetan Plateau form the *P. vlangalii* complex and have a complicated taxonomic history. Here, the following names are recognized *P. vlangalii*, *P. roborowskii*, and *P. hongyuanensis*.

Phrynocephalus vlangalii, Strauch 1876; type locality “Kuku-noor dictum” [= Qinghai Lake, Qinghai Province, China]. The name *P. vlangalii* predates *P. putjatai* Bedriaga 1907; type locality “Gui-dui am Hoang-ho” [= Guide County (36° 00' N, 101° 40' E), southeast of Qinghai (Kuku-Nor) Lake, Qinghai Province, China]. Phylogenetic results in Jin & Brown (2013) are consistent with results reported here with a reassignment of names for populations sampled in Jin & Brown (2013). If *P. putjatai* is a junior synonym of *P. vlangalii* because their type localities appear to overlap, then populations assigned to that species in Jin & Brown (2013) are actually *P. vlangalii*. Populations assigned to *P. vlangalii* in Jin & Brown (2013) are *P. roborowskii* and *P. hongyuanensis*.

Phrynocephalus roborowskii Bedriaga “1905” 1906; restricted type locality “Provinz Zaidam” [= Qaidam Depression, Qinghai Province, China].

Phrynocephalus hongyuanensis Zhao, Jiang & Huang 1980 (in Jiang *et al.* 1980); type locality “Waqên, Hongyuan County, 33° 03' N; 102° 37' E, Sichuan Province, China; 3500 m.” This species was originally described as a subspecies of *P. vlangalii* (see below).

Phrynocephalus vlangalii hongyuanensis is elevated to species status as *P. hongyuanensis* based on phylogenetic information reported here. *P. hongyuanensis* from the northeastern portion of the Tibetan Plateau is either sister to *P. roborowskii* from the northwestern portion of the Tibetan Plateau (mt-DNA bootstrap 100%, decay index 17; combined analysis bootstrap 100%, decay index 20), or nested inside *P. roborowskii* in the nuclear RAG-1 DNA analysis with little support (decay index 1). Hence, in all analyses *P. vlangalii* appears outside of the clade containing *P. hongyuanensis* and *P. roborowskii*, while being located in the geographical middle of those species. Jin *et al.* (2008) sampled only *P. vlangalii* and *P. roborowskii*, leaving out *P. hongyuanensis* in sampling, therefore not discovering this distinction. Pang *et al.* (2003) showed *P. hongyuanensis* inside of *P. vlangalii*, but did not consider *P. roborowskii* as a taxon or did not sample it [sampling between this study and Pang *et al.* (2003) is not the same].

a). Sex Determinate Dispersal—In our sampling, Tibetan Plateau species of *P. vlangalii*, *P. roborowskii*, *P. hongyanensis*, and *P. theobaldi*, as well as *P. forsythii*, are all viviparous. All are high elevation ecotypes except *P. forsythii*, which is from the low elevation Taklimakan Desert north of the Tibetan Plateau. There is evidence of sex determinate dispersal favoring males in this clade (Qi *et al.* 2013). While collecting during summer months in sandy soil habitats of the Tibetan Plateau, Macey and others would commonly dig up to one meter down to find gravid females, and sometimes females who had just given birth with their young in the burrow. Females lack an evolutionary drive to disperse because once impregnated they must dig deep burrows of a meter or more to carry out their two month incubation period needed before parturition (Qi *et al.* 2013), and remain in the burrow for hibernation during winter months possibly with their young (Wu *et al.* 2015), who are too small to dig burrows of their own. Males disperse for breeding purposes and have the additional ability to disperse for livelihood purposes.

b). Analogous Natural History with Salamanders of the Genus *Ensatina*—Mitochondrial DNA is maternally inherited, and nuclear DNA is bisexually inherited. Females of the subspecies *Ensatina eschscholtzii platensis* brood their eggs, (which means to guard their eggs) and as such males have a greater home range than females, dispersing in wider distances (Staub *et al.* 1995). Kutcha *et al.* (2009) reported a sharp mt-DNA break between northern and southern populations of *E. e. platensis* at the Stanislaus River, which serves as the border between the California counties of Calaveras and Tuolumne. For reference, in the central Sierra Nevada where the mt-DNA break occurs, sample 190 refers to the northern clade of *E. e. platensis* taken near Arnold in Calaveras County, while sample 192 refers to the southern clade taken near Alder Spring, central Tuolumne County south of the Stanislaus River and north of the Tuolumne River (refer to figure 3 and appendix S1 for locality information in Kutcha *et al.* 2009). The two clades of *E. e. platensis* show an intergradation of breaks at eight nuclear encoded allozyme loci ranging from Wagner Ridge in Mariposa County (sample number 27 in Jackman & Wake 1994) to the south and Panther Creek in Amador County to the north in the region of the Mokelumne River (sample number 22 in Jackman & Wake 1994), with indications of significant allozyme variation within populations of the southern clade of *E. e. platensis* (Wake & Schneider 1998). Unpublished data recognize a major break between northern and southern *E. e. platensis* clades, as well as a hybridization zone with *E. e. xanthoptica* near the area of Wagner Ridge (David B. Wake pers. comm.). Hence, the *Ensatina* complex shows alternative patterns in the degree of genetic breaks from maternally inherited mitochondrial DNA and bisexually inherited nuclear encoded allozyme alleles that may be attributed to life history traits.

Noble *et al.* (2010) reported a possible area east of Qinghai Lake in which two different populations of *Phrynocephalus* of uncertain taxonomic identity come in contact with nuclear DNA and mitochondrial DNA appearing to have discordant breaks. A possible explanation for this could be females must make deep burrows and sit tight (Wu *et al.* 2015), while males move around, and as such mitochondrial DNA remains localized, with bisexually inherited nuclear DNA spreading by males as they look for breeding partners (Noble *et al.* 2010). As discussed above, we believe populations on the east side of Qinghai Lake should be referred to as *P. vlangalii*, and populations on the west side of the lake referred to as *P. roborowskii*. Maternally inherited mitochondrial DNA and bisexually inherited nuclear DNA should not show a discordance based on the sampling strategy adopted in this study.

B. Geologic Activity and *Phrynocephalus* Cladogenesis

Phylogenetic patterns discovered are shaped by complex geologic activity and seaway inundations involving serial tectonic collisions of plates that originated in Gondwanaland, crossed the Tethys Sea, and collided with Eurasia several hundred million years ago (see Introduction for review). The more modern tectonic collisions of the Indian Plate 50 MYBP (Windley 1988; Royden *et al.* 2008) and the Arabian Plate 18 MYBP (Dercourt *et al.* 1986; Steininger & Rogl 1984) caused major compression of ancient plates inducing plate boundaries to be rejuvenated as strike-slip fault zones that formed the current major mountain belts of Asia, which are directly responsible for *Phrynocephalus* speciation. Figure 9 illustrates major directional plate movements within Asia caused by Indian and Arabian compression, along with estimated crustal shortening and deformation rates influenced by the Indian collision (Dewey *et al.* 1989). Details of the docking of Arabia, and the continued movement of India into Eurasia are illustrated in figures 10, 11, and 12 (35, 22, and 10 MYBP respectively). These figures show the evolution of land areas, seaways, and tectonic activity with major uplift. *Phrynocephalus* is part of the subfamily Agaminae that is hypothesized to have originated in Afro-Arabia (Macey *et al.* 2000b). As Arabia is connecting with Eurasia, and India is continuing to move into Eurasia there is a dramatic emergence of land in internal Asia, providing diversity of habitats for *Phrynocephalus* to occupy as they disperse out of Arabia 18 MYBP (Dercourt *et al.* 1986; Steininger & Rogl 1984).

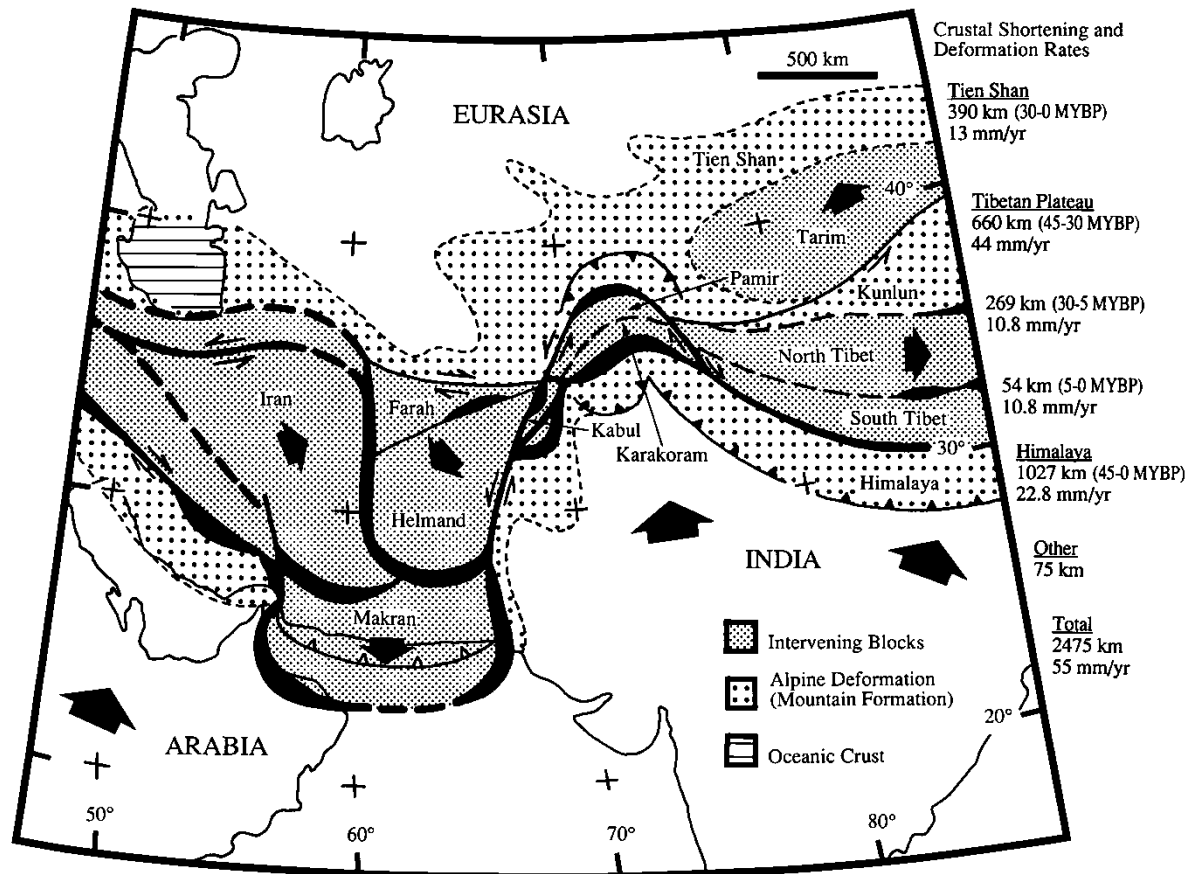


FIGURE 9. Movements of tectonic plates. During the middle Eocene, 50–45 MYBP, India first contacted Eurasia. Since that time, India and Laurasian plates have converged 2365 km in the west, 2475 in the center, and 2750 km in the east (Dewey *et al.* 1989; Molnar *et al.* 1987; Royden *et al.* 2008; Windley 1988). The high altitudes now present in the Hindu Kush, Karakoram, Tien Shan, and Pamir are attributed to the Indian collision (Dewey *et al.* 1988, 1989). The Hindu Kush between the Helmand and Farah blocks is associated with the uplift of the trans-Himalaya, which includes the Karakoram and is one of the earlier uplifting events. The Tien Shan and Pamir, which now separate the Taklimakan Desert (Tarim Plate) from the Caspian Basin and Farah Block, were formed approximately 10 MYBP (Abdrakhmatov *et al.* 1996; Tapponier *et al.* 1981). Crustal shortening and deformation rates are from Dewey *et al.* (1989). The map is modified from Tapponier *et al.* (1981).

Phylogenetic patterns recovered are highly suggestive of divergences caused by geologic mountain building and tectonic induced sea level evolution. While taking a conservative approach of using non-corrected pairwise nucleotide substitutional data, and applying a pairwise rate of 1.3% sequence divergence per million years for the segment of mitochondrial DNA reported, our estimates should not be overestimates. Among all comparisons presented in table 4 and discussed below (also see Results), estimated ages from nucleotide substitution data either match expected times from geologic information, or exceed them in age. This is highly suggestive that the geologic evolution of Asia as it formed had a major impact on speciation events that shape the genus *Phrynocephalus*.

a). Eastern Tien Shan Mountain Building—In the eastern Tien Shan (mountains), the divergence of *P. guttatus* and *P. salenskyi* populations from *P. versicolor* and *P. przewalskii* populations is estimated to be 6.0 MYBP, which is slightly older than the geologic date 5 MYBP (Smit *et al.* 2013). The broad range of the Tien Shan (mountains) is an ancient plate suture zone rejuvenated with activity from the Tibetan collision, and shows continual activity over the last 10 MYBP (Abdrakhmatov *et al.* 1996).

TABLE 4. Pairwise comparisons of taxa evaluating mitochondrial DNA distance with geologic events. All comparisons use the ND1-COI segment except the *P. mystaceus* populations which apply the subset of ND1-half of ND2. The *P. helioscopus* to *P. turcomanus* comparison is north-south across the Caspian Basin. The Paratethys Sea refers to the closing of the Tethys Sea in the area now known as the Caspian Basin. There are three comparisons across the Tibetan Plateau that include all Tibetan Plateau taxa because of a polytomy (listed as Tibet Comparison 1-3); the placement of *P. forsythii* would not affect these estimates significantly as this species is either outside of the groups compared or part of one of the groups compared.

Taxa Compared	Geologic Event	Geologic Date	Distance	Estimated Age
<i>P. guttatus</i> & <i>P. salenskyi</i> to <i>P. versicolor</i> & <i>P. przewalskii</i>	Eastern Tien Shan	5 MYBP Smit <i>et al.</i> 2013	7.81%	6.0 MYBP
<i>P. bannikovi</i> to <i>P. raddei</i>	Late Miocene Drying of Paratethys Sea	5.5-6 MYBP Steininger & Rogl 1984	8.60%	6.6 MYBP
<i>P. golubewii</i> to <i>P. helioscopus</i> & <i>P. turcomanus</i>	Late Miocene Drying of Paratethys Sea	5.5-6 MYBP Steininger & Rogl 1984	11.60%	8.9 MYBP
<i>P. helioscopus</i> to <i>P. turcomanus</i>	Pliocene Inundation of Caspian Basin	3-3.5 MYBP Steininger & Rogl 1984	4.45%	3.4 MYBP
<i>P. interscapularis</i> & <i>P. sogdianus</i> to <i>P. vindumi</i>	Kopet-Dagh	5 MYBP Smit <i>et al.</i> 2013	15.63%	12.0 MYBP
<i>P. scutellatus</i> populations 1 & 2	North-South Iranian Plateau Compression	5-10 MYBP Mouthereau <i>et al.</i> 2012 Smit <i>et al.</i> 2013	10.43%	8.0 MYBP
<i>P. arabicus</i> 1-2 & <i>P. longicaudatus</i> to <i>P. maculatus</i>	Zagroz	5-10 MYBP Rapid Uplift Mouthereau <i>et al.</i> 2012	11.28%	8.7 MYBP
<hr/>				
Tibet Comparison 1				
<i>P. roborowskii</i> & <i>P. hongyuanensis</i> to <i>P. theobaldi</i>	North-South Tibet	5 MYBP Rapid Uplift 5-10 MYBP Plain-Stage Shackleton & Chang 1988	7.64%	5.9 MYBP
Tibet Comparison 2				
<i>P. vlangalii</i> populations 1-3 to <i>P. theobaldi</i>	North-South Tibet	5 MYBP Rapid Uplift 5-10 MYBP Plain-Stage Shackleton & Chang 1988	10.60%	8.2 MYBP
Tibet Comparison 3				
<i>P. roborowskii</i> , <i>P. hongyuanensis</i> , & <i>P. vlangalii</i> populations 1-3 to <i>P. theobaldi</i>	North-South Tibet	5 MYBP Rapid Uplift 5-10 MYBP Plain-Stage Shackleton & Chang 1988	9.12%	7.0 MYBP

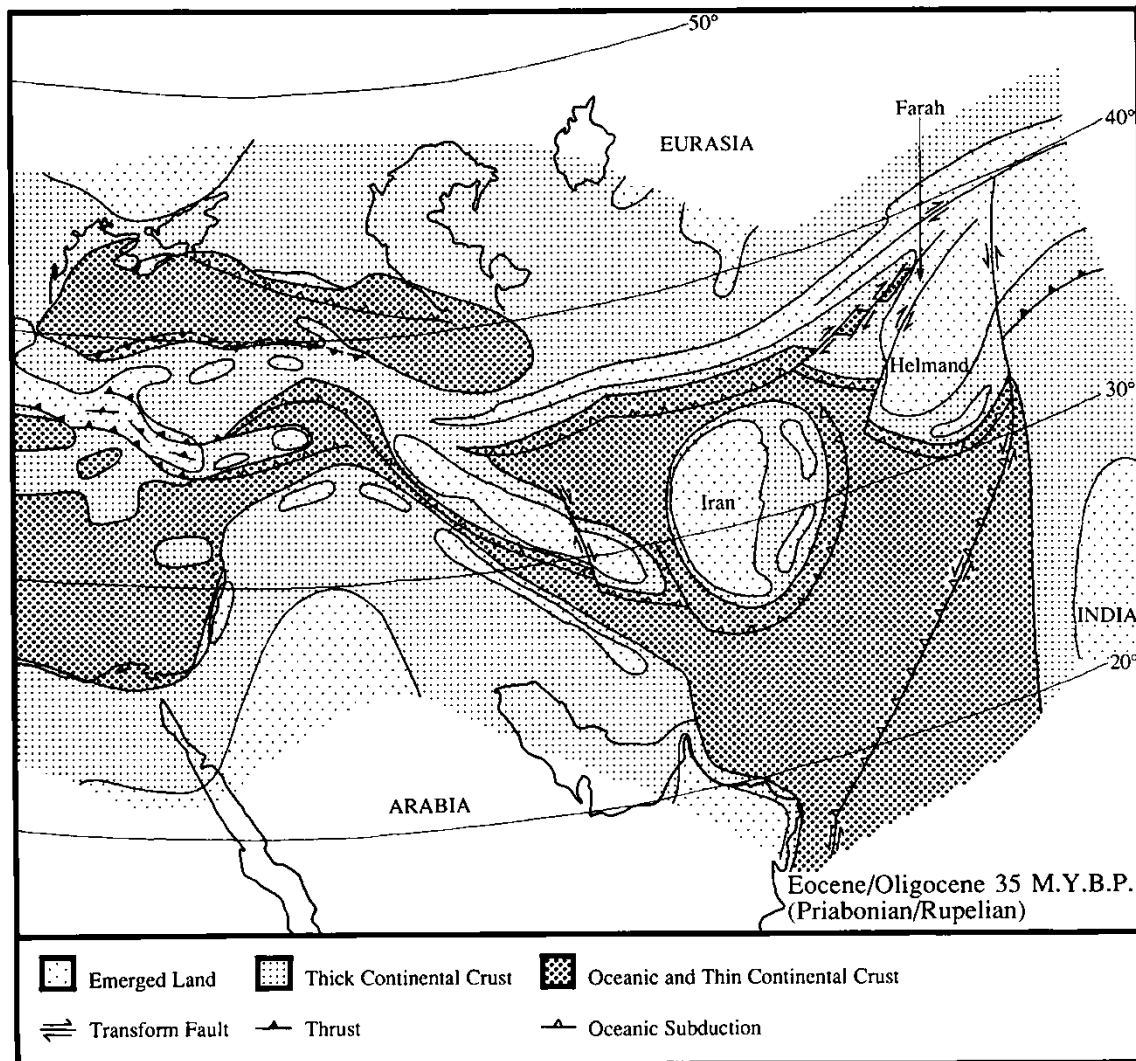


FIGURE 10. Tectonic setting for the formation of mountain belts in central and Southwest Asia at 35 MYBP, Eocene/Oligocene. The map is after Dercourte *et al.* (1986). Note the approaching Arabian Plate, with much of Southwestern Asia in front of the Indian Plate.

b). *Drying and Inundation Cycles of the Paratethys Sea in the Caspian Basin*—As the Tethys Sea closed, when Afro-Arabia smashed into Eurasia, there were a series of drying and inundation events in the Caspian Basin that are expected to have influenced speciation among *Phrynocephalus*, during and following invasion from the south (Figs. 13 and 14). **When the Paratethys Sea inundated the Caspian Basin 5.5–6 MYBP**, two comparisons revolve around this event (Steininger & Rogl 1984; Fig. 13). *P. bannikovi* and *P. raddei* have a divergence estimate of 6.6 MYBP, which is slightly older than the geologic estimate of 5.5–6 MYBP. *P. golubewii* is estimated to have diverged from *P. helioscopus* and *P. turcomanus* around 8.9 MYBP, which is considerably older than the geologic estimate of 5.5–6 MYBP. Following the drying of the Paratethys Sea, the Pliocene inundation of the Caspian Basin is estimated to have occurred 3–3.5 MYBP (Steininger & Rogl 1984; Fig. 14), which matches the nucleotide sequence divergence between *P. helioscopus* and *P. turcomanus* of 3.4 MYBP, suggesting a north-south divergence of these taxa, with rejuvenated seaway development. The tight relationship of *P. golubewii* in a sister position to the clade containing *P. helioscopus* and *P. turcomanus* is suggestive of a first phase of speciation from the drying of the Paratethys Sea (*P. golubewii* to *P. helioscopus* + *P. turcomanus*), and a second speciation event with Pliocene rejuvenation of a seaway in the Caspian Basin (*P. helioscopus* to *P. turcomanus*). An additional speciation event suggested to revolve around the late Miocene drying of the Paratethys Sea 5.5–6 MYBP (Steininger & Rogl 1984) is the separation of *P. bannikovi* from *P. raddei*, both inhabiting gravel habitats. The nucleotide based divergence

estimate is 6.6 MYBP, which is slightly older than the geologic estimate. The Paratethys Sea in the Caspian Basin may have formed evaporitic areas, which may have looked like those now observed to the south of the Caspian Sea in Iran and Azerbaijan with high-levels of rainfall. Localized water systems may have formed that created alluvial fans spilling gravel into lowland areas from mountains experiencing increased rainfall and uplifting. In this hypothesis, gravel is placed in lowland areas as the Paratethys Sea is drying up creating a number of unique environments, including those with salt deposits, promoting speciation among *Phrynocephalus* populations.

c). *Kopet-Dagh Mountain Building on the Northern Margin of the Iranian Plateau*—Two taxon comparisons cross the Kopet-Dagh (mountains), spanning the northern border of Iran with the southern border of Turkmenistan, and have a geologic estimate of 5 MYBP (Smit *et al.* 2013). Populations of *P. mystaceus* are distributed in the Caspian Basin (population 1), with an isolated population in northwestern Iran (population 2), and exclusively inhabit large sand dunes. The nucleotide divergence estimate of 5.2 MYBP is almost exactly as expected from geologic estimates. *P. interscapularis* and *P. sogdianus*, which dwell on the edges of large sand dunes in the Caspian Basin, show an estimated nucleotide divergence from *P. vindumi*, a large sand dune dweller of northwestern Iran, of 12.0 MYBP, which is considerably older than expected based on the geologic estimate and probably reflects an older history than the rise of the Kopet-Dagh.

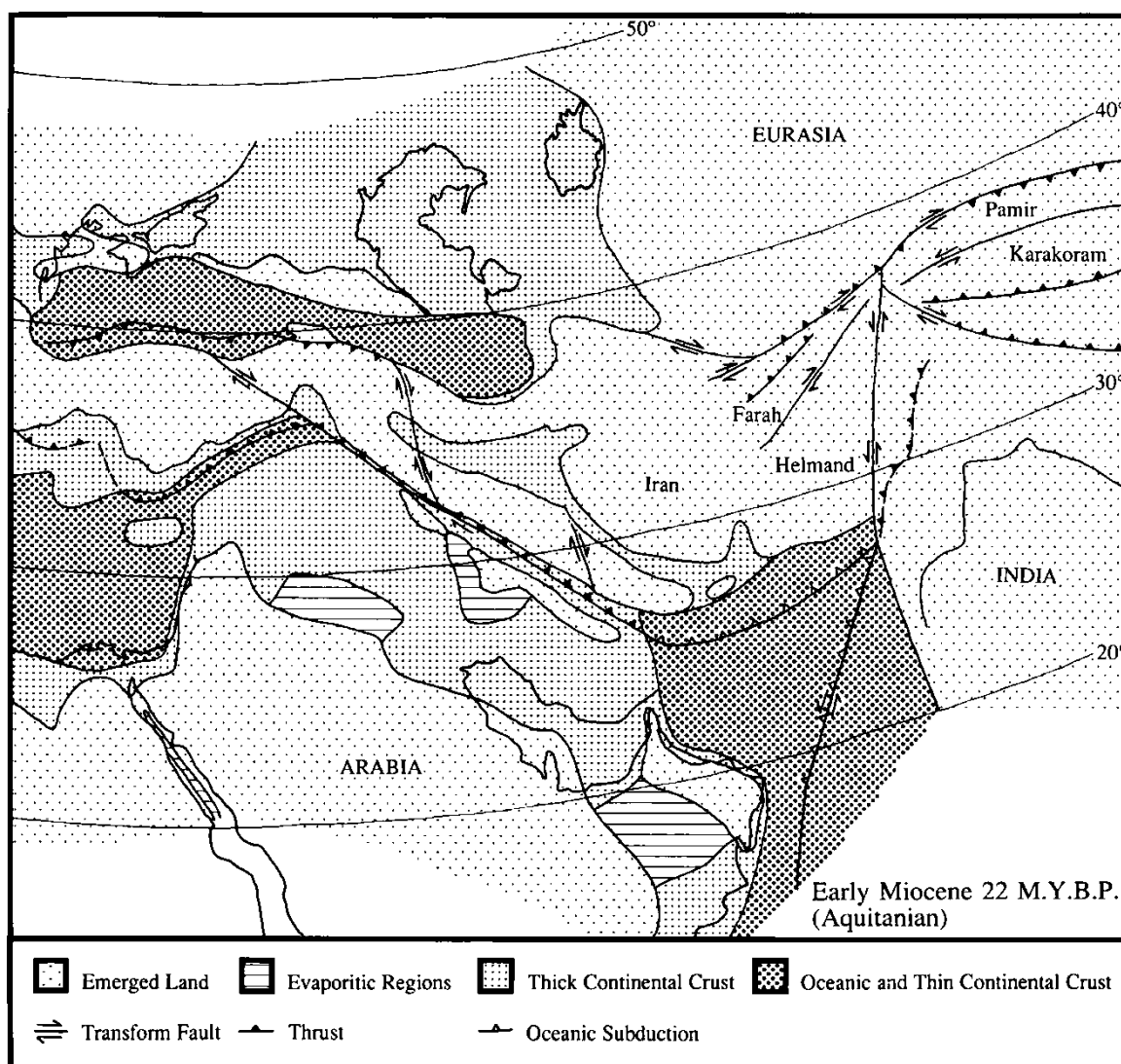


FIGURE 11. Tectonic setting for the formation of mountain belts in central and Southwest Asia at 22 MYBP, Early Miocene. The map is after Dercourte *et al.* (1986) and uplifting in the Pamir and Karakoram mountains is schematic after Tapponnier *et al.* (1981). Note the near docking of the Arabian Plate with Eurasia, forward movement of India into Eurasia, and Southwest movement of ancient Gondwanan Plates (Farah, Helmand, Iran).

d). **Iranian Plateau Geologic Compression**—Geologic compression north-south across the Iranian Plateau is estimated to have taken place over a 5–10 MYBP period (Mouthereau *et al.* 2012; Smit *et al.* 2013). Population diversity of *P. scutellatus* is dated at 8.0 MYBP based on nucleotide sequence divergence, which is within the range of the geologic estimate.

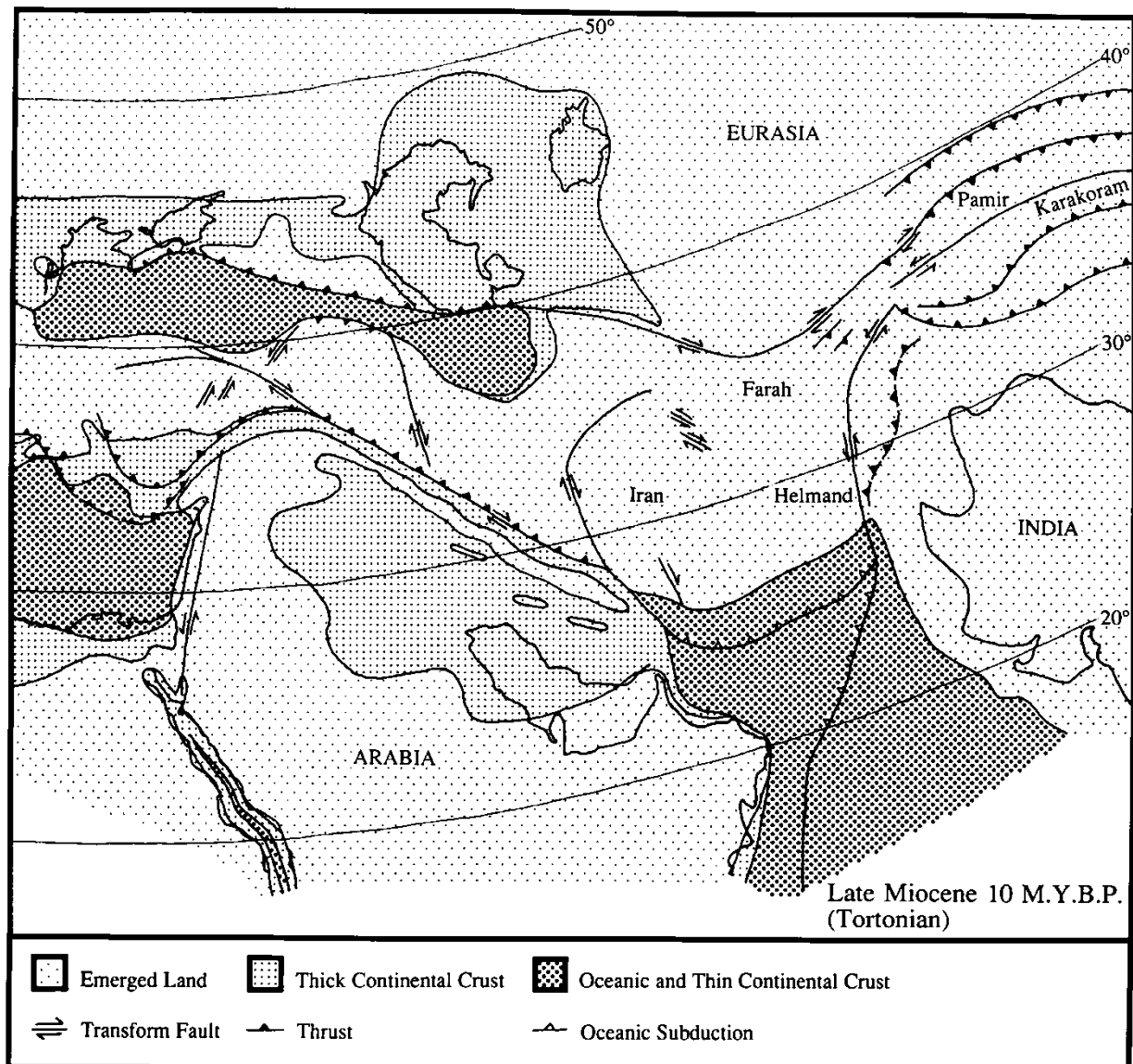


FIGURE 12. Tectonic setting for the formation of mountain belts in central and Southwest Asia at 10 MYBP, Late Miocene. The map is after Dercourte *et al.* (1986) and uplifting in the Pamir and Karakoram mountains is schematic after Tapponnier *et al.* (1981). Tectonic processes depicted here continue today. During the late Miocene (10 MYBP, Tortonian), India wedged deeply into Eurasia, and Arabia began indentation into Iran (composed of Cimmerian Plates). The Pamir Mountains were experiencing intense uplifting during the Late Miocene (10 MYBP). The indentation of Arabia into Iran in the Late Miocene (10 MYBP) began the formation of the Zagros Mountains in the southern part of the Iranian Plateau. In the northern part of the Iranian Plateau, the Lesser Caucasus Mountains and Kopet-Dagh began uplifting in the early Pliocene (5 MYBP). Plates are labeled in capital letters and ancient Gondwanan Plates (Cimmerian Plates) are Iran (Lut), Farah, and Helmand. Note that the indentations of both India and Arabia are compressing the Cimmerian Plates and causing intense mountain building along paleo-sutures of these plates.

e). **Zagros Mountain Building on the Southern Margin of the Iranian Plateau**—Taxa that are distributed in the Arabian Peninsula, *P. arabicus* and *P. longicaudatus*, are separated from their sister taxon *P. maculatus* of the Iranian Plateau by the Zagros mountains, which are estimated to have formed 5–10 MYBP (Mouthereau *et al.*

2012). Based on nucleotide sequence divergence, these taxa are estimated to have diverged 8.7 MYBP, which is within the expected divergence time based on geologic evidence. Mouthereau *et al.* (2012) suggest an uplift period of 7–14.8 MYBP for the formation of the central Zagros. This is the highest elevation-area in the mountain range, and probably representing the first region to experience uplift, which still is in the timeframe of the estimate presented here based on nucleotide sequence divergence.

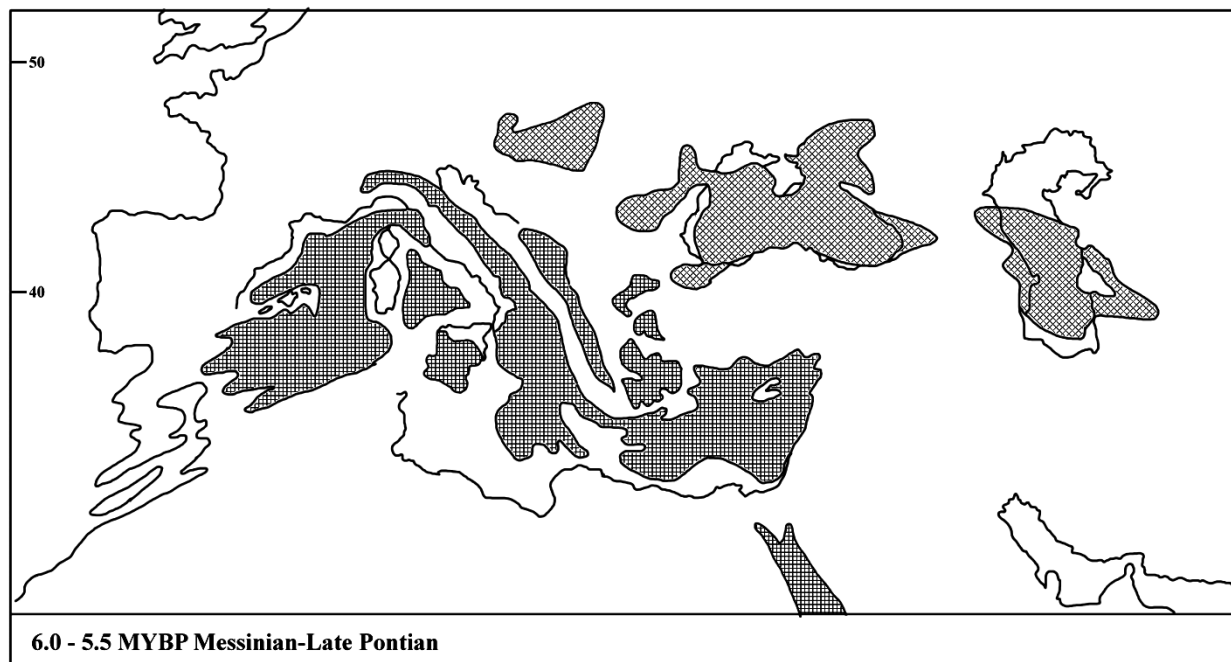


FIGURE 13. Late Miocene (6.0–5.5 MYBP) with the Caspian Basin, Black Sea and Mediterranean Sea as evaporitic regions. The minimal extent of water in the Caspian Basin may have promoted dispersal events among *Phrynocephalus* populations. The map is after Steininger & Rogl (1984).

f). Tibetan Uplift—Tibet is composed of a series of Gondwanan blocks that migrated across the Tethys Sea, smashing into Eurasia several hundred MYBP (Figs. 3 and 9). This was subsequently compressed and under-plated by the Indian Plate, creating the Tibetan Plateau, and a series of east-west mountain ranges on suture zones of ancient Tibetan blocks, which provide barriers for *Phrynocephalus* dispersal. Comparisons here cross from north to south these geologic events, and are organized around the third phase of Tibetan uplift 5 MYBP. Following the second phase of Tibetan uplift, the plateau was maintained as a plain of 3000 m elevation by an equilibrium of gradual uplifting, faulting, and erosion 5–10 MYBP (pediplanation cycle; Dewey *et al.* 1989; Shackleton & Chang 1988) that was followed by the third phase of rapid uplift doubling the plateau’s elevation at 5 MYBP (Shackleton & Chang 1988). Among samples from northern Tibet compared to the single sample from southern Tibet, *P. theobaldi*, we estimate three different divergence times depending on which taxa from northern Tibet are included in comparisons; comparison 1, 5.9 MYBP; comparison 2, 8.2 MYBP; and comparison 3, 7.0 MYBP. These estimates from nucleotide data are older than that of the third phase of Tibetan uplift but well within the pediplanation cycle of 5–10 MYBP, that followed the second phase of Tibetan uplift (Dewey *et al.* 1989; Shackleton & Chang 1988).

C. Glacial History and the Root of *Phrynocephalus*

Unlike North America and Europe, Asia was not heavily glaciated at high latitudes during the last ice age 18,000 years before present (McIntyre *et al.* 1976; Fig. 15), which is also the case in much of high elevation Tibet. This opens up the potential for an old north that was not erased by glaciation, and in fact Nikolsky (1916) suggested an old Eocene origin for *Phrynocephalus* in Sino-Mongolian Central Asia including Tibet. *Phrynocephalus* inhabiting northern regions of Central Asia and Tibet have dramatic size and color pattern diversities, with the greatest

number of available scientific names (see Barabanov & Ananjeva 2007). Statistical results using mt-DNA data and combined data largely reject a basal position for northern lowland taxa, viviparous/Tibetan taxa, or these two clades combined (Table 3). Hence, it is highly unlikely that *Phrynocephalus* originated in northern Central Asia and/or Tibet.

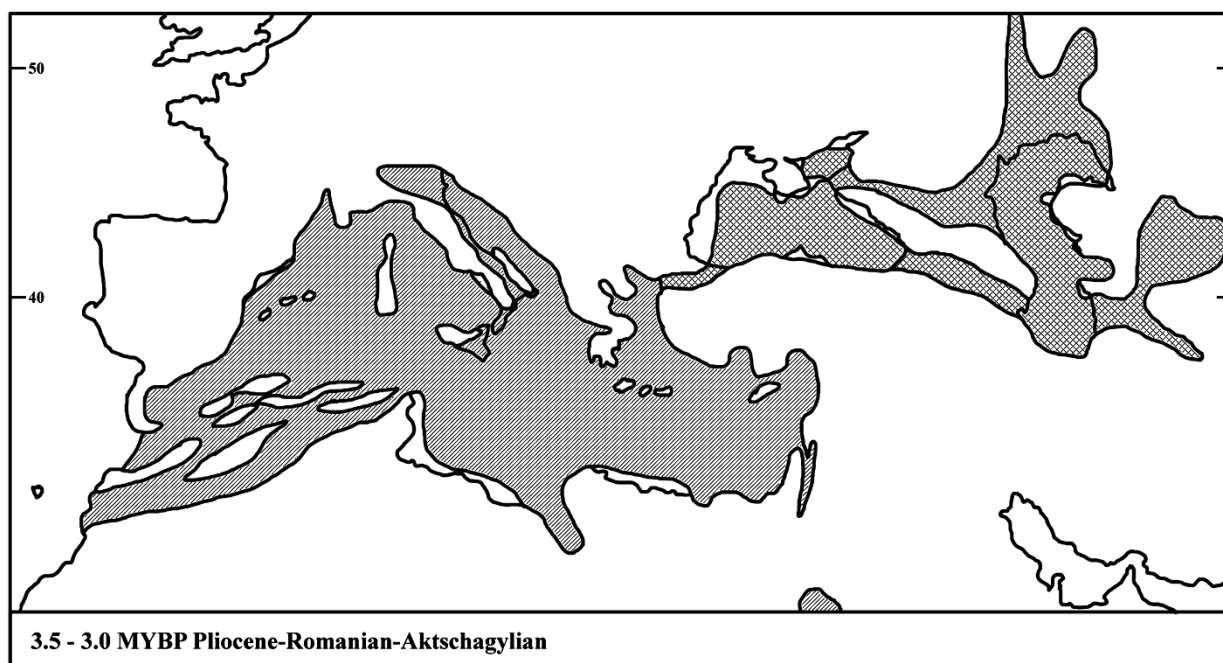


FIGURE 14. Pliocene (3.5–3.0 MYBP) extent of the rejuvinted Paratethys Sea. Note that the Caspian Basin is reconnected with the Black Sea and Mediterranean Sea. This period of water inundation may have further subdivided populations of *Phrynocephalus*. Note the rejuvenated inundation to the southeast of the current Caspian Sea outline, which is at the base of the Kopet-Dagh (mountains) uplifting that initiated approximately 5 MYBP (Smit *et al.* 2013). The map is after Steininger & Rogl (1984).

D. Habitat Evolution Among *Phrynocephalus*

The description of habitat types among all sampled *Phrynocephalus* and outgroups is presented in table 5. Examples of most species sampled and habitats are presented in plates I–VIII. The outgroup *Laudakia caucasia* occupies mountain areas with large boulders where *Phrynocephalus* species do not occur, and therefore treated separately.

Phrynocephalus and additional outgroup taxa sampled in this study inhabit either hard or soft substrates. Hard substrates are comprised of gravel, clay, and dry lakebed habitats while soft substrates consist of large and small sand dunes. The complex nature of these subcategories within the major categories of hard substrates and soft substrates complicates an easy understanding of the evolution of habitat usage. Presented in figure 16 is a plot of hard and soft substrates on the strict consensus of the three most parsimonious trees discovered in the combined analysis of mt-DNA, nuclear RAG-1 DNA, and allozyme data (for combined parsimony tree see Fig. 8).

The subfamily Agaminae, including *Phrynocephalus*, has been hypothesized to originate in the Gondwanan block of Afro-Arabia (Macey *et al.* 2000b). As Afro-Arabia separated from other Gondwanan plates, and moved north across the Tethys Sea, Arabia separated from Africa (40 MYBP), caused by the Red Sea rift. As Arabia began to collide with Eurasia (18 MYBP), a route was provided for *Phrynocephalus* to migrate north into Eurasia.

Results from plotting hard and soft substrate are presented in figure 16 and indicate a soft substrate niche being the ancestral characteristic for *Phrynocephalus*. *Phrynocephalus* may have opportunistically taken advantage of a sand-niche developed in the Arabian–Eurasian collision zone (18 MYBP), providing an advantageous set of adaptations for new habitat utilization. As plates collide, habitats form and the smashing of rocks can create sand, as well as the inclusion of sea-sand with the closing of seaways, such as the Tethys Sea.

TABLE 5. Habitat types and general geographic distribution of *Phrynocephalus* and outgroups (see Plates I-VIII for examples of habitats and Materials and Methods for definition details).

Habitat Definitions		
Rock (R)	—a large rock boulder area	
Clay (C)	—hard clay soil, which does not have gravel	
Gravel (G)	—complex soils that tend to be isolated with unique gravel covers, or gravel from alluvial fans draining mountain regions	
Dry Lakebed (DL)	—flat desert dry lakebeds that often have salt deposits.	
Small Sand Dune (SS)	—light sand, small sand dunes or edge of large shifting sand dunes	
Large Sand Dune (LS)	—large shifting sand dunes	

Taxon	Distribution	Habitat
<i>L. caucasia</i>	Northern Iranian Plateau	Rock
<i>B. laungwalaensis</i>	Thar Desert, India	Large Sand Dune
<i>T. persicus</i>	Arabian Plate	Clay/Gravel/Small Sand Dune
<i>T. sanguinolentus</i>	Caspian Basin	Clay/Gravel/Small Sand Dune
<i>P. scutellatus-1</i>	SE Iranian Plateau	Gravel
<i>P. scutellatus-2</i>	NE Iranian Plateau	Gravel
<i>P. arabicus-1</i>	Arabian Plate, Saudi Arabia	Large Sand Dune
<i>P. arabicus-2</i>	Arabian Plate, Oman	Small Sand Dune
<i>P. longicaudatus</i>	Arabian Plate, Oman	Gravel
<i>P. maculatus-1</i>	NW Iranian Plateau	Dry Lakebed
<i>P. maculatus-2</i>	SE Iranian Plateau	Dry Lakebed
<i>P. clarkorum</i>	Helmand Block	Small Sand Dune
<i>P. ornatus</i>	Helmand Block	Small Sand Dune
<i>P. luteoguttatus-1</i>	Helmand Block	Small Sand Dune
<i>P. luteoguttatus-2</i>	Helmand Block	Small Sand Dune
<i>P. interscapularis</i>	Caspian Basin	Small Sand Dune
<i>P. sogdianus</i>	Farah Block	Small Sand Dune
<i>P. vindumi</i>	NE Iranian Plateau	Small Sand Dune
<i>P. persicus</i>	Northern Iranian Plateau	Clay/Gravel
<i>P. golubewii</i>	Southern Caspian Basin	Dry Lakebed
<i>P. helioscopus</i>	Northern Caspian Basin	Clay/Small Sand Dune
<i>P. turcomanus</i>	Southern Caspian Basin	Clay
<i>P. mystaceus-1</i>	Caspian Basin	Large Sand Dune
<i>P. mystaceus-2</i>	NE Iranian Plateau	Large Sand Dune
<i>P. axillaris</i>	Tarim Basin	Clay
<i>P. bannikovi</i>	SW Caspian Basin	Gravel
<i>P. raddei</i>	Southern Caspian Basin	Gravel
<i>P. rossikowi</i>	Southern Caspian Basin	Gravel
<i>P. strauchi</i>	Fergan Valley	Gravel
<i>P. forsythii-1</i>	Tarim Basin	Gravel
<i>P. forsythii-2</i>	Tarim Basin	Gravel
<i>P. roborowskii-1</i>	Chaka Basin, NW Tibet	Gravel
<i>P. roborowskii-2</i>	Qaidam/Altun, NW Tibet	Gravel

.....continued on the next page

TABLE 5. (Continued)

Taxon	Distribution	Habitat
<i>P. hongyuanensis</i>	Eastern Tibet	Small Sand Dune
<i>P. vlangalii-1</i>	Qinghai Basin, NE Tibet	Gravel
<i>P. vlangalii-2</i>	Qinghai Basin, NE Tibet	Small Sand Dune
<i>P. vlangalii-3</i>	NE Tibet	Small Sand Dune
<i>P. theobaldi</i>	Southern Tibet	Gravel
<i>P. guttatus</i>	Northern Caspian Basin	Small Sand Dune
<i>P. salenskyi-1</i>	Junggar Depression	Large Sand Dune
<i>P. salenskyi-2</i>	Zaysan Depression	Small Sand Dunes
<i>P. versicolor</i>	Gobi-Junggar-Tarim	Clay/Gravel
<i>P. przewalskii-1</i>	Gobi Desert	Clay/Gravel
<i>P. przewalskii-2</i>	Gobi Desert	Small Sand Dune
<i>P. przewalskii-3</i>	Gobi Desert	Large Sand Dune
<i>P. przewalskii-4</i>	Gobi Desert	Large Sand Dune

Note: (1) Caspian Basin refers to areas in former Soviet Central Asia mainly draining into the Aral and Caspian seas; (2) Farah Block is mainly in northern Afghanistan but reaches Uzbekistan; (3) Fergan Valley is a separate valley near the China border surrounded by the Tien Shan (mountains) that drains into the Aral Sea; (4) Gobi Desert is located in northcentral China and southern Mongolia; (5) Helmand Block of southern Afghanistan extends to adjacent Pakistan; (6) Junggar Depression is located in extreme northwestern China; (7) Qaidam Depression and Altun mountains are on the northwestern portion of the Tibetan Plateau; (8) Tarim Basin (=Taklimakan Desert) is in northwest China; (9) Thar Desert is located in northwestern India; (10) Zaysan Depression is located in eastern Kazakhstan adjacent to China.

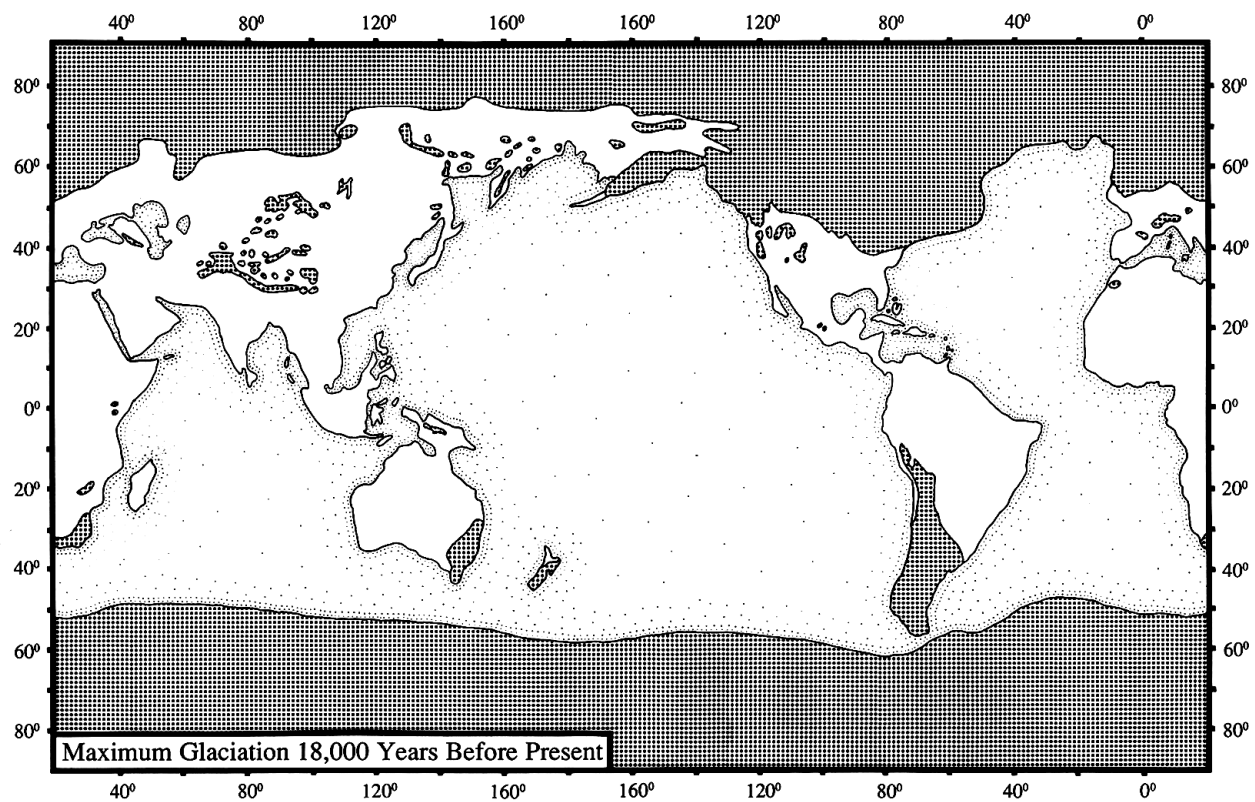


FIGURE 15. Maximum glaciation 18,000 years before present. Much of northern Asia was never fully glaciated, unlike most of high-latitude North America and Europe, lending the possibility of an old history in the north. The map is redrawn from McIntyre *et al.* (1976).

Habitat Evolution in *Phrynocephalus*

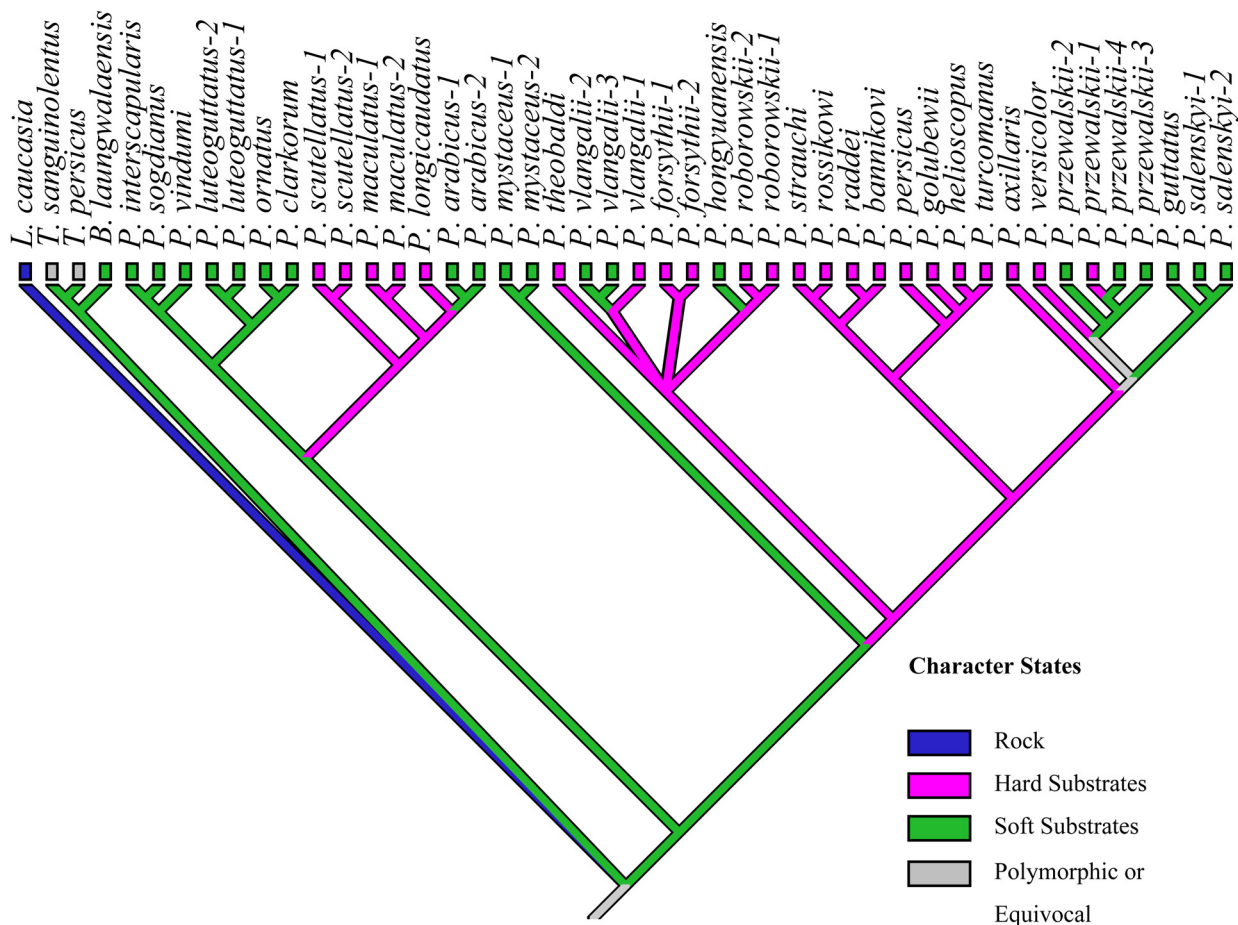


FIGURE 16. Evolution of habitat usage among *Phrynocephalus* species and populations including outgroups. Rock habitat is only used by the outgroup *Laudakia*. Hard substrates are clay, gravel, and dry lakebed. Soft substrates are small sand dune and large sand dune. See table 5 and the methods section for details of habitat categories, and plates I–VIII for images of habitats with species.

Taxa in Southwest Asia and some from the Caspian Basin show a root of being sand dwelling with a switch to hard substrates (*P. scutellatus* populations, *P. maculatus* populations, and *P. longicaudatus*); a reversal to sand habitats is observed among *P. arabicus* populations.

Additional taxa in the Caspian Basin occupy hard substrates with no reversal to a soft substrate (*P. strauchi*, *P. rossikowi*, *P. raddei*, *P. bannikovi*, *P. persicus*, *P. golubewii*, *P. helioscopus*, and *P. turcomanus*).

The ancestral state for taxa in low elevation Chinese deserts is hard substrate with at least one switch to soft substrate, followed by a reversal to hard substrate (*P. przewalskii* population 1).

The viviparous/Tibetan clade which includes taxa from high elevation Tibet and adjacent low elevation Taklimakan Desert consisting of *P. forsythii* populations, *P. roborowskii* populations, *P. hongyuanensis*, *P. vlangalii* populations, and *P. theobaldi*, generally occupy gravel soil types, but require loose soil to dig burrows in which to incubate their young. There are two examples of sampled elements switching from a hard to soft substrate in the viviparous/Tibetan clade: *P. vlangalii* (populations 2 and 3) and *P. hongyuanensis*.

E. *Phrynocephalus* Size Diversity

Phrynocephalus show a variety of snout vent lengths and tail lengths, (Table 6, Appendix 5). Body size per sample ranged from 106 mm for *P. mystaceus* to 35 mm for *P. vindumi* and *P. interscapularis*. Tail length per sample ranges from 133 mm for *P. maculatus* population 1 to 35 mm for *P. luteoguttatus* population 2. *P. mystaceus* and *P.*

interscapularis are sympatric in the Caspian Basin, and habitat partition with *P. mystaceus* in large floating sand dunes, with *P. interscapularis* living on the edge of those large sand dunes, which may revolve around ecotype evolution in a predator-prey relationship. In northwestern Iran *P. vindumi* replaces the role of *P. interscapularis*, and is sympatric with *P. mystaceus*. Tail length appears to be the most sexually dimorphic characteristic.

TABLE 6. Snout-vent lengths (SVL) and tail lengths (TL) for *Phrynocephalus* and outgroups. See appendix 5 for details on sampling. Habitat definitions are: Rock (R), a large rock boulder area; Clay (C), hard clay soil, which does not have gravel; Gravel (G), complex soils that tend to be isolated with unique gravel covers or gravel from alluvial fans draining mountain regions; Dry Lakebed (DL), flat desert dry lakebeds that often have salt deposits; Small Sand Dune (SS), light sand, small sand dunes or edge of large shifting sand dunes; and Large Sand Dune (LS), large shifting sand dunes.

Taxon	Sample No.	Reference	N	SVL	TL	Habitat
<i>L. caucasia</i>	25	CAS:Herp:184561	10	104	110	R
<i>B. laungwalaensis</i>	45	Sharma 1978	male	69	42	LS
			female	54	32	
<i>T. persicus</i>	46	Anderson 1999		97	147	C/G/SS
<i>T. sanguinolentus</i>	26	CAS:Herp:179879	10	102	161	C/G/SS
		CAS:Herp:179850		98	172	
<i>P. scutellatus-1</i>	39	MVZ:Herp:243994	6	50	70	G
		MVZ:Herp:243893		44	71	
<i>P. scutellatus-2</i>	40	CAS:Herp:141193	10	49	72	G
		CAS:Herp:228686		48	73	
<i>P. arabicus-1</i>	27	CAS:Herp:84384	17	57	65	LS
<i>P. arabicus-2</i>	28	CAS:Herp:25573	5	54	74	SS
<i>P. longicaudatus</i>	31	CAS:Herp:251100	Oman 1	62	90	G
		CAS:Herp:84449	Saudi Arabia 11	80	116	
<i>P. maculatus-1</i>	34	MVZ:Herp:250470	8	90	133	DL
<i>P. maculatus-2</i>	35	MVZ:Herp:243677	1	71	78	DL
<i>P. clarkorum</i>	29	CAS:Herp:120232	15	40	59	SS
<i>P. ornatus</i>	37	MVZ:Herp:236917	10	40	59	SS
<i>P. luteoguttatus-1</i>	32	MVZ:Herp:236904	10	45	44	SS
		MVZ:Herp:236907		40	45	
<i>P. luteoguttatus-2</i>	33	CAS:Herp:232122	2	38	35	SS
<i>P. interscapularis</i>	8	CAS:Herp:179189	10	37	36	SS
		CAS:Herp:179172		35	41	
<i>P. sogdianus</i>	20	CAS:Herp:182980	10	41	50	SS
<i>P. vindumi</i>	42	CAS:Herp: 228793	10	37	42	SS
		CAS:Herp: 228794		35	44	
<i>P. persicus</i>	38	CAS:Herp:140824	5	60	49	C/G
<i>P. golubewii</i>	5	CAS:Herp:185159	4	60	86	DL
		ZISP	21	63	63	
		Shammokov 1981	male	67	87	
			female	62	77	
<i>P. helioscopus</i>	7	CAS:Herp:183380	11	51	49	C/SS
		CAS:Herp:183386		42	55	

.....continued on the next page

TABLE 6. (Continued)

Taxon	Sample No.	Reference	N	SVL	TL	Habitat	
<i>P. turcomanus</i>	22	CAS:Herp:184795	10	57	67	C	
		CAS:Herp:184796		50	68		
<i>P. mystaceus</i> -1	9	CAS:Herp:179754	11	106	110	LS	
<i>P. mystaceus</i> -2	36	CAS:Herp: 228633	10	106	103	LS	
		CAS:Herp: 228632		104	107		
<i>P. axillaris</i>	1	MVZ:Herp:208893	10	57	72	C	
		MVZ:Herp:208891		56	85		
<i>P. bannikovi</i>	2	CAS:Herp:184585	10	50	64	G	
		CAS:Herp:184584		49	68		
<i>P. raddei</i>	14	CAS:Herp:179779	10	46	53	G	
		CAS:Herp:179772		45	54		54
<i>P. rossikowi</i>	17	CAS:Herp:179645	18	40	46	G	
		CAS:Herp:179646		36	48		
<i>P. strauchi</i>	41	ZISP	6	55	82	G	
		Sattarov 1993		males	50		82
				females	49		72
<i>P. forsythii</i> -1	3	CAS:Herp:197127	2	45	61	G	
<i>P. forsythii</i> -2	4	CAS:Herp:167820	7	44	46	G	
		CAS:Herp:167822		38	51		
<i>P. roborowskii</i> -1	15	MVZ:Herp:211585	10	63	57	G	
		MVZ:Herp:211572		60	66		
<i>P. roborowskii</i> -2	16	CAS:Herp:167510	8	60	68	G	
<i>P. hongyuanensis</i>	30	MVZ:Herp:216685	14	55	56	SS	
		MVZ:Herp:216689		54	59		
<i>P. vlangalii</i> -1	24	MVZ:Herp:211539	10	64	56	G	
		MVZ:Herp:211555		62	65		
<i>P. vlangalii</i> -2	43	MVZ:Herp:272845	5	61	58	SS	
<i>P. vlangalii</i> -3	44	MVZ:Herp:272849	4	57	58	SS	
<i>P. theobaldi</i>	21	CAS:Herp:171731	10	56	42	G	
		CAS:Herp:171733		48	51		
<i>P. guttatus</i>	6	MVZ:Herp:216024	10	49	59	SS	
		MVZ:Herp:216028		46	62		
<i>P. salenskyi</i> -1	18	CAS:Herp:171631	10	59	70	LS	
		CAS:Herp:171596		57	75		
<i>P. salenskyi</i> -2	19	CAS:Herp:183390	5	56	70	SS	
		CAS:Herp:183391		51	76		
<i>P. versicolor</i>	23	CAS:Herp: 170915	10	49	59	C/G	
		CAS:Herp: 170916		48	65		
<i>P. przewalskii</i> -1	10	CAS:Herp:166171	10	62	90	C/G	
<i>P. przewalskii</i> -2	11	CAS:Herp:166970	10	55	80	SS	
<i>P. przewalskii</i> -3	12	CAS:Herp:166823	11	68	90	LS	
		CAS:Herp:166844		65	102		
<i>P. przewalskii</i> -4	13	CAS:Herp:167167	10	66	90	LS	

Snout vent lengths for clay ecotypes range from 62 mm for *P. przewalskii* population 1 to 49 mm for *P. versicolor*, with tail lengths ranging from 90 mm for *P. przewalskii* population 1 to 49 mm for *P. persicus*.

The snout vent length for gravel ecotypes range from 64 mm for *P. vlangalii* population 1 to 40 mm for *P. rossikowi*, with tail lengths ranging from 90 mm for *P. longicaudatus* to 42 mm for *P. theobaldi*.

Snout vent lengths for dry lakebed ecotypes range from 90 mm for *P. maculatus* population 1 to 60 mm for *P. golubewii*, with tail length ranging from 133 mm for *P. maculatus* population 1 to 78 mm for *P. maculatus* population 2.

Snout vent lengths for small sand dune ecotypes range from 61 mm for *P. vlangalii* population 2 to 35 mm for both *P. vindumi* and *P. interscapularis*, with tail length ranging from 80 mm for *P. przewalskii* population 2 to 35 mm for *P. luteoguttatus* population 2.

Snout vent lengths for large sand dune ecotypes range from 106 mm for *P. mystaceus* populations to 59 mm for *P. salenskyi* population 1, with tail lengths ranging from 110 mm for *P. mystaceus* population 1 to 70 mm for *P. salenskyi* population 1.

The largest *Phrynocephalus* occupy large floating sand dunes, and the smallest *Phrynocephalus* species are found on the fringes of large floating sand dunes in the Caspian Basin and northern Iran. *P. mystaceus* occupying large sand dunes in these habitats coexists with the two smallest species that occupy the fringes of those sand dunes, *P. interscapularis* in the Caspian Basin, and *P. vindumi* in northwestern Iran. It has not escaped our attention that size and habitat partitioning may have occurred in these regions because it is likely that smaller species (*P. interscapularis* or *P. vindumi*) serve as a food source for larger species (*P. mystaceus*). Further work is needed for phylogenetic assessment of size evolution among *Phrynocephalus* species and populations considering the sexually dimorphic nature of this genus, both with body size and tail length.

F. *Phrynocephalus* Species Diversity as Related to Geology, Habitat and Size

Two regions show high species numbers in close proximity. Six species are found on the northern side of the Kopet-Dagh (mountains) along the southern margin of the Caspian Basin in Turkmenistan. Species that inhabit hard substrates are *P. rossikowi*, *P. raddei*, *P. bannikovi*, *P. golubewii*, and *P. turcomanus*, with *P. interscapularis* and *P. mystaceus* occurring in soft substrates (Table 5, Fig. 16). Among these species there are major size differences (Table 6).

Six species are also found at the juncture of the Helmand Basin of southern Afghanistan with the Baluchistan Plateau including the base of the Sulaiman Range of southern Pakistan. Species that inhabit hard substrates are *P. maculatus* and *P. scutellatus* (Table 5, Fig. 16). Smaller species that inhabit soft substrates are *P. clarkorum*, *P. ornatus*, and *P. luteoguttatus* (Clade C in Figs. 4 and 8). A larger species inhabiting soft substrates in large floating sand dunes is *P. euptilopus*, which was not sampled in this study even though repeated efforts were made in both Afghanistan and Pakistan by the last author. Among these species there are major size differences (Table 6).

Both of these examples share a plate tectonic past around the northern migration of the Arabian Plate and its impact on ancient tectonic plates to the north in Eurasia. The Kopet-Dagh (mountains), on the northern margin of the Iranian Plateau, descends into the Caspian Basin. This region of the Caspian Basin experienced the most dramatic changes via tectonic uplift, erosion, and sea floor drying of the Paratethys Sea creating unique and diversified habitats (see Figs. 3, 9–14; Table 4). Additionally, the Helmand Block of southern Afghanistan is being pushed south by impinging Arabia and further northern invasion of the Indian Plate (Fig. 9). This has created uplift in the Gulf of Oman creating the push-back of the Makran in southern Pakistan (Figs. 9–12).

It is dynamic tectonics of this nature that created a series of habitats leading to speciation among *Phrynocephalus*. As adaptive niches were created, size diversity, morphological specializations, background matching, and defensive mimicry developed (Plates I–VIII). Future work on *Phrynocephalus* will need to take into account these aspects with particular attention to plate tectonic induced events in order to investigate phyletic patterns, taxonomy, and evolutionary diversity among one of the world's most interesting and confusing lizard genera.



A



B



C



D



E



F

PLATE I. Species of the Arabian Peninsula and Iranian Plateau. (A) *P. arabicus*-2; (B) habitat of A, near Al Ashkhara, Oman; (C) *P. longicaudatus*; (D) habitat of C, near Al Hij, Bar Al Hikman Peninsula, Oman; (E) *P. maculatus*-2; and (F) habitat of E, near Sirjan, southern Iran.



A



B



C



D



E



F

PLATE II. Species of the Helmand Basin in Afghanistan and Iranian Plateau. (A) *P. luteoguttatus*; (B) *P. clarkorum*; (C) *P. ornatus*; (D) habitat of A and B, Registan Desert, Afghanistan; (E) *P. scutulatus*; and (F) habitat of E, near Khabr, southern Iran.



A



B



C



D



E



F

PLATE III. Species of southern Tibet and soft substrate habitats in the Caspian Basin. (A) *P. theobaldi*; (B) habitat of A, near Yangbajain, north of Lhasa, southern Tibet; (C) *P. sogdianus*; (D) *P. interscapularis*; (E) *P. mystaceus*; and (F) habitat of D and E, Karakum Desert, north of Ashkhabad, Turkmenistan.



A



B



C



D



E



F

PLATE IV. Small species inhabiting hard substrates in the Caspian Basin of Turkmenistan. (A) *P. rossikowi*; (B) habitat of A, along the Amu-Darya River; (C) *P. raddei*; (D) habitat of C, Karakum Desert, north of Ashkhabad; (E) *P. bannikovi*; and (F) habitat of E, Big Balkan Mountains.



A



B



C



D



E



F

PLATE V. Large species inhabiting hard substrates in the Caspian Basin of Turkmenistan (A-D) and Kazakhstan (E-F). (A) *P. golubewii*; (B) habitat of A, near Bami, southern edge of Karakum Desert; (C) *P. turcomanus*; (D) habitat of C, southern edge of Karakum Desert; (E) *P. helioscopus*; and (F) habitat of E, Barsakel'mes Island, Aral Sea.



A



B



C



D



E



F

PLATE VI. Species of the northern Tibetan Plateau. (A) *P. hongyuanensis*; (B) habitat of A, near Waqên, northeastern Tibet in Sichuan Province; (C) *P. roborowskii*-1; (D) habitat of C, Chaka Depression, Qinghai Province; (E) *P. vlangalii*-1; and (F) habitat of E, near Heimahe, south side of Qinghai Lake, Qinghai Province.



A



B



C



D



E



F

PLATE VII. Species of the low elevation deserts in China (A-D) and northern Caspian Basin in Russia (E-F). (A) *P. przewalskii*-3; (B) habitat of A, Shapatou (foreground), Yellow River, Gobi Desert, Ningxia; (C) *P. salenskyi*-1; (D) habitat of C, near Jimsar, Junggar Depression, Xinjiang; (E) *P. guttatus*; and (F) habitat of E, west side of Caspian Sea in Dagestan.



A



B



C



D



E



F

PLATE VIII. Outgroup taxa and *Phrynocephalus* mimicry adaptations. (A) *Laudakia caucasia*; (B) habitat of A, Big Balkan Mountains, Turkmenistan; (C) *Trapelus sanguinolentus*; (D) habitat of C, Repetek, Karakum Desert, Turkmenistan; (E) *P. turcomanus* illustrating false large head with eyes on body-back; and (F) *P. mystaceus* illustrating false enlarged mouth with red capillary-beds.

Acknowledgments

Carol Spencer provided information on collection database networks. Jens Vindum assisted with specimens and tissues at the California Academy of Sciences, San Francisco. Johnathan B. Losos advised on measurement data. David B. Wake provided information on *Ensatina* salamanders. Zhili Fang, Hooman Jokar, Azita N. Macey, Sakhat M. Shammakov, Boris S. Tuniyev, Ermi Zhao and Hooshang Ziaie assisted with fieldwork. Henry Fabian facilitated work at Merritt College. The late Ilya S. Darevsky and late Ermi Zhao fostered collaborations in China and the USSR. Robert I. Macey provided the atlas that allowed JRM to come up with the idea to go to China and the USSR in the 1980's. JRM thanks Dr. Lamont D. Paxton for correcting a major health crisis, thus ensuring this work is published. Support provided by Russian Foundation Basic Research Grant No. RFBR 18-04-00040. Isabella C. Espinoza, Emily C. Chau, Giovanni L. Lara, and Theodore W. Wismar provided editorial assistance.

References

- Abdrakhmatov, K.Ye., Aldazhanov, S.A., Hager, B.H., Hamburger, M.W., Herring, T.A., Kalabaev, K.B., Makakarov, V.I., Molnar, P., Pananasyuk, S.V., Prilepin, M.T., Reilinger, R.E., Sadybakasov, I.S., Souter, B.J., Trapeznikov, Y.A., Tsurkov, V.Ye. & Zubovich, A.V. (1996) Relatively recent construction of the Tien Shan inferred from GPS measurements of present-day crustal deformation rates. *Nature*, 384, 450–453.
<https://doi.org/10.1038/384450a0>
- Anderson, J. (1872) On some Persian, Himalayan, and other Reptiles. *Proceedings of the Zoological Society of London*, 1872 (2), 371–404.
- Anderson, S.C. (1999) *The Lizards of Iran*. Contribution to Herpetology 15, Society for the Study of Amphibians and Reptiles, Oxford, Ohio, 442 pp.
- Baig, K.J., Wagner, P., Ananjeva, N.B. & Böhme, W. (2012) A morphology-based taxonomic revision of *Laudakia* Gray, 1845 (Squamata: Agamidae). *Vertebrate Zoology*, 62 (2), 213–260.
- Bannikov, A.G., Darevsky, I.S., Ischchenko, V.G., Rustamov, A.K. & Szczerbak, N.N. (1977) *Opredelitel' Zemnovodnikh i Presmikayushchikhsya Fauni SSSR* [Guide to the Reptile and Amphibian Fauna of the USSR]. Prosveshchenie, Moscow, 415 pp., figs. 1–108, 135 maps, 32 col. pls. [in Russian]
- Barabanov, A.V. & Ananjeva, N.B. (2007) Catalogue of the available scientific species-group names for lizards of the genus *Phrynocephalus* Kaup, 1825 (Reptilia, Sauria, Agamidae). *Zootaxa*, 1399, 1–56.
<https://doi.org/10.11646/zootaxa.1399.1.1>
- Bedriaga, J. (“1905” 1906) Verzeichnis der von der Central-Asiatischen Expedition unter Stabs-Kapitän W. Roborowski in den Jahren 1893-1895 gesammelten Reptilien. *Annuaire du Musée Zoologique de l'Académie Impériale des Sciences de St.-Pétersbourg*, 10 (3–4), 159–200.
- Bedriaga, J. (1907) Amphibien und Reptilien (Reptilia Przewalskiana). *Wissenschaftliche Resultate der von N.M. Przewalski nach Central-Asien unternommenen Reisen*. Zoologischer Theil, Bd. 3, Abth. 1, Lfrg. 2, St. Petersburg, pp. 71–278.
- Bedriaga, J. (1909) Amphibien und Reptilien (Reptilia Przewalskiana). *In: Wissenschaftliche Resultate der von N.M. Przewalski nach Central-Asien unternommenen Reisen*. Zoologischer Theil, Bd. 3, Abth. 1, Lfrg. 3, St. Petersburg, pp. 279–502.
- Bermingham, E., McCafferty, S.S. & Martin, A.P. (1997) Fish biogeography and molecular clocks: Perspectives from the Panamanian Isthmus. *In: Kocher, T.D & Stepien C.A, (Eds.), Molecular Systematics of Fishes*. Academic Press, San Diego, pp. 113–128.
<https://doi.org/10.1016/B978-012417540-2/50009-9>
- Blanford, W.T. (1876) List of Reptilia and Amphibia collected by the late Dr. Stoliczka in Kashmir, Ladák, Eastern Turkestan and Wakhán, with descriptions of new species. *Journal of the Asiatic Society of Bengal*, 44 (3), 191–196.
- Bogdanov, O.P., Atayev, Ch. & Shammakov, S. (1974) The finding of *Phrynocephalus maculatus* in the USSR. *Zoologicheskij Zhurnal*, Moscow, 53 (2), 304–305. [in Russian]
- Boettger, O. (1888) Über die Reptilien und Batrachier Transcaspiens. *Zoologischer Anzeiger*, Leipzig, 11 (279), 259–263.
- Boulenger, G.A. (1887) *Catalogue of the Lizards in the British Museum (Natural History), Second Edition. Vol. 3. Lacertidae, Gerrhosauridae, Scincidae, Anelytropidae, Dibamidae, Chamaeleontidae*. Trustees of the British Museum, London, 575 pp.
- Buth, D.G. (1984) The application of electrophoretic data in systematic studies. *Annual Review of Ecology and Systematics*, 15, 501–522.
<https://doi.org/10.1146/annurev.es.15.110184.002441>
- Chernov, S.A. (1948) Reptiles — Reptilia. *In: Pavlovsky, E.N. & Vinogradova, B.S. (Eds.), The Animals of the USSR. Vol. 2. The desert zone*. USSR Academy of Sciences, Moscow-Leningrad, pp. 127–161. [in Russian]
- Clayton, J.W. & Tretiak, D.N. (1972) Amine-citrate buffers for pH control in starch gel electrophoresis. *Journal of the Fisheries Research Board Canada*, 29, 1169–1172.

<https://doi.org/10.1139/f72-172>

- Darevsky, I.S., Rustamov, A.K. & Shammakov, S. (1976) Status and distribution of *Phrynocephalus reticulatus* Eichwald (Sauria, Agamidae) in Central Asia. *Teoreticheskiye i prikladnyye aspekty okhrany prirody i okhotovedeniya*, Moscow, 84, 113–119. [in Russian]
- Dercourte, J., Zonenshain, L.P., Ricou, L.-E., Kazmin, V.G., Le Pichon, X., Knipper, A.L., Grandjacquet, C., Sbornikov, I.M., Geysant, J., Lepvrier, C., Pechersky, D.H., Boulin, J., Sibuet, J.-C., Savostin, L.A., Sorokhtin, O., Westphal, M., Bazhenov, M.L., Lauer, J.P. & Biju-Duval, B. (1986) Geological evolution of the Tethys belt from the Atlantic to the Pamirs since the Lias. *Tectonophysics*, 123, 241–315. [with maps, plates I–X]
- Dewey, J.F., Shackleton, R.M., Chang, C. & Sun, Y. (1988) The tectonic evolution of the Tibetan Plateau. In: *The Geological Evolution of Tibet. Report of the 1985 Royal Society – Academia Sinica Geotraverse of the Qinghai – Xizang Plateau Led by Chang Chengfu, Robert M. Shackleton, F.R.S, John F. Dewey, F.R.S., and Yin Jixiang*. Philosophical Transactions of the Royal Society of London, London, A 327 (1594), pp. 379–313.
<https://doi.org/10.1098/rsta.1988.0135>
- Dewey, J.F., Cande, S. & Pitman, W.C., III. (1989) Tectonic evolution of the India/Eurasia collision zone. *Eclogae Geologicae Helveticae*, 82 (3), 717–734.
<https://doi.org/10.5169/seals-166399>
- Dunayev, E.A. (1995) Reviewed description of the types of *Phrynocephalus strauchi* Nikolsky, 1899 (Squamata, Agamidae) and materials on the history of its study, distribution, and variability. *Russian Journal of Herpetology*, 2 (2), 87–94.
- Eichwald, E. (1831) *Zoologia specialis quam expositis animalibus tum vivis, tum fossilibus potissimum Rossiae in universum, et Poloniae in specie, in usum lectionum publicarum in Universitate Caesarea Vilnensi habendarum. Pars posterior*. Josephi Zawadzki, Vilnae, 396 pp.
- Felsenstein, J. (1985) Confidence limits on phylogenies with a molecular clock. *Systematic Zoology*, 34 (4), 152–161.
<https://doi.org/10.1111/j.1558-5646.1985.tb00420.x>
- Feng, Y., Coleman, R.G., Tilton, G. & Xiao, X. (1989) Tectonic evolution of the west Junggar region, Xinjiang, China. *Tectonics*, 8 (4), 729–752.
<https://doi.org/10.1029/TC008i004p00729>
- Golubev, M.L. (1991) About the name *Agama ocellata* Lichtenstein in Eversmann, 1823 (Reptilia, Agamidae) with redescription of the types. *Herpetological Researches*, Leningrad, 1, 12–17. [in Russian with English summary]
- Golubev, M.L. (1998) A new subspecies of *Phrynocephalus ornatus* Boulenger (Reptilia: Agamidae) from Eastern Iran, with a key to South-Western and Middle Asian microphrynocephalids. *Hamadryad*, 23 (2), 162–168.
- Gozdik, A. & Fu, J. (2009) Are Toad-Headed lizards *Phrynocephalus przewalskii* and *P. frontalis* (family Agamidae) the same species? Defining species boundaries with morphological and molecular data. *Russian Journal of Herpetology*, 16 (2), 107–118.
- Haas, G. (1957) Some amphibians and reptiles from Arabia. *Proceedings of the California Academy of Sciences*, 29 (3), 47–86.
- Hall, R. (1996) Reconstructing Cenozoic SE Asia. In: Hall, R. & Blundell, D. (Eds.), *Reconstructing Cenozoic SE Asia*. Geological Society of London Special Publication No. 106, London, pp. 153–184.
<https://doi.org/10.1144/GSL.SP.1996.106.01.11>
- Harris, H. & Hopkinson, D.A. (1976 et seq.) *Handbook of Enzyme Electrophoresis in Human Genetics*. Oxford: North Holland Publishing Co., Amsterdam. [loose leaf with supplements in 1977 and 1978]
- Jackman, T.R. & Wake, D.B. (1994) Evolutionary and historical analysis of protein variation in the blotched forms of salamanders of the *Ensatina* complex (Amphibia: Plethodontidae). *Evolution*, 48 (3), 876–897.
<https://doi.org/10.1111/j.1558-5646.1994.tb01369.x>
- Jiang, Y.-M., Huang, Q.-Y. & Zhao, E.-M. (1980) A new subspecies of *Phrynocephalus vlangalii* (Strauch) and preliminary observation on its ecology. *Acta Zoologica Sinica*, Beijing, 26 (2), 178–183. [in Chinese with English summary]
- Jin, Y.-T., Brown, R.P. & Liu, N.-F. (2008) Cladogenesis and phylogeography of the lizard *Phrynocephalus vlangalii* (Agamidae) on the Tibetan plateau. *Molecular Ecology*, 17 (8), 1971–1982.
<https://doi.org/10.1111/j.1365-294X.2008.03721.x>
- Jin, Y.-T. & Brown, R.P. (2013) Species history and divergence times of viviparous and oviparous Chinese toad-headed sand lizards (*Phrynocephalus*) on the Qinghai-Tibetan Plateau. *Molecular Phylogenetics and Evolution*, 68 (2), 259–268.
<https://doi.org/10.1016/j.ympev.2013.03.022>
- Kamali, K. & Anderson, S.C. (2015) A new Iranian *Phrynocephalus* (Reptilia: Squamata: Agamidae) from the hottest place on earth and a key to the genus *Phrynocephalus* in southwestern Asia and Arabia. *Zootaxa*, 3904 (2), 249–260.
<https://doi.org/10.11646/zootaxa.3904.2.4>
- Kaup, J.J. (1825) Einige Bemerkungen zu Merrems Handbuch [Some Remarks on Merrem's Handbook]. *Isis von Oken*, 16, cols., 589–593. [in German]
- Kuchta, S.R., Parks, D.S., Mueller, R.L. & Wake, D.B. (2009) Closing the ring: Historical biogeography of the salamander ring species *Ensatina eschscholtzii*. *Journal of Biogeography*, 36 (5), 982–995.
<https://doi.org/10.1111/j.1365-2699.2008.02052.x>
- Kumazawa, Y. & Nishida, M. (1993) Sequence evolution of mitochondrial transfer RNA genes and deep-branch animal phylogenetics. *Journal of Molecular Evolution*, 37 (4), 380–398.
<https://doi.org/10.1007/BF00178868>

- Kwon, S.-T., Tilton, R.G., Coleman, R.G. & Feng, Y. (1989) Isotopic studies bearing on the tectonics of the west Junggar region, Xinjiang, China. *Tectonics*, 8 (4), 719–727.
<https://doi.org/10.1029/TC008i004p00719>
- Lanfear, R., Calcott, B., Ho, S.Y.W. & Guindon, S. (2012) PartitionFinder: Combined selection of partitioning schemes and substitution models for phylogenetic analyses. *Molecular Biology and Evolution*, 29 (6), 1695–1701.
<https://doi.org/10.1093/molbev/mss020>
- Larson, A. (1994) The comparison of morphological and molecular data in phylogenetic systematics. In: Schierwater, B., Streit, B., Wagner, G.P. & DeSalle, R. (Eds.), *Molecular Ecology and Evolution: Approaches and Applications*. Birkhäuser Verlag, Basel, pp. 371–390.
https://doi.org/10.1007/978-3-0348-7527-1_22
- Leviton, A.E. & Anderson, S.C. (2010) The herpetological literature for Southwestern Asia: An indexed bibliography. *Occasional Papers of the California Academy of Sciences*, No. 157, i–vii, 1–622.
- Leviton, A.E. & Anderson, S.C. (2013) The herpetological literature for Southwestern Asia: An indexed bibliography Second Edition. *Occasional Papers of the California Academy of Sciences*, No. 161, i–x, 1–944.
- Lichtenstein, H. (1856) *Nomenclator Reptilium et Amphibiorum Musei Zoologici Berolinensis. Namenverzeichnis der in der zoologischen Sammlung der Königlichen Universität zu Berlin aufgestellten Arten von Reptilien und Amphibien nach ihren Ordnungen, Familien und Gattungen*. Königlich Preussischen Akademie der Wissenschaften, Berlin, 48 pp. [in German]
- Mabee, P.M. & Humphries, J. (1993) Coding polymorphic data: Examples from allozymes and ontogeny. *Systematic Biology*, 42 (2), 166–181.
<https://doi.org/10.1093/sysbio/42.2.166>
- Macey, J.R. (2005) Plethodontid salamander mitochondrial genomics: A parsimony evaluation of character conflict and implications for historical biogeography. *Cladistics*, 21 (2), 194–202.
<https://doi.org/10.1111/j.1096-0031.2005.00054.x>
- Macey, J.R., Larson, A., Ananjeva, N.B., Fang, Z.L. & Papenfuss, T.J. (1997a) Two novel gene orders and the role of light-strand replication in rearrangement of the vertebrate mitochondrial genome. *Molecular Biology and Evolution*, 14 (1), 91–104.
<https://doi.org/10.1093/oxfordjournals.molbev.a025706>
- Macey, J.R., Larson, A., Ananjeva, N.B. & Papenfuss, T.J. (1997b) Replication slippage may cause parallel evolution in the secondary structures of mitochondrial transfer RNAs. *Molecular Biology and Evolution*, 14 (1), 30–39.
<https://doi.org/10.1093/oxfordjournals.molbev.a025699>
- Macey, J.R., Larson, A., Ananjeva, N.B. & Papenfuss, T.J. (1997c) Evolutionary shifts in three major structural features of the mitochondrial genome among iguanian lizards. *Journal of Molecular Evolution*, 44 (6), 660–674.
<https://doi.org/10.1007/PL00006190>
- Macey, J.R. & Verma, A. (1997) Homology in phylogenetic analysis: Alignment of transfer RNA genes and the phylogenetic position of snakes. *Molecular Phylogenetics and Evolution*, 7 (2), 272–279.
<https://doi.org/10.1006/mpev.1997.0379>
- Macey, J.R., Schulte, J.A. II, Ananjeva, N.B., Larson, A., Rastegar-Pouyani, N., Shammakov, S.M. & Papenfuss, T.J. (1998a) Phylogenetic relationships among agamid lizards of the *Laudakia caucasia* species group: Testing hypotheses of biogeographic fragmentation and an area cladogram for the Iranian Plateau. *Molecular Phylogenetics and Evolution*, 10 (1), 118–131.
<https://doi.org/10.1006/mpev.1997.0478>
- Macey, J.R., Schulte, J.A. II, Larson, A., Fang, Z., Wang, Y., Tuniyev, B.S. & Papenfuss, T.J. (1998b) Phylogenetic relationships of toads in the *Bufo bufo* species group from the eastern escarpment of the Tibetan Plateau: A case of vicariance and dispersal. *Molecular Phylogenetics and Evolution*, 9 (1), 80–87.
<https://doi.org/10.1006/mpev.1997.0440>
- Macey, J.R., Wang, Y., Ananjeva, N.B., Larson, A. & Papenfuss, T.J. (1999) Vicariant patterns of fragmentation among gekkonid lizards of the genus *Teratoscincus* produced by the Indian Collision: A molecular phylogenetic perspective and an area cladogram for Central Asia. *Molecular Phylogenetics and Evolution*, 12 (3), 320–332.
<https://doi.org/10.1006/mpev.1999.0641>
- Macey, J.R., Schulte, J.A. II & Larson, A. (2000a) Evolution and phylogenetic information content of mitochondrial genomic structural features illustrated with acrodont lizards. *Systematic Biology*, 49 (1), 257–277.
<https://doi.org/10.1093/sysbio/49.2.257>
- Macey, J.R., Schulte, J.A. II, Larson, A., Ananjeva, N.B., Wang, Y., Pethiyagoda, R., Rastegar-Pouyani, N. & Papenfuss, T. J. (2000b) Evaluating trans-Tethys migration: An example using acrodont lizard phylogenetics. *Systematic Biology*, 49 (2), 233–256.
<https://doi.org/10.1093/sysbio/49.2.233>
- Macey, J.R., Schulte, J.A. II, Fong, J.J., Das, I. & Papenfuss, T.J. (2006) The complete mitochondrial genome of an agamid lizard from the Afro-Asian subfamily Agaminae and the phylogenetic position of *Bufoinceps* and *Xenagama*. *Molecular Phylogenetics and Evolution*, 39 (3), 881–886.
<https://doi.org/10.1016/j.ympev.2005.08.020>

- Maddison, W.P. & Maddison, D.R. (2000) *MacClade4: Analysis of Phylogeny and Character Evolution*. Sinauer Associates, Sunderland, MA.
- Maniatis, T.E., Fritsch, F. & Sambrook, J. (1982) *Molecular Cloning: A Laboratory Manual*. Cold Spring Harbor Laboratory, Cold Spring Harbor, NY, 545 pp.
- McIntyre, A., Moore, T.C., Andersen, B., Balsam, W., Bé, A., Brunner, C., Cooley, J., Crowley, T., Denton, G., Gardner, J., Geitzenauer, K., Hays, J.D., Hutson, W., Imbrie, J., Irwing, G., Kellogg, T., Kennett, J., Kipp, N., Kukla, G., Kukla, H., Lozano, J., Luz, B., Mangion, S., Matthews, R.K., Mayewski, P., Molfino, B., Ninkovich, D., Opdyke, N., Prell, W., Robertson, J., Ruddiman, W.F., Sachs, H., Saito, T., Shackleton, N., Thierstein, H. & Thompson, P. (1976) The surface of the ice-age earth. *Science*, 191 (4232), 1131–1137.
<https://doi.org/10.1126/science.191.4232.1131>
- Melnikov, D., Melnikova, E., Nazarov, R., Al-Johany, A. & Ananjeva, N.B. (2015) A new species of *Phrynocephalus* (Agamidae, Sauria) from Al Sharqiyah sands, northeastern Oman, dedicated to the memory of Sako Tuniyev (1983 – 2015). *Russian Journal of Herpetology*, 22 (4), 301–309.
- Melville, J., Hale, J., Mantziou, G., Ananjeva, N.B., Milto, K. & Clemann, N. (2009) Historical biogeography, phylogenetic relationships and intraspecific diversity of agamid lizards in the Central Asian deserts of Kazakhstan and Uzbekistan. *Molecular Phylogenetics and Evolution*, 53 (1), 99–112.
<https://doi.org/10.1016/j.ympev.2009.05.011>
- Mertens, R. & Müller, L. (1928) Liste der Amphibien und Reptilien Europas. *Abhandlungen der Senckenbergischen Naturforschenden Gesellschaft*, 41 (1), 1–62.
- Metcalfe, I. (1996) Pre-Cretaceous evolution of SE Asia terranes. In: Hall, R. & Blundell, D. (Eds.), *Tectonic Evolution of Southeast Asia*. Geological Society of London Special Publication No. 106, London, pp. 97–122.
- Miller, M.A., Pfeiffer, W. & Schwartz, T. (2010) Creating the CIPRES Science Gateway for inference of large phylogenetic trees. *Proceedings of the Gateway Computing Environments Workshop (GCE)*, 14 Nov. 2010, 1–8.
<https://doi.org/10.1109/GCE.2010.5676129>
- Molnar, P., Burchfiel, B.C., Liang, K. & Zhao, Z. (1987) Geomorphic evidence for active faulting in the Altyn Tagh and northern Tibet and qualitative estimates of its contribution to the convergence of India and Eurasia. *Geology*, 15 (3), 249–253.
[https://doi.org/10.1130/0091-7613\(1987\)15<249:GEFAFI>2.0.CO;2](https://doi.org/10.1130/0091-7613(1987)15<249:GEFAFI>2.0.CO;2)
- Moritz, C., Dowling, T.E. & Brown, W.M. (1987) Evolution of animal mitochondrial DNA: Relevance for population biology and systematics. *Annual Review of Ecology and Systematics*, 18, 269–292.
<https://doi.org/10.1146/annurev.es.18.110187.001413>
- Mouthereau, F., Lacombe, O. & Vergés, J. (2012) Building the Zagros collisional orogen: Timing, strain distribution and the dynamics of Arabia/Eurasia plate convergence. *Tectonophysics*, 532–535, 27–60.
<https://doi.org/10.1016/j.tecto.2012.01.022>
- Murphy, R.W., Sites, J.W. Jr., Buth, D.G. & Haufler, C.H. (1990) Proteins I: Isozyme electrophoresis. In: Hillis, D.M. & Moritz, C. (Eds.), *Molecular Systematics*. Sinauer Associates, Sunderland, MA, pp. 45–126.
- Nikolsky, A.M. (1899) Reptiles and amphibians of the Turkestan general-governorship (Herpetologia Turanica). In: Fedchenko, A.P. (Ed.), *Travel to the Turkestan of the member-founder of the A.P. Fedchenko Society, accomplished on behalf of the Imperial Society of Amateurs of natural history, anthropology, and ethnography*. Zoogeographical Investigations. University Publishing, Moscow, Issue 23, Vol. 2, part 7, pp. 21–84. [in Russian]
- Nikolsky, A.M. (1905) Reptiles and amphibians of the Russian Empire (Herpetologica Rossica). *Mémoires de l'Académie Impériale des Sciences de St.-Petersbourg*, 17 (1), 518 pp. [in Russian]
- Nikolsky A. M. (1916) *Faunae de la Russie et des pays limitrophes fondée principalement sur les collections du Musée Zoologique de l'Académie Impériale des Sciences de Petrograd. Reptiles (Reptilia). Vol. II. Ophidia*. Imperial Academy of Sciences, Petrograd. 349 pp. [in Russian with French title]
- Noble, D.W.A., Qi, Y. & Fu, J. (2010) Species delineation using Bayesian model-based assignment tests: A case study using Chinese toad-headed agamas (genus *Phrynocephalus*). *BMC Evolutionary Biology*, 2010 (10), 197.
<https://doi.org/10.1186/1471-2148-10-197>
- Pallas, P.S. (1771) *Reise durch verschiedene Provinzen des Russischen Reichs*. Bd.I. St.Petersburg: Kayserliche Academie der Wissenschaften, 540 pp.
- Pang, J., Wang, Y., Zhong, Y., Hoelzel, A.R., Papenfuss, T.J., Zeng, X., Ananjeva, N.B. & Zhang, Y.-P. (2003) A phylogeny of Chinese species in the genus *Phrynocephalus* (Agamidae) inferred from mitochondrial DNA sequences. *Molecular Phylogenetics and Evolution*, 27 (3), 398–409.
[https://doi.org/10.1016/S1055-7903\(03\)00019-8](https://doi.org/10.1016/S1055-7903(03)00019-8)
- Qi, Y., Yang, W., Lu, B. & Fu, J. (2013) Genetic evidence for male-biased dispersal in the Qinghai toad-headed agamid *Phrynocephalus vlangalii* and its potential link to individual social interactions. *Ecology and Evolution*, 3 (5), 1219–1230.
<https://doi.org/10.1002/ece3.532>
- Richardson, B.J., Baverstock, P.R. & Adams, M. (1986) *Allozyme Electrophoresis. A Handbook for Animal Systematics and Population Studies*. Academic Press, Sydney, 410 pp.
- Richter, B. & Fuller, M. (1996) Palaeomagnetism of the Sibumasu and Indochina blocks: Implications for the extrusion tectonic model. In: Hall, R. & Blundell, D. (Eds.), *Reconstructing Cenozoic SE Asia*. Geological Society of London Special

- Publication No. 106, London, pp. 203–224.
<https://doi.org/10.1144/GSL.SP.1996.106.01.13>
- Royden, L.H., Burchfiel, B.C. & van der Hilst, R.D. (2008) The Geological Evolution of the Tibetan Plateau. *Science*, 321 (5892), 1054–1058.
<https://doi.org/10.1126/science.1155371>
- Sattarov, T.S. (1993) *Reptiles of North Tajikistan*. Donish, Dushanbe, 276 pp. [in Russian]
- Selander, R.K., Smith, H.M., Yang, S.Y., Johnson, W.E. & Gentry, J.R. (1971) Biochemical polymorphism and systematics in the genus *Peromyscus*. I. Variation in the old-field mouse (*Peromyscus polionotus*). *Studies in Genetics VI, University of Texas Publication*, 7103, 49–90.
- Sengör, A.M.C. (1984) The Cimmeride orogenic system and the tectonics of Eurasia. *Geological Society of America, Special Paper No. 195*, 1–82.
<https://doi.org/10.1130/SPE195-p1>
- Sengör, A.M.C., Altiner, D., Cin, A., Ustaomer, T. & Hsu, K.J. (1988) Origin and assembly of the Tethyside orogenic collage at the expense of Gondwana Land. In: Audley-Charles, M.G. & Hallam, A. (Eds.), *Gondwana and the Tethys*. Geological Society Special Publication No. 37, Oxford University Press, Oxford, pp. 119–181.
- Schulte, J.A. II, Macey, J.R., Larson, A. & Papenfuss, T.J. (1998) Molecular tests of phylogenetic taxonomies: A general procedure and example using four subfamilies of the lizard family Iguanidae. *Molecular Phylogenetics and Evolution*, 10 (3), 367–376.
<https://doi.org/10.1006/mpev.1998.0541>
- Shammakov, S. (1981) *Reptiles of the Turkmenian plains*. Ilym, Ashkhabad, 312 pp. [in Russian]
- Sharma, R.C. (1978) A new species of *Phrynocephalus* Kaup (Reptilia: Agamidae) from the Rajasthan Desert, India with notes on its ecology. *Bulletin of the Zoological Survey of India*, 1 (3), 291–294.
- Shackleton, R.M. & Chang, C. (1988) Cenozoic uplift and deformation of the Tibetan Plateau: The geomorphological evidence. In: *The Geological Evolution of Tibet. Report of the 1985 Royal Society – Academia Sinica Geotraverse of the Qinghai – Xizang Plateau Led by Chang Chengfu, Robert M. Shackleton, F.R.S, John F. Dewey, F.R.S., and Yin Jixiang*. Philosophical Transactions of the Royal Society of London, London, A 327 (1594), pp. 365–377.
<https://doi.org/10.1098/rsta.1988.0134>
- Shenbrot, G.I. & Semenov (as Semyonov), D.V. (1990) New species of the genus *Phrynocephalus* (Reptilia, Agamidae) from Turkmenia. *Zoologicheskyy Zhurnal*, Moscow, 69 (9), 154–156. [in Russian with English summary]
- Smit, J.H.W., Cloetingh, S.A.P.L., Burov, E., Tesauro, M., Sokoutis, D. & Kaban, M. (2013) Interference of lithospheric folding in western Central Asia by simultaneous Indian and Arabian plate indentation. *Tectonophysics*, 602, 176–193.
<https://doi.org/10.1016/j.tecto.2012.10.032>
- Solovyeva, E.N., Poyarkov, N.A., Dunaev, E.A., Duysebayeva, T.N. & Bannikova, A.A. (2011) Molecular differentiation and taxonomy of the Sunwatcher Toad-Headed Agama species complex *Phrynocephalus* superspecies *helioscopus* (Pallas 1771) (Reptilia: Agamidae). *Russian Journal of Genetics*, 47 (7), 842–856.
<https://doi.org/10.1134/S1022795411070155>
- Solovyeva, E.N., Dunayev, E.A. & Poyarkov, N.A. (2012) Interspecific taxonomy of Sunwatcher Toadhead Agama species complex (*Phrynocephalus helioscopus*, Squamata). *Zoologicheskyy Zhurnal*, Moscow, 91 (11), 1377–1396. [in Russian with English summary]
- Solovyeva, E.N., Poyarkov, N.A., Dunayev, E.A., Nazarov, R.A., Lebedev, V.S. & Bannikova, A.A. (2014) Phylogenetic relationships and subgeneric taxonomy of Toad Headed Agamas *Phrynocephalus* (Reptilia, Squamata, Agamidae) as determined by mitochondrial DNA sequencing. *Doklady Biological Sciences*, 455, 119–124.
<https://doi.org/10.7868/S0869565214100260>
- Stamatakis, A., Hoover, P. & Rougemont, J. (2008) A rapid bootstrap algorithm for the RAxML web servers. *Systematic Biology*, 57 (5), 758–771.
<https://doi.org/10.1080/10635150802429642>
- Staub, N.L., Brown, C.W. & Wake, D.B. (1995) Patterns of growth and movements in a population of *Ensatina eschscholtzii platensis* (Caudata: Plethodontidae) in the Sierra Nevada, California. *Journal of Herpetology*, 29 (4), 593–599.
<https://doi.org/10.2307/1564743>
- Steininger, F.F. & Rögl, F. (1984) Paleogeography and palinspastic reconstruction of the Neogene of the Mediterranean and Paratethys. In: Dixon, J.E. & Robertson, A.H.F. (Eds.), *The Geological Evolution of the Eastern Mediterranean*. Geological Society Special Publication No. 17, Blackwell Science, Oxford, pp. 659–668.
<https://doi.org/10.1144/GSL.SP.1984.017.01.52>
- Strauch, A.A. (1876) Part III. Reptilia and Amphibia. In: Imperial Russian Geographic Society (Ed.), *Przevalsky N. M., Mongolia and the Tangut Lands, a Three-Year Journey in Eastern High Asia. Vol. II. Reptiles and Amphibians*. V.S. Balashov printing house, St. Petersburg, pp. 1–55. [in Russian]
- Swofford, D.L. (2002) *PAUP*. Phylogenetic Analysis Using Parsimony (*and Other Methods)*. Sinauer Associates, Sunderland, Massachusetts.
- Tapponier, P., Mattauer, M., Proust, F. & Cassaigneau, C. (1981) Mesozoic ophiolites, sutures, and large-scale tectonic movements in Afghanistan. *Earth and Planetary Science Letters*, 52 (2), 355–371.
[https://doi.org/10.1016/0012-821X\(81\)90189-8](https://doi.org/10.1016/0012-821X(81)90189-8)

- Templeton, A.R. (1983) Phylogenetic inference from restriction endonuclease cleavage site maps with particular reference to the evolution of humans and the apes. *Evolution*, 37 (2), 221–244.
<https://doi.org/10.1111/j.1558-5646.1983.tb05533.x>
- Townsend, T., Larson, A., Louis, E. & Macey, J.R. (2004) A new hypothesis of squamate evolutionary relationships from nuclear and mitochondrial DNA sequence data. *Systematic Biology*, 53 (5), 735–757.
<https://doi.org/10.1080/10635150490522340>
- Tsarevsky (as Carevskij), S. (1926) Contributions sur la systématique et la distribution des lézards du genre *Phrynocephalus* (Reptilia). *Comptes Rendus de l'Académie des Sciences de l'URSS*, 1926, 211–214. [in Russian with French title]
- Urquhart, J., Wang, Y. & Fu, J. (2009) Historical vicariance and male-mediated gene flow in the toad-headed lizards *Phrynocephalus przewalskii*. *Molecular Ecology*, 18 (17), 3714–3729.
<https://doi.org/10.1111/j.1365-294X.2009.04310.x>
- Wake, D.B. & Schneider, C.J. (1998) Taxonomy of the plethodontid salamander genus *Ensatina*. *Herpetologica*, 54 (2), 279–298.
- Wang, Y. & Fu, J. (2004) Cladogenesis and vicariance patterns in the toad-headed lizard *Phrynocephalus versicolor* species complex. *Copeia*, 2004 (2), 199–206.
<https://doi.org/10.1643/CG-03-082R1>
- Wagner, P., Bauer, A.M., Leviton, A.E., Wilms, T.M. & Böhme, W. (2016) A checklist of the amphibians and reptiles of Afghanistan exploring herpetodiversity using biodiversity archives. *Proceedings of the California Academy of Sciences*, Series 4, 63, 457–565.
- Weisrock, D.W., Macey, J.R., Ugurtas, I.H., Larson, A. & Papenfuss, T.J. (2001) Molecular phylogenetics and historical biogeography among salamandrids of the “true” salamander clade: Rapid branching of numerous highly divergent lineages with the rise of Anatolia in *Mertensiella luschani*. *Molecular Phylogenetics and Evolution*, 18 (3), 434–448.
<https://doi.org/10.1006/mpev.2000.0905>
- Weisrock, D.W., Macey, J.R., Matsui, M., Mulcahy, D.G. & Papenfuss, T.J. (2013) Molecular phylogenetic reconstruction of the endemic Asian salamander family Hynobiidae (Amphibia, Caudata). *Zootaxa*, 3626 (1), 77–93.
<https://doi.org/10.11646/zootaxa.3626.1.3>
- Windley, B.F. (1988) Tectonic framework of the Himalaya, Karakorum and Tibet, and problems of their evolution. In: Shackleton, R.M., Dewey, J.F. & Windley, B.F. (Eds.), *Tectonic Evolution of the Himalayas and Tibet*. Philosophical Transactions of the Royal Society of London, Series A, Vol. 326, No. 1589, Cambridge University Press, Cambridge, pp. 3–16.
- Wu, Y., Fu, J., Yue, B. & Yin, Q. (2015) An atypical reproductive cycle in a common viviparous Asia Agamid *Phrynocephalus vlangalii*. *Ecology and Evolution*, 5 (21), 5138–5147.
<https://doi.org/10.1002/ece3.1783>
- Zhao, K. (1979) A survey of the classification and distribution of the toad-headed agamids (*Phrynocephalus*) in China. *Acta Scientiarum Naturalium Universitatis Intramongolicae*, Hohhot, 1979 (2), 111–121. [in Chinese with English summary]

APPENDIX 1

A. Allozyme Data—The 220 individuals examined for allozyme data are listed by species, population numbers when more than one are used, sample sizes, localities and museum numbers. All voucher specimens are deposited in the California Academy of Sciences, San Francisco (CAS:Herp), and the Museum of Vertebrate Zoology, University of California, Berkeley (MVZ:Herp). *Phrynocephalus* taxa are listed in alphabetical order with the two outgroups at the end.

(Sample 1) *P. axillaris*, N=10: Ruins near Hanoi Maydan Ruins, 27.5 km SE of Kashgar Hotel in Kashi (Kashgar), (39° 29' N 75° 58'), Kashi Prefecture, Xinjiang Autonomous Region, China, MVZ:Herp:208887-96. **(Sample 2)** *P. bannikovi*, N=10: Elev. 650 m, 39° 45' N 54° 33' E, foothills adjacent to the northern slope of the Bolshoy (Big) Balkan Mountains, 12 km ESE of Akrobat (Tasharvat) [39° 45' N 54° 22' E] and the Jebel to Oglany Station Rd., Akrobat (Tasharvat) is 18 km NE of Jebel on the Jebel to Oglany Station Rd., Krasnovodsk Region, Turkmenistan CAS:Herp:184580-89. **(Sample 3)** *P. forsythii* population 1, N=4: 47.1 km SW Yengisar (41° 55' N 84° 34' E), MVZ:Herp:208876-8; 47.5 km W Qarqi (41° 54' N 85° 35' E), Bayingolin Mongol Autonomous Prefecture, Xinjiang Autonomous Region, China, MVZ:Herp:208859. **(Sample 4)** *P. forsythii* population 2, N=4: Sand dunes 4.0 km ENE Tikanlik (40° 42' N 87° 38' E), Bayingolin Mongol Autonomous Prefecture, Xinjiang Autonomous Region, China, CAS:Herp:167820-23. **(Sample 5)** *P. golubewii*, N=4: Elev. 80 m, 38° 49' N 56° 53' E, 12 km NE (airline) of Bami, Ashgabad (Ashkabad) Region, Turkmenistan, CAS:Herp:185159-185162. **(Sample 6)** *P. guttatus*, N=10: Chervlenye Buruni, 14 km W (airline) of Terekli-Mekteb (44° 10' N 45° 52' E), Nogaisky District, Dagestan, Russia, MVZ:Herp:216020-29. **(Sample 7)** *P. helioscopus*, N=9: Barsakel'mes Island (45° 42' N 59° 52' E), Aral Sea, vicinity of Aral'sk (46° 48' N 61° 40' E), Aral'sk Region, Kazakhstan, CAS:Herp:183043-46, 380-84. **(Sample 8)** *P. interscapularis*, N=10: Chardjou Region, 1 km north of Repetek Desert Reserve Station, Repetek (38° 34' N 63° 11' E), Chardjou Region, Turkmenistan, CAS:Herp:179150-59. **(Sample 9)** *P. mystaceus* (population 1 for DNA), N=10: 55 km N of Ashkabad (37° 57' N 58° 23' E) on the Ashkabad—Bakhardok (38° 46' N 58° 30' E) Rd. then 21 km WNW on dirt Rd., Ashkabad Region, Turkmenistan, CAS:Herp:179754, 818-19, 876, 890, 892-93, 936-38. **(Sample 10)** *P. przewalskii* population 1, N=10: 23 km SW Baiyin (36° 32' N 104° 12' E) on Baotou-Lanzhao Rd., CAS:Herp:166722, 24; Wujiachuan (36° 47' N 104° 30' E),

Lanzhao Municipality, Gansu Province, China, CAS:Herp:166768-71, 73-75, 77. **(Sample 11)** *P. przewalskii* population 2, N=6: South shore of Yellow River, south across from Shapotou (37° 30' N 104° 58' E), Yinnan Prefecture, Ningxia Autonomous Region, China, CAS:Herp:166963, 65-67, 70-71. **(Sample 12)** *P. przewalskii* population 3, N=6: North shore of Yellow River, Shapotou (37° 30' N 104° 58' E), Yinnan Prefecture, Ningxia Autonomous Region, China, CAS:Herp:166822-25, 27; 47.3 km South of the Center of Luanning (37° 58' N 105° 23' E) on the Luanning-Zhenluopu Rd., Alxa League, Nei Mongol Autonomous Region, China, MVZ:Herp:210850. **(Sample 13)** *P. przewalskii* population 4, N=8: 3 km E main gate of Shamogongyuan Desert Park, 19 km NNE of Wuwei (31° 18' N 117° 54' E), then 3.5 km S, Wuwei Prefecture, Gansu Province, China, CAS:Herp:167167-74. **(Sample 14)** *P. raddei*, N=10: 55 km N of Ashkabad (37° 57' N 58° 23' E) on the Ashkabad—Bakhardok (38° 46' N 58° 30' E) Rd. then 21 km WNW on dirt Rd., Ashkabad Region, Turkmenistan, CAS:Herp:179770-79. **(Sample 15)** *P. roborowskii* population 1, N=9: Elev. 3120 m, E edge of Chaka (36° 45' N 99° 06' E), northern part of Haixi Mongol Zangzu Kazakzu Autonomous Prefecture, Qinghai Province, China, MVZ:Herp:211571-72, 74-80. **(Sample 16)** *P. roborowskii* population 2, N=8: [Lao (old)] Mangnai (37° 48' N 91° 46' E), Haixi Mongolzu Zangzu Kazakzu Autonomous Prefecture, Qinghai Province, China, CAS:Herp:167503-5; 146 km WSW of Ruoqiang (39° 02' N 88° 00' E) on Golmud-Ruoqiang Rd., Altun Mnts., Bayingolin Mongol Autonomous Prefecture, Xinjiang Autonomous Region, China, CAS:Herp:167506; elev. 2350 m, 97 km WSW of Ruoqiang (39° 02' N 88° 00' E) on Golmud-Ruoqiang Rd., Altun Mnts., Bayingolin Mongol Autonomous Prefecture, Xinjiang Autonomous Region, China, CAS:Herp:167507-9; approx. 87 km WSW of Ruoqiang (39° 02' N 88° 00' E) on Golmud-Ruoqiang Rd., Altun Mnts., Bayingolin Mongol Autonomous Prefecture, Xinjiang Autonomous Region, China, CAS:Herp:167510. **(Sample 17)** *P. rossikowi*, N=10: East side of Nephtezavodsk which is 30 km WNW of Deynau (39° 15' N 63° 11' E), Chardjou Region, Turkmenistan, CAS:Herp:179640-44, 684-88. **(Sample 18)** *P. salenskyi* population 1, N=10: 8.4 km NNE of Wujiacqu, also approx. 30 km NE of Bayi Nongchang (44° 20' N 87° 35' E), CAS:Herp:168285; Elev. 600 m, 3.4 km NW of the 2nd branch 10th team of Red Flag Farm (Hong Qi Long Chang), which is 8.2 km N Jimsar (43° 59' N 89° 04' E) on main st. then 4.7 km NW on Rd. to Beiting, from Beiting 25.3 km west on Rd. to Red Flag Farm, then 4.4 km north on dirt Rd., Changji Huizu Autonomous Prefecture, Xinjiang Autonomous Region, China, CAS:Herp:171566-74. **(Sample 19)** *P. salenskyi* population 2, N=5: Beach of Zaysan Lake (48° 00' N 84° 00' E), Zaysan Depression, Kazakhstan, CAS:Herp:183389-93. **(Sample 20)** *P. sogdianus*, N=7: Sand dunes on W side of Surkhan Darya (River), on Kumkurgan-Denau Rd., Surkhan Darjinskaya Region, Uzbekistan, CAS:Herp:182988-94. **(Sample 21)** *P. theobaldi*, N=10: Elev. 3740 m, Sera Monastery, Lhasa (29° 39' N 91° 06' E), Lhasa Municipality, Xizang (Tibet) Autonomous Region, China, CAS:Herp:171730-9. **(Sample 22)** *P. turcomanus*, N=10: Elev. 50 m, 39° 14' N 54° 58' E, Chalsu Valley, base of the Maly (Little) Balkan Mountains, 36 km west of the 2 km long Rd. south to Kazandjik on the Ashgabad (Ashkabad) to Krasnovodsk Rd., then 4-5 km north on dirt Rd., Krasnovodsk Region, Turkmenistan, CAS:Herp:184794-03. **(Sample 23)** *P. versicolor*, N=10: Elev. 1340 m, 17.3 km NNW Anxi (40° 30' N 96° 00' E) on Lanzhou-Urumqi Rd., Jiuquan Prefecture, Gansu Province, China, CAS:Herp:170914-23. **(Sample 24)** *P. vlangalii* (population 1 for DNA), N=10: Elev. 3220 m, 5.2 km east of Heimahe (36° 44' N 99° 46' E) on Xining-Golmud Rd., Hainan Zangzu Autonomous Prefecture, Qinghai Province, China, MVZ:Herp:211536-45. **(Sample 25)** *Laudakia caucasia*, N=10: Between Geok-tepen (38° 09' N 57° 58' E) and Bezmein (38° 05' N 58° 12' E), Ashkabad Region, Turkmenistan, CAS:Herp:179114-18; Mt. Dushak, near Germab (38° 01' N 57° 44' E), Ashkabad Region, Turkmenistan, CAS:Herp:179119-21, 23; Firyruza (37° 56' N 58° 04' E), Ashkabad Region, Turkmenistan, CAS:Herp:179728. **(Sample 26)** *Trapelus sanguinolentus*, N=10: 55 km N of Ashkabad (37° 57' N 58° 23' E) on the Ashkabad—Bakhardok (38° 46' N 58° 30' E) Rd. then 21 km WNW on dirt Rd., Ashkabad Region, Turkmenistan, CAS:Herp:179758-67.

B. DNA Data—All samples used in the allozyme study are also used in the mitochondrial DNA data set with the exception of a replacement sample for the outgroup *Laudakia caucasia*, which is CAS:Herp:184561, AF028685 (Macey *et al.* 1998a) from Elev. 650 m, 39° 45' N 54° 33' E, foothills adjacent to the northern slope of the Bolshoy (Big) Balkan Mountains, 12 km ESE of Akrobat (Tasharvat) [39° 45' N 54° 22' E] and the Jebel to Oglany Station Rd., Akrobat (Tasharvat) is 18 km NE of Jebel on the Jebel to Oglany Station Rd., Krasnovodsk Region, Turkmenistan. The individuals sequenced are as follows with the first GenBank number referring to mitochondrial DNA. If the sample is also sequenced for RAG-1 DNA a second GenBank number is listed.

(Sample 1) *P. axillaris*, MVZ:Herp:208887, KJ195924, KJ195965. **(Sample 2)** *P. bannikovi*, CAS:Herp:184580, KJ195925, KJ195966. **(Sample 3)** *P. forsythii* population 1, MVZ:Herp:208859, KJ195928, KJ195968. **(Sample 4)** *P. forsythii* population 2, CAS:Herp:167820, KJ195929, KJ195969. **(Sample 5)** *P. golubewii*, CAS:Herp:185159, KJ195920, KJ195960. **(Sample 6)** *P. guttatus*, MVZ:Herp:216020, KJ195937, KJ195977. **(Sample 7)** *P. helioscopus*, CAS:Herp:183380, KJ195921, KJ195961. **(Sample 8)** *P. interscapularis*, CAS:Herp:179151, AF128517 (Macey *et al.* 2000b), KJ195956. **(Sample 9)** *P. mystaceus*, CAS:Herp:179754, AF128518 (Macey *et al.* 2000b), KJ195963. **(Sample 10)** *P. przewalskii* population 1, CAS:Herp:166769, KJ195941, KJ195981. **(Sample 11)** *P. przewalskii* population 2, CAS:Herp:166963, KJ195942, KJ195982. **(Sample 12)** *P. przewalskii* population 3, CAS:Herp:166822, KJ195943, KJ195983. **(Sample 13)** *P. przewalskii* population 4, CAS:Herp:167167, KJ195944, KJ195984. **(Sample 14)** *P. raddei*, CAS:Herp:179770, U82691 (Macey *et al.* 1997c), AY662586 (positions 26-2785; Townsend *et al.* 2004). **(Sample 15)** *P. roborowskii* population 1, MVZ:Herp:211571, KJ195930, KJ195970. **(Sample 16)** *P. roborowskii* population 2, CAS:Herp:167503, KJ195931, KJ195971. **(Sample 17)** *P. rossikowi*, CAS:Herp:179640, KJ195926, KJ195967. **(Sample 18)** *P. salenskyi* population 1, CAS:Herp:171566, KJ195938, KJ195978. **(Sample 19)** *P. salenskyi* population 2, CAS:Herp:183389, KJ195939, KJ195979. **(Sample 20)** *P. sogdianus*, CAS:Herp:182988, KJ195917, KJ195957. **(Sample 21)** *P. theobaldi*, CAS:Herp:171730,

KJ195936, KJ195976. **(Sample 22)** *P. turcomanus*, CAS:Herp:184794, KJ195922, KJ195962. **(Sample 23)** *P. versicolor*, CAS:Herp:170914, KJ195940, KJ195980. **(Sample 24)** *P. vlangalii* (population 1 for DNA), MVZ:Herp:211536, KJ195933, KJ195973. **(Sample 25)** *Laudakia caucasia*, replacement CAS:Herp:184561, AF028685 (Macey *et al.* 1998a), KJ195945. **(Sample 26)** *Trapelus sanguinolentus*, CAS:Herp:179758, AF128511 (Macey *et al.* 2000b).

Additional samples were used in the mitochondrial DNA data set and most of these are included in the RAG-1 DNA data set. These are listed in alphabetical order with the first GenBank number referring to mitochondrial DNA and the second referring to RAG-1 DNA. When more than one sample is used a population number is assigned, and outgroups are listed at the end. In addition to the CAS:Herp and MVZ:Herp collections listed above, voucher specimens are deposited in Göteborg Natural History Museum Reptilia Exotica, Goteborg, Sweden (GNHM Re. ex.), Kunming Institute of Zoology, Yunnan, China (KIZ), Raffles Museum of Biodiversity Research, National University of Singapore (ZRC), and the Zoological Institute, St. Petersburg, Russia (ZISP).

(Sample 27) *P. arabicus* population 1, soft sand just north of Abqaiq (25° 56' N 49° 40' E) and to the east of the waste water run off, Saudi Arabia, CAS:Herp:183068, KJ195908. **(Sample 28)** *P. arabicus* population 2, Elev. 40 m, 21.7199° N, 59.4718° E, 21.5 km SW (by road) Al Ashkhara, Ash Sharqiyah Region, Oman, CAS:Herp:251008, KJ195909, KJ195950. **(Sample 29)** *P. clarkorum*, Elev. 3350 ft, N 31° 23.0' E 65° 53.5', Rigestan Sand Dunes at W side of Kadeney Rud (=River), 5 km (airline) of Takhteh Pol, approx 40 km SSE Kandahar (by rd to Quetta), Kandahar Prov., Afghanistan, MVZ:Herp:236888, KJ195913. **(Sample 30)** *P. hongyuanensis*, Elev. 3150 m, sand dunes, 5.0 km of Wasong Rd. (Waqên - Songpan Rd.) at Waqên (33° 03' N 102° 37' E), on Chengdu-Lanzhou Rd., Rd. # 213, then 2.0 km north (magnetic) by 20 Deg East on dirt Rd., Aba (Ngawa) Zangzu Autonomous Prefecture, Sichuan Province, China, MVZ:Herp:216686, KJ195932, KJ195972. **(Sample 31)** *P. longicaudatus*, Elev. 25 m, 20.6888° N, 58.2949° E, 8.6 km S (airline) Al Hij, Barr Al Hikman Peninsula, Mahut Wilayat, Al Wusta Region, Oman, CAS:Herp:251100, KJ195910, KJ195951. **(Sample 32)** *P. luteoguttatus* population 1, Elev. 2350 ft, N 31° 00.7' E 64° 16.7', Rigestan Sand Dunes, 12 km SE (airline) of Daruishan, Helmund Prov., Afghanistan, MVZ:Herp:236906, KJ195915, KJ195954. **(Sample 33)** *P. luteoguttatus* population 2, Elev. 935 m, 29° 26.86' N, 66° 00.20' E, Sayap Chashma (spring), Batto Village, 15 km W (by road) Nushki, Chagai District, Pakistan, CAS:Herp:232112, KJ195916, KJ195955. **(Sample 34)** *P. maculatus* population 1, Marengab sand dunes, 50 km NE (airline) Kasan, Esfahan Province, Iran, MVZ:Herp:236911, KJ195911, KJ195952. **(Sample 35)** *P. maculatus* population 2, Elev. 5700 ft., 29° 25.039' N 55° 29.581' E, West of Sirjan, Kerman Province, Iran, MVZ:Herp:243677, KJ195912, KJ195953. **(Sample 36)** *P. mystaceus* population 2, Elev., 1060 M, 35° 40 38.4' N, 56° 38 17.0' E, Kalateh-rey Sand Dunes ca 10 km SE of Ahmabad (which is 110 km airline WSW of Sabzevar) or 15.7 km (by road) NW of Zamanabad, Semnan Province, Iran, CAS:Herp:228621, KJ195923, KJ195964. **(Sample 37)** *P. ornatus*, Elev. 3200', N 31° 40.3' E 64° 55.5', 81 km W (by Herat Rd) of Kandahar, Kandahar Prov., Afghanistan, MVZ:Herp:236918, KJ195914. **(Sample 38)** *P. persicus*, Elev. 4300', N 35° 44.0' E 50° 04.5', 3 km S (airline) Buin (which is 55 km S of Qazuin), Zanjan Prov., Iran, MVZ:Herp:236928, KJ195919, KJ195959. **(Sample 39)** *P. scutellatus* population 1, Elev. 7185 ft., 28° 55.750' N 56° 30.420' E, near Khahr, Kerman Province, Iran, MVZ:Herp:243893, KJ195906, KJ195948. **(Sample 40)** *P. scutellatus* population 2, Elev. 1855 M, 32° 40.25' N, 59° 47.86' E, 5 km (airline) east of Birjand Zahedan Highway at about 7.2 km (by road) N of Sarbisheh or at about 55 km (by road) S of Birjand, Khorasan Province, Iran, CAS:Herp:228686, KJ195907, KJ195949. **(Sample 41)** *P. strauchi*, 1.5-2 km from nature monument "Yazyavan Desert", Fergan Valley, Yazyavansky District, Fergan Region, Uzbekistan, ZISP 21288, KJ195927. **(Sample 42)** *P. vindumi*, Elev. 925 m, 34° 37.28' N, 58° 43.86' E, Sand Dunes 26.4 km N (by road) Gonabad, Khorasan Province, Iran, CAS:Herp:228790, KJ195918, KJ195958. **(Sample 43)** *P. vlangalii* population 2, Elev. 3243 m, 36.7165° N, 100.7880° E, East side of Qinghai Lake, Hainan Zangzu Autonomous Prefecture, Qinghai Province, China, MVZ:Herp:272842, KJ195934, KJ195974. **(Sample 44)** *P. vlangalii* population 3, Elev. 4100 m, 34.3104° N, 99.1812° E, 4 kilometers North (by road) of Youyun Township, Maqên County, Golog Tibetan Autonomous Prefecture, Qinghai Province, China, KIZ 020262, KJ195935, KJ195975. **(Sample 45)** *Bufoniceps laungwalaensis*, Elev. 192 m, 26.50.26 N 70.32.24 E, vicinity of Sam, Rajasthan State, India, ZRC 2.5681, DQ008214 (Macey *et al.* 2006), KJ195946. **(Sample 46)** *Trapelus persicus*, Chehar-Rustaei Village, 25 km E of Bandar-e-Genaveh on the road to Borazjan, Khuzistan Province, Iran, GNHM Re. ex. 5211, AF128510 (Macey *et al.* 2000b), KJ195947.

C. Information on Plates I-VIII—All localities of samples and habitats are as provided for DNA sequencing samples except: Plate II A, B and D are from the same place as the *P. clarkorum* DNA sample. Plate III, A and B are from Elev. 3990 m, 52.4 km south of the Yangbajain—Margyang Rd. at the north side of Yangbajain (30° 13' N 90° 25' E), also at km 1900.8 from Xining on the Xining- Golmud—Lhasa Rd., Lhasa Municipality, Xizang (Tibet) Autonomous Region, China; Plate III D and E as well as Plate VIII F are from Elev. 40 m, 38° 10' N 54° 44' E, 14.2 km SW of Madau, also 65.8 km SW of Bugdaili on the Bugdaili to Kizil-Atrek Rd., Krasnovodsk Region, Turkmenistan; Plate III F is from the same locality as the *P. interscapularis* DNA sample. Plate V C and D as well as Plate VIII E are from Elev. 40 m, 39° 12' N 55° 00' E, 36 km west of the 2 km long Rd. south to Kazandjik on the Ashgabad (Ashkabad) to Krasnovodsk Rd., Krasnovodsk Region, Turkmenistan. Plate VIII C and D are from the same locality, which is the same as that for the DNA sample of *P. interscapularis*. All photos are by J. Robert Macey except: Plate I A-D by Todd W. Pierson (Oman); Plate II A-D by Theodore J. Papenfuss (Afghanistan); Plate III C by Roman Nazarov (*P. sogdianus*); Plate V E-F by M. Milto (*P. helioscopus* and habitat); and Plate VII A by Kellar A. Autumn (*P. przewalskii*).

APPENDIX 2

Step matrix charts for the 25 allozyme loci used in this study.

#NEXUS

begin data;

dimensions ntax=26 nchar=25;
format symbols="0123456789ABCDEFGHIJK";
matrix

[Where multiple populations of a species are reported, a number follows the species name: *P. przewalskii* population 1 is from Wujiaochuan and Baiyin, population 2 from across the Yellow River from Shapotou, population 3 from Shapotou and north of Shapotou, population 4 from Wuwei; *P. salenskyi* population 1 from Jimsar and Wujiaqu, population 2 from Zaysan Lake; *P. forsythii* population 1 from Yengisar, population 2 from Tikanlik; *P. roborowskii* population 1 from Chaka, population 2 from Magnai and Ruoqiang. See Appendix 1 for full locality information and museum numbers.]

```
[
      G
      A H I I I L L M M P P P
      C A A E S F G P A D D D D D D M E E P G P S]
      A O D A S T B P D D D H H H H H P P P G D N P O]
      B N H T T D A I H H H 1 2 1 2 1 2 I B D M H P K D]

P_przewalskii_1 2 2 E 5 2 6 5 1 5 0 C 2 4 1 5 5 1 5 8 2 4 I 9 2 4
P_przewalskii_2 2 3 8 5 2 6 4 7 5 6 4 1 6 1 4 5 1 5 3 2 4 J A 2 4
P_przewalskii_3 2 3 7 5 2 6 4 7 5 2 C 1 4 1 5 5 1 5 2 2 4 H 9 2 4
P_przewalskii_4 2 3 H 5 2 6 4 7 5 3 4 1 4 1 5 5 1 5 3 2 4 A 9 2 4
P_versicolor 2 3 6 5 2 A 4 7 5 F C 3 5 2 2 2 1 5 7 2 4 8 9 2 4
P_salenskyi_1 2 3 0 1 3 1 3 7 7 4 C 9 0 4 3 1 1 5 8 2 4 D A 2 1
P_salenskyi_2 2 3 D 2 2 6 1 7 5 5 9 9 4 4 0 1 1 5 8 2 4 4 A 2 4
P_guttatus 2 3 F 2 2 6 5 7 4 8 C 1 4 4 0 1 1 7 8 2 4 G 4 2 4
P_axillaris 2 3 3 1 2 5 0 2 8 5 8 0 0 4 0 1 0 0 6 2 4 G 4 3 2
P_forsythii_1 2 3 J 1 5 4 4 7 5 9 C 7 4 4 5 1 1 6 9 2 4 C 4 2 3
P_forsythii_2 2 3 J 1 5 2 4 7 5 B 6 1 4 4 5 1 2 6 5 2 3 7 4 2 3
P_vlangalii 2 3 K 1 2 9 4 3 9 C 3 7 4 4 5 1 1 9 8 5 0 E 4 0 5
P_roborowskii_1 2 3 K 3 2 6 4 3 0 E 6 7 4 3 5 1 1 1 3 5 4 9 4 0 5
P_roborowskii_2 2 3 K 1 2 0 4 6 6 G 5 7 4 4 5 1 1 5 3 5 4 6 5 0 5
P_theobaldi 2 4 K 0 2 6 4 0 2 G 0 7 2 4 5 1 1 2 4 5 4 5 4 0 5
P_helioscopus 2 3 B 4 2 6 1 7 5 H D B 4 1 0 1 1 5 8 6 4 5 0 1 4
P_turcomanus 2 3 2 4 2 7 2 7 5 H D B 4 1 0 1 1 5 8 6 5 3 2 0 4
P_golubewii 2 6 B 2 2 6 4 9 3 C C 7 4 1 0 1 1 5 8 6 4 B 2 0 4
P_bannikovi 2 3 4 2 2 6 4 7 5 A C 4 4 0 1 1 1 4 8 1 4 5 4 0 6
P_raddei 2 3 5 1 5 7 4 7 5 D C 9 0 1 0 1 1 A C 6 4 5 1 0 6
P_rossikowi 2 0 C 1 4 6 4 9 8 C 7 6 0 0 0 4 1 5 1 3 5 0 8 0 6
P_mystaceus 2 3 9 1 2 7 6 0 0 5 B 8 4 1 6 0 1 6 8 2 4 2 4 0 0
P_interscapularis 1 6 A 1 0 3 4 5 5 7 4 5 4 1 5 1 3 6 1 4 4 1 4 2 6
P_sogdianus 1 6 G 1 1 8 4 4 5 C 1 5 1 1 5 3 3 5 0 4 2 3 3 2 6
L_caucasia 3 1 1 1 6 C 4 A 5 I A A 4 0 5 6 1 8 A 0 4 K 7 0 7
T_sanguineolentus 0 5 I 1 6 B 4 8 1 1 2 0 3 1 5 1 1 3 B 0 1 F 6 0 8
; end;
```

begin assumptions;

usertype 1.AB=4 [4 STATES, DIRECT TRANSFORMATIONS]

	0	1	2	3
[a]	.	2	2	2
[b]	2	.	2	2
[c]	2	2	.	2
[d]	2	2	2	;

usertype 2.ACON=7 [7 STATES, DIRECT TRANSFORMATIONS]

	0	1	2	3	4	5	6
[a]	.	2	3	2	3	2	2
[b]	2	.	1	2	3	2	2
[bc]	3	1	.	1	2	3	3
[c]	2	2	1	.	1	2	2
[ce]	3	3	2	1	.	3	1
[d]	2	2	3	2	3	.	2
[e]	2	2	3	2	1	2	;

usertype 3.ADH=21 [21 STATES, DIRECT TRANSFORMATIONS]

	0	1	2	3	4	5	6	7	8	9	A	B	C	D	E	F	G	H	I	J	K
[acfjo]	.	4	5	4	6	3	2	3	3	6	5	4	4	3	4	4	5	5	6	6	6
[bcf]	4	.	3	2	4	1	2	3	3	4	3	2	4	3	4	4	3	5	4	4	4
[bfgj]	5	3	.	1	7	4	3	4	4	5	4	3	3	2	3	3	4	6	3	5	5
[bfj]	4	2	1	.	6	3	2	3	3	6	3	2	2	1	2	2	3	5	4	4	4
[cei]	6	4	7	6	.	3	4	5	5	4	5	4	4	5	6	6	5	7	4	4	4
[cf]	3	1	4	3	3	.	1	2	2	3	2	1	3	2	3	3	2	4	3	3	3
[cfj]	2	2	3	2	4	1	.	1	1	4	3	2	2	1	2	2	3	5	4	4	4
[cfjm]	3	3	4	3	5	2	1	.	2	5	4	3	3	2	3	1	4	6	5	5	5
[cfjn]	3	3	4	3	5	2	1	2	.	3	4	3	3	2	3	3	4	4	5	5	3
[cgn]	6	4	5	6	4	3	4	5	3	.	5	4	6	5	6	6	5	5	2	4	2
[df]	5	3	4	3	5	2	3	4	4	5	.	1	3	2	3	3	2	4	3	3	3
[f]	4	2	3	2	4	1	2	3	3	4	1	.	2	1	2	2	1	3	2	2	2
[fij]	4	4	3	2	4	3	2	3	3	6	3	2	.	1	2	2	3	5	4	4	4
[fj]	3	3	2	1	5	2	1	2	2	5	2	1	1	.	1	1	2	4	3	3	3
[fjl]	4	4	3	2	6	3	2	3	3	6	3	2	2	1	.	2	3	3	4	4	4
[fjm]	4	4	3	2	6	3	2	1	3	6	3	2	2	1	2	.	3	5	4	4	4
[fk]	5	3	4	3	5	2	3	4	4	5	2	1	3	2	3	3	.	4	3	3	3
[flno]	5	5	6	5	7	4	5	6	4	5	4	3	5	4	3	5	4	.	5	5	3
[g]	6	4	3	4	4	3	4	5	5	2	3	2	4	3	4	4	3	5	.	2	2
[h]	6	4	5	4	4	3	4	5	5	4	3	2	4	3	4	4	3	5	2	.	2
[n]	6	4	5	4	4	3	4	5	3	2	3	2	4	3	4	4	3	3	2	2	;

usertype 4.AAT=6 [6 STATES, DIRECT TRANSFORMATIONS]

	0	1	2	3	4	5
[a]	.	2	3	3	2	2
[b]	2	.	1	1	2	2
[bc]	3	1	.	2	1	3
[bd]	3	1	2	.	3	3
[c]	2	2	1	3	.	2
[e]	2	2	3	3	2	;

usertype 5.EST=7 [7 STATES, DIRECT TRANSFORMATIONS]

	0	1	2	3	4	5	6
[ac]	.	3	1	2	3	3	3
[b]	3	.	2	3	2	2	2
[c]	1	2	.	1	2	2	2
[ce]	2	3	1	.	3	3	3
[d]	3	2	2	3	.	2	2
[f]	3	2	2	3	2	.	2
[g]	3	2	2	3	2	2	;

usertype 6.EST_D=13 [13 STATES, DIRECT TRANSFORMATIONS]

	0	1	2	3	4	5	6	7	8	9	A	B	C
[ad]	.	1	2	3	3	2	1	2	2	2	3	4	5
[adg]	1	.	3	4	2	3	2	1	3	3	4	5	6
[bd]	2	3	.	1	1	2	1	2	2	2	3	4	5
[bdf]	3	4	1	.	2	3	2	3	3	3	4	5	6
[bdg]	3	2	1	2	.	3	2	1	3	3	4	5	6
[cd]	2	3	2	3	3	.	1	2	2	2	3	4	5
[d]	1	2	1	2	2	1	.	1	1	1	2	3	4
[dg]	2	1	2	3	1	2	1	.	2	2	3	4	5
[dh]	2	3	2	3	3	2	1	2	.	2	3	4	5
[di]	2	3	2	3	3	2	1	2	2	.	1	4	5
[dik]	3	4	3	4	4	3	2	3	3	1	.	3	4
[ek]	4	5	4	5	5	4	3	4	4	4	3	.	3
[jkl]	5	6	5	6	6	5	4	5	5	5	4	3	;

usertype 7.FBA=7 [7 STATES, DIRECT TRANSFORMATIONS]

	0	1	2	3	4	5	6
[ad]	.	2	3	2	1	2	2
[bd]	2	.	1	2	1	2	2
[bde]	3	1	.	3	2	1	3
[cd]	2	2	3	.	1	2	2
[d]	1	1	2	1	.	1	1
[de]	2	2	1	2	1	.	2
[df]	2	2	3	2	1	2	;

usertype 8.GPI=11 [11 STATES, DIRECT TRANSFORMATIONS]

	0	1	2	3	4	5	6	7	8	9	A
[a]	.	3	3	2	2	3	3	2	3	2	2
[bg]	3	.	2	3	3	4	4	1	2	3	3
[cg]	3	2	.	3	3	4	4	1	2	3	3
[d]	2	3	3	.	2	3	3	2	3	2	2
[e]	2	3	3	2	.	1	1	2	3	2	2
[ef]	3	4	4	3	1	.	2	3	4	3	3
[eh]	3	4	4	3	1	2	.	3	4	3	3
[g]	2	1	1	2	2	3	3	.	1	2	2
[gk]	3	2	2	3	3	4	4	1	.	3	3
[i]	2	3	3	2	2	3	3	2	3	.	2
[j]	2	3	3	2	2	3	3	2	3	2	;

usertype 9.GAPDH=10 [10 STATES, DIRECT TRANSFORMATIONS]

	0	1	2	3	4	5	6	7	8	9
[af]	.	3	3	2	2	1	3	2	2	3
[b]	3	.	2	3	3	2	4	3	3	2
[c]	3	2	.	3	3	2	4	3	3	2
[df]	2	3	3	.	2	1	3	2	2	3
[ef]	2	3	3	2	.	1	3	2	2	3
[f]	1	2	2	1	1	.	2	1	1	2
[fgk]	3	4	4	3	3	2	.	3	3	4
[fh]	2	3	3	2	2	1	3	.	2	3
[fi]	2	3	3	2	2	1	3	2	.	3
[j]	3	2	2	3	3	2	4	3	3	;

usertype 10.HADH=19 [19 STATES, DIRECT TRANSFORMATIONS]

	0	1	2	3	4	5	6	7	8	9	A	B	C	D	E	F	G	H	I
[abcf]	.	3	1	3	4	2	3	3	4	4	4	5	3	4	5	4	5	5	5
[b]	3	.	2	2	3	1	2	2	1	5	3	4	2	3	4	3	2	2	2
[bcf]	1	2	.	2	3	1	2	2	3	3	3	4	2	3	4	3	4	4	4
[bef]	3	2	2	.	1	1	2	2	3	5	3	4	2	3	4	3	4	4	4
[befi]	4	3	3	1	.	2	3	1	2	4	4	5	3	4	5	2	5	3	5
[bf]	2	1	1	1	2	.	1	1	2	4	2	3	1	2	3	2	3	3	3
[bfg]	3	2	2	2	3	1	.	2	3	5	3	4	2	1	4	3	2	4	4
[bfi]	3	2	2	2	1	1	2	.	1	3	3	4	2	3	4	1	4	2	4
[bi]	4	1	3	3	2	2	3	1	.	4	4	5	3	4	5	2	3	1	3
[cfji]	4	5	3	5	4	4	5	3	4	.	4	3	3	4	3	2	5	3	5
[df]	4	3	3	3	4	2	3	3	4	4	.	1	1	2	3	2	3	3	3
[dfj]	5	4	4	4	5	3	4	4	5	3	1	.	2	3	2	3	4	4	4
[f]	3	2	2	2	3	1	2	2	3	3	1	2	.	1	2	1	2	2	2
[fg]	4	3	3	3	4	2	1	3	4	4	2	3	1	.	3	2	1	3	3
[fhj]	5	4	4	4	5	3	4	4	5	3	3	2	2	3	.	3	4	4	4
[fi]	4	3	3	3	2	2	3	1	2	2	2	3	1	2	3	.	3	1	3
[g]	5	2	4	4	5	3	2	4	3	5	3	4	2	1	4	3	.	2	2
[i]	5	2	4	4	3	3	4	2	1	3	3	4	2	3	4	1	2	.	2
[k]	5	2	4	4	5	3	4	4	3	5	3	4	2	3	4	3	2	2	;

usertype 11.IDDH=14 [14 STATES, DIRECT TRANSFORMATIONS]

	0	1	2	3	4	5	6	7	8	9	A	B	C	D
[a]	.	1	2	2	3	2	3	2	3	3	3	4	2	2
[ac]	1	.	3	1	2	3	4	3	4	4	4	5	3	3
[b]	2	3	.	2	3	2	3	2	3	3	3	4	2	2
[c]	2	1	2	.	1	2	3	2	3	3	3	4	2	2
[ci]	3	2	3	1	.	3	2	3	2	2	2	3	1	3
[d]	2	3	2	2	3	.	1	2	3	3	3	4	2	2
[di]	3	4	3	3	2	1	.	3	2	2	2	3	1	3
[e]	2	3	2	2	3	2	3	.	1	3	3	4	2	2
[ei]	3	4	3	3	2	3	2	1	.	2	2	3	1	3
[fi]	3	4	3	3	2	3	2	3	2	.	2	3	1	3
[gi]	3	4	3	3	2	3	2	3	2	2	.	3	1	3
[hik]	4	5	4	4	3	4	3	4	3	3	3	.	2	4
[i]	2	3	2	2	1	2	1	2	1	1	1	2	.	2
[j]	2	3	2	2	3	2	3	2	3	3	3	4	2	;

usertype 12.IDH_1=12 [12 STATES, DIRECT TRANSFORMATIONS]

	0	1	2	3	4	5	6	7	8	9	A	B
[a]	.	1	2	2	3	2	3	2	3	3	2	2
[ad]	1	.	1	1	2	3	2	1	2	2	3	3
[adg]	2	1	.	2	3	4	3	2	3	1	4	4
[adh]	2	1	2	.	3	4	3	2	3	3	4	2
[bd]	3	2	3	3	.	3	2	1	2	2	3	3
[c]	2	3	4	4	3	.	1	2	3	3	2	2
[cd]	3	2	3	3	2	1	.	1	2	2	3	3
[d]	2	1	2	2	1	2	1	.	1	1	2	2
[df]	3	2	3	3	2	3	2	1	.	2	3	3
[dg]	3	2	1	3	2	3	2	1	2	.	3	3
[e]	2	3	4	4	3	2	3	2	3	3	.	2
[h]	2	3	4	2	3	2	3	2	3	3	2	;

usertype 13.IDH_2=7 [7 STATES, DIRECT TRANSFORMATIONS]

	0	1	2	3	4	5	6
[af]	.	3	3	3	1	2	2
[bef]	3	.	4	4	2	3	3
[c]	3	4	.	2	2	3	3
[d]	3	4	2	.	2	3	3
[f]	1	2	2	2	.	1	1
[fg]	2	3	3	3	1	.	2
[fh]	2	3	3	3	1	2	;

usertype 14.LDH_1=5 [5 STATES, DIRECT TRANSFORMATIONS]

	0	1	2	3	4
[a]	.	2	3	3	2
[b]	2	.	1	3	2
[bd]	3	1	.	2	1
[cd]	3	3	2	.	1
[d]	2	2	1	1	;

usertype 15.LDH_2=7 [7 STATES, DIRECT TRANSFORMATIONS]

	0	1	2	3	4	5	6
[a]	.	1	1	1	3	2	3
[ab]	1	.	2	2	4	3	4
[ac]	1	2	.	2	2	3	4
[ad]	1	2	2	.	2	1	2
[cd]	3	4	2	2	.	1	2
[d]	2	3	3	1	1	.	1
[de]	3	4	4	2	2	1	;

usertype 16.MDH_1=7 [7 STATES, DIRECT TRANSFORMATIONS]

	0	1	2	3	4	5	6
[ab]	.	1	3	2	3	3	3
[b]	1	.	2	1	2	2	2
[bce]	3	2	.	3	4	2	4
[bd]	2	1	3	.	1	3	3
[d]	3	2	4	1	.	2	2
[e]	3	2	2	3	2	.	2
[f]	3	2	4	3	2	2	;

usertype 17.MDH_2=4 [4 STATES, DIRECT TRANSFORMATIONS]

	0	1	2	3
[a]	.	2	3	2
[b]	2	.	1	2
[bc]	3	1	.	3
[d]	2	2	3	;

usertype 18.MPI=11 [11 STATES, DIRECT TRANSFORMATIONS]

	0	1	2	3	4	5	6	7	8	9	A
[ac]	.	4	3	3	7	3	4	4	3	4	3
[bg]	4	.	3	3	5	1	2	2	3	4	3
[d]	3	3	.	2	6	2	3	3	2	3	2
[e]	3	3	2	.	6	2	3	3	2	3	2
[fghkm]	7	5	6	6	.	4	5	5	6	5	6
[g]	3	1	2	2	4	.	1	1	2	3	2
[gj]	4	2	3	3	5	1	.	2	3	2	3
[gl]	4	2	3	3	5	1	2	.	3	4	1
[i]	3	3	2	2	6	2	3	3	.	3	2
[jm]	4	4	3	3	5	3	2	4	3	.	3
[l]	3	3	2	2	6	2	3	1	2	3	;

usertype 19.PEP_B=13 [13 STATES, DIRECT TRANSFORMATIONS]

	0	1	2	3	4	5	6	7	8	9	A	B	C
[ab]	.	2	3	4	3	6	4	5	3	4	4	5	4
[bf]	2	.	1	2	3	4	2	3	1	2	4	5	4
[bfj]	3	1	.	3	4	3	3	4	2	1	5	6	3
[cf]	4	2	3	.	3	4	2	3	1	2	4	5	4
[d]	3	3	4	3	.	3	3	4	2	3	3	4	3
[dfji]	6	4	3	4	3	.	4	5	3	2	6	5	4
[ef]	4	2	3	2	3	4	.	1	1	2	4	5	4
[efh]	5	3	4	3	4	5	1	.	2	3	5	6	5
[f]	3	1	2	1	2	3	1	2	.	1	3	4	3
[fj]	4	2	1	2	3	2	2	3	1	.	4	5	2
[gl]	4	4	5	4	3	6	4	5	3	4	.	3	2
[ikl]	5	5	6	5	4	5	5	6	4	5	3	.	3
[jl]	4	4	3	4	3	4	4	5	3	2	2	3	;

usertype 20.PEP_D=7 [7 STATES, DIRECT TRANSFORMATIONS]

	0	1	2	3	4	5	6
[a]	.	2	2	3	2	2	2
[b]	2	.	2	3	2	2	2
[c]	2	2	.	1	2	2	2
[cg]	3	3	1	.	3	3	3
[d]	2	2	2	3	.	2	2
[e]	2	2	2	3	2	.	2
[f]	2	2	2	3	2	2	;

usertype 21.PGM=6 [6 STATES, DIRECT TRANSFORMATIONS]

	0	1	2	3	4	5
[abde]	.	2	1	4	3	2
[bd]	2	.	1	2	1	2
[bde]	1	1	.	3	2	1
[cd]	4	2	3	.	1	2
[d]	3	1	2	1	.	1
[de]	2	2	1	2	1	;

usertype 22.PGDH=21 [21 STATES, DIRECT TRANSFORMATIONS]

	0	1	2	3	4	5	6	7	8	9	A	B	C	D	E	F	G	H	I	J	K
[ace]	.	3	2	1	6	2	5	4	5	3	4	4	5	6	7	4	4	5	6	5	4
[bc]	3	.	1	2	5	3	6	5	6	4	5	3	4	5	6	3	3	4	5	4	3
[c]	2	1	.	1	4	2	5	4	5	3	4	2	3	4	5	2	2	3	4	3	2
[ce]	1	2	1	.	5	1	4	3	4	2	3	3	4	5	6	3	3	4	5	4	3
[dmo]	6	5	4	5	.	4	5	4	5	3	4	4	5	4	7	4	2	3	4	3	4
[e]	2	3	2	1	4	.	3	2	3	1	2	2	3	4	5	2	2	3	4	3	2
[ehmq]	5	6	5	4	5	3	.	3	4	2	3	5	6	3	8	5	3	2	5	4	3
[eim]	4	5	4	3	4	2	3	.	3	1	2	4	3	4	5	4	2	3	4	3	4
[ekmt]	5	6	5	4	5	3	4	3	.	2	3	5	6	5	8	5	3	4	5	4	5
[em]	3	4	3	2	3	1	2	1	2	.	1	3	4	3	6	3	1	2	3	2	3
[ems]	4	5	4	3	4	2	3	2	3	1	.	4	5	4	7	4	2	3	2	1	4
[f]	4	3	2	3	4	2	5	4	5	3	4	.	3	4	5	2	2	3	4	3	2
[gi]	5	4	3	4	5	3	6	3	6	4	5	3	.	5	4	3	3	4	5	4	3
[hjm]	6	5	4	5	4	4	3	4	5	3	4	4	5	.	5	4	2	3	4	3	4
[ijnp]	7	6	5	6	7	5	8	5	8	6	7	5	4	5	.	5	5	6	7	6	5
[l]	4	3	2	3	4	2	5	4	5	3	4	2	3	4	5	.	2	3	4	3	2
[m]	4	3	2	3	2	2	3	2	3	1	2	2	3	2	5	2	.	1	2	1	2
[mq]	5	4	3	4	3	3	2	3	4	2	3	3	4	3	6	3	1	.	3	2	1
[mrs]	6	5	4	5	4	4	5	4	5	3	2	4	5	4	7	4	2	3	.	1	4
[ms]	5	4	3	4	3	3	4	3	4	2	1	3	4	3	6	3	1	2	1	.	3
[q]	4	3	2	3	4	2	3	4	5	3	4	2	3	4	5	2	2	1	4	3	;

usertype 23.PNP=11 [11 STATES, DIRECT TRANSFORMATIONS]

	0	1	2	3	4	5	6	7	8	9	A
[abc]	.	3	2	3	4	5	5	5	5	4	5
[bd]	3	.	3	2	1	2	2	2	2	3	4
[c]	2	3	.	1	2	3	3	3	3	2	3
[cd]	3	2	1	.	1	2	2	2	2	3	4
[d]	4	1	2	1	.	1	1	1	1	2	3
[de]	5	2	3	2	1	.	2	2	2	3	4
[df]	5	2	3	2	1	2	.	2	2	1	2
[dg]	5	2	3	2	1	2	2	.	2	3	4
[dh]	5	2	3	2	1	2	2	2	.	3	4
[f]	4	3	2	3	2	3	1	3	3	.	1
[fi]	5	4	3	4	3	4	2	4	4	1	;

usertype 24.PK=4 [4 STATES, DIRECT TRANSFORMATIONS]

	0	1	2	3
[a]	.	1	2	2
[ad]	1	.	3	3
[b]	2	3	.	2
[c]	2	3	2	;

usertype 25.SOD=9 [9 STATES, DIRECT TRANSFORMATIONS]

	0	1	2	3	4	5	6	7	8
[a]	.	4	2	2	2	2	2	2	2
[beg]	4	.	4	4	2	4	4	4	4
[c]	2	4	.	2	2	2	2	2	2
[d]	2	4	2	.	2	2	2	2	2
[e]	2	2	2	2	.	2	2	2	2
[f]	2	4	2	2	2	.	2	2	2
[h]	2	4	2	2	2	2	.	2	2
[i]	2	4	2	2	2	2	2	.	2
[j]	2	4	2	2	2	2	2	2	.; end;

APPENDIX 3. Maximum-likelihood Results

The best-fit partitioning scheme using the Akaike Information Criterion in PartitionFinder (Lanfear *et al.* 2012) estimated six partitions that best explained the data in the mitochondrial DNA only dataset: (1) first codon positions of ND1 and ND2; (2) second codon positions of ND1 and ND2; (3) third codon positions of ND1 and ND2; (4) mitochondrial DNA tRNA and noncoding positions; (5) first and third codon positions in COI; and (6) second codon positions in COI. For the RAG-1 gene only dataset three partitions best explained the data, one for each codon position. Although not all models estimated a general time reversible sequence evolution model with gamma distributed rate variation (GTR + Gamma) as the optimal model for each partition, all maximum-likelihood analyses assumed this model for all partitions as the alternative models are not implemented in RAxML and likelihood scores of this model compared to optimal models estimated by PartitionFinder analyses did not greatly differ. Maximum-likelihood phylogenetic estimates are provided in figures 17 and 18.

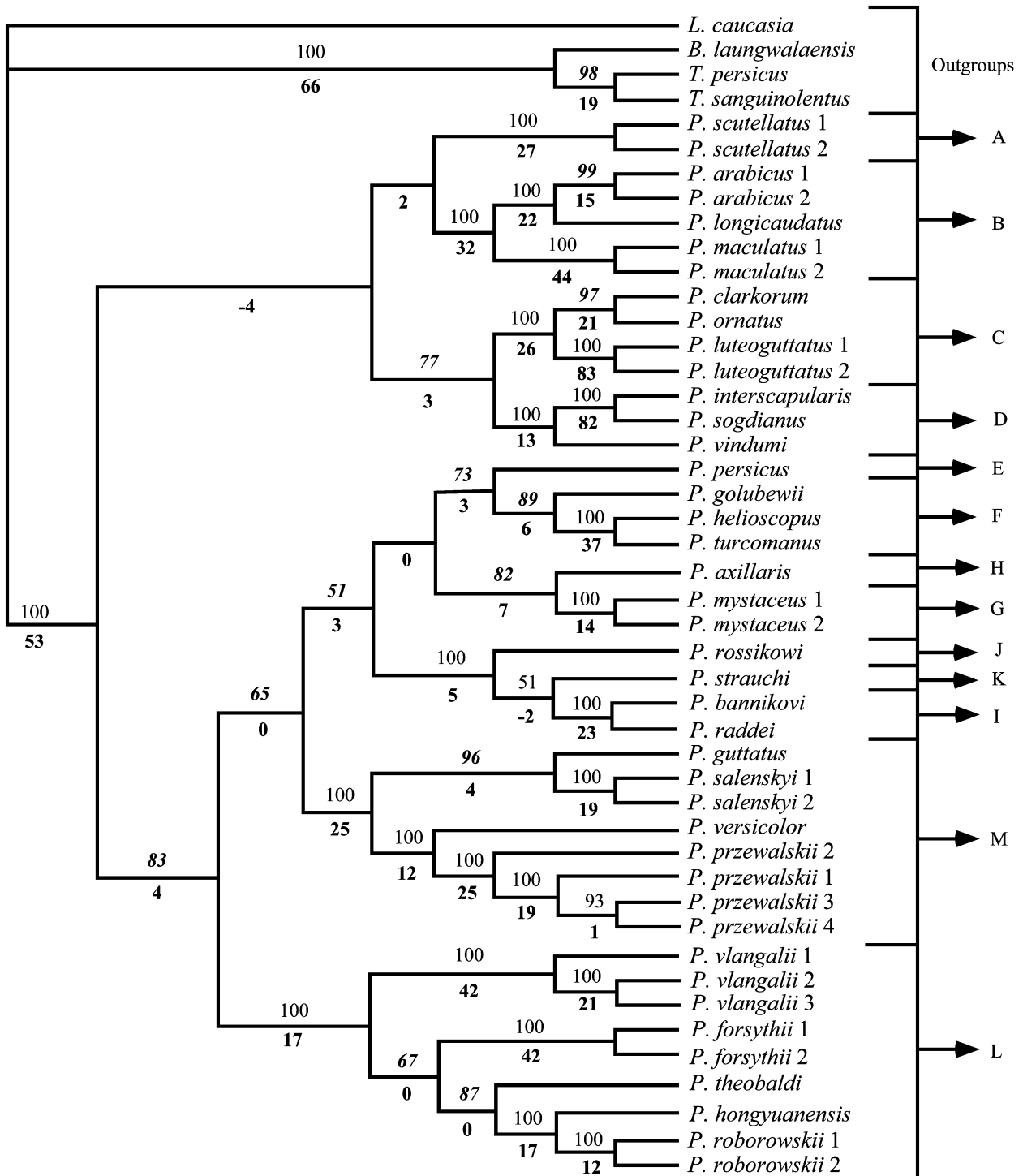


FIGURE 17. Highest maximum-likelihood tree ($-\ln = 19894.22$) from the 1595 included aligned mitochondrial DNA positions. Bootstrap values are presented above branches and comparative parsimony decay indices are presented below branches in bold (Macey 2005). Branches that appear in parsimony analyses have the parsimony decay index plotted. Branches with no parsimony cost but are not present in strict consensus trees are listed as a "0" decay value. Branches that conflict with the parsimony analysis have a negative decay value representing the number of parsimony steps cost to obtain the maximum-likelihood branch. Bold italic bootstraps are those that differ from parsimony analysis. Outgroups (*Laudakia*, *Bufo*, and *Trapelus*), and *Phrynocephalus* clades and lineages previously identified are labeled to the right as A–M.

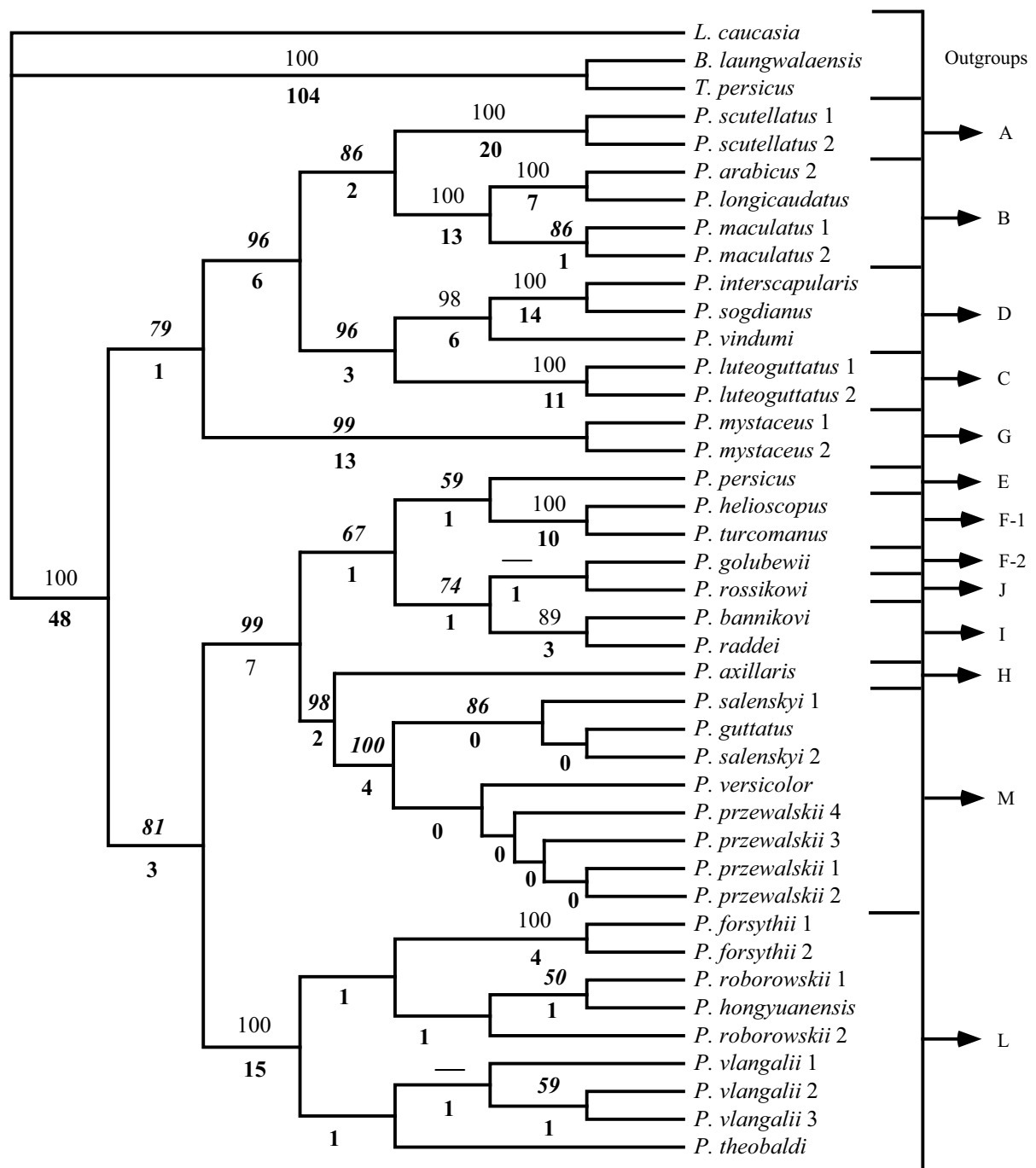


FIGURE 18. Highest maximum-likelihood tree ($-\ln = 8673.71$) from the 2760 aligned nuclear RAG-1 DNA positions. The maximum-likelihood analysis chose one of the 62 equally parsimonious trees. Bootstrap values are presented above branches and comparative parsimony decay indices are presented below branches in bold (Macey 2005). Branches that appear in parsimony analyses have the parsimony decay index plotted. Branches with no parsimony cost but are not present in strict consensus trees are listed as a "0" decay value. Branches that conflict with the parsimony analysis have a negative decay value representing the number of parsimony steps cost to obtain the maximum-likelihood branch. Bold italic bootstraps are those that differ from parsimony analysis. A dash above a branch is one that had a bootstrap value above 50% in the parsimony analysis but does not in this analysis. Outgroups (*Laudakia*, *Bufoinceps*, and *Trapelus*), and *Phrynocephalus* clades and lineages previously identified are labeled to the right as A–M (clades that are broken are numbered).

APPENDIX 4

Trees used in Wilcoxon sign-ranks tests (Felsenstein 1985; Templeton 1983) examined for statistical significance of shortest trees relative to alternative hypotheses are described with trees in standard bracket format including taxa and populations numbered as follows: (1) *L. caucasia*, (2) *B. laungwalaensis*, (3) *T. persicus*, (4) *T. sanguinolentus*, (5) *P. scutellatus-1*, (6) *P. scutellatus-2*, (7) *P. arabicus-1*, (8) *P. arabicus-2*, (9) *P. longicaudatus*, (10) *P. maculatus-1*, (11) *P. maculatus-2*, (12) *P. clarkorum*, (13) *P. ornatus*, (14) *P. luteoguttatus-1*, (15) *P. luteoguttatus-2*, (16) *P. interscapularis*, (17) *P. sogdianus*, (18) *P. vindumi*, (19) *P. persicus*, (20) *P. golubewii*, (21) *P. helioscopus*, (22) *P. turcomanus*, (23) *P. mystaceus-1*, (24) *P. mystaceus-2*, (25) *P. axillaris*, (26) *P. bannikovi*, (27) *P. raddei*, (28) *P. rossikowi*, (29) *P. strauchii*, (30) *P. forsythii-1*, (31) *P. forsythii-2*, (32) *P. roborowskii-1*, (33) *P. roborowskii-2*, (34) *P. hongyuanensis*, (35) *P. vlangalii-1*, (36) *P. vlangalii-2*, (37) *P. vlangalii-3*, (38) *P. theobaldi*, (39) *P. guttatus*, (40) *P. salenskyi-1*, (41) *P. salenskyi-2*, (42) *P. versicolor*, (43) *P. przewalskii-1*, (44) *P. przewalskii-2*, (45) *P. przewalskii-3*, and (46) *P. przewalskii-4*. The northern lowland clade (Clade M in Figs. 4 and 8) consists of *P. guttatus*, *P. salenskyi* populations, *P. versicolor*, and *P. przewalskii* populations. Viviparous/Tibetan taxa (Clade L in Figs. 4 and 8) consists of *P. forsythii*, *P. roborowskii* populations, *P. hongyuanensis*, *P. vlangalii* populations, and *P. theobaldi*. Lineage H is *P. axillaris* in figures 4 and 8. *P. axillaris* is not included in the northern lowland clade comparisons applying mitochondrial DNA data because it is not placed in a monophyletic position with the northern lowland clade defined as Clade M, but is sister to the northern lowland clade in the combined analysis, and therefore tests were done with and without *P. axillaris* (Clade H) in tests using the combined data.

The three overall shortest parsimony trees (A1-A3) used in mitochondrial DNA data comparisons have a length of 4442 changes:

Tree A1, mt-DNA data—

(1,((2,(3,4)),(5,6),(((7,8),9),(10,11))),(((12,13),(14,15)),(16,17),18)),(((19,(20,(21,22))),((23,24),25),(26,27),(28,29))),(((30,31),((32,33),34),38)),(35,(36,37))),((39,(40,41)),(42,((43,(45,46)),44))))))));

Tree A2, mt-DNA data—

(1,((2,(3,4)),(5,6),(((7,8),9),(10,11))),(((12,13),(14,15)),(16,17),18)),(((19,(20,(21,22))),((23,24),25),(26,27),(28,29))),((39,(40,41)),(42,((43,(45,46)),44))),(((30,31),((32,33),34),38)),(35,(36,37))))))));

Tree A3, mt-DNA data—

(1,((2,(3,4)),(5,6),(((7,8),9),(10,11))),(((12,13),(14,15)),(16,17),18)),(((19,(20,(21,22))),((23,24),25),(26,27),(28,29))),((39,(40,41)),(42,((43,(45,46)),44))),(((30,31),((32,33),34),38))))))));

The three overall shortest parsimony trees (B1-B3) used in combined mitochondrial DNA data, nuclear RAG-1 DNA data, and allele presence/absence coding of allozyme data comparisons have a length of 5683 changes:

Tree B1, combined data—

(1,((2,(3,4)),(((5,6),(((7,8),9),(10,11))),(((12,13),(14,15)),(16,17),18))),((((19,(20,(21,22))),((26,27),(28,29))),25,((39,(40,41)),(42,((43,46),45),44))))),(((30,31),((32,33),34),38)),(23,24)))));

Tree B2, combined data—

(1,((2,(3,4)),(((5,6),(((7,8),9),(10,11))),(((12,13),(14,15)),(16,17),18))),((((19,(20,(21,22))),((26,27),(28,29))),25,((39,(40,41)),(42,((43,46),45),44))))),(((30,31),((32,33),34),38)),(23,24)))));

Tree B3, combined data—

(1,((2,(3,4)),(((5,6),(((7,8),9),(10,11))),(((12,13),(14,15)),(16,17),18))),((((19,(20,(21,22))),((26,27),(28,29))),25,((39,(40,41)),(42,((43,46),45),44))))),(((30,31),((32,33),34),38)),(35,(36,37))))),((23,24)))));

Alternative trees (C1-E1) derived from constrained mitochondrial DNA data analyses used in Wilcoxon sign-ranks tests are described below:

Tree C1, northern lowland clade basal (Clade M), length 4442 steps—

(1,((2,(3,4)),(((5,6),(((7,8),9),(10,11))),(((12,13),(14,15)),(16,17),18))),(((19,(20,(21,22))),((23,24),25),(26,27),(28,29))),((30,31),((32,33),34),38))),((39,(40,41)),(42,((43,(45,46)),44))))));

Tree D1, viviparous/Tibetan clade basal (Clade L), length 4443 steps—

(1,((2,(3,4)),(((5,6),(((7,8),9),(10,11))),(((12,13),(14,15)),(16,17),18))),(((19,(20,(21,22))),((23,24),25),(26,27),(28,29))),((39,(40,41)),(42,((43,(45,46)),44))))),(((30,31),((32,33),34),38)),(35,(36,37))))));

Tree E1, northern lowland and viviparous/Tibetan clades basal (clades L and M), length 4425 steps—

(1,((2,(3,4)),((5,6),(((7,8),9),(10,11))),((12,13),(14,15)),((16,17),18)),((19,(20,(21,22))),((23,24),25)),((26,27),(28,29))),(((30,31),((32,33),34),38)),(35,(36,37))),((39,(40,41)),(42,((43,(45,46)),44))))))));

Alternative trees (F1-J1) derived from constrained combined data analyses used in Wilcoxon sign-ranks tests are described below:

Tree F1, northern lowland clade not including *P. axillaris* as basal (Clade M), length 5710 steps—

(1,((2,(3,4)),((((5,6),(((7,8),9),(10,11))),((12,13),(14,15)),((16,17),18))),((30,31),(((32,33),34),38)),(35,(36,37))),((23,24)),((19,(20,(21,22))),((26,27),(28,29))),((25,((39,(40,41)),(42,((43,46),45),44))))));

Tree G1, northern lowland clade including *P. axillaris* as basal (clades H and M), length 5713 steps—

(1,((2,(3,4)),((((5,6),(((7,8),9),(10,11))),((12,13),(14,15)),((16,17),18))),((30,31),35,(36,37))),((32,33),34),38)),((19,(20,(21,22))),((23,24),25)),((26,27),(28,29))),((39,(40,41)),(42,((43,46),45),44))))));

Tree H1, viviparous/Tibet clade basal (Clade L), length 5702 steps—

(1,((2,(3,4)),((((5,6),(((7,8),9),(10,11))),((12,13),(14,15)),((16,17),18))),((19,(20,(21,22))),((26,27),(28,29))),((25,((39,(40,41)),(42,((43,46),45),44))))),((30,31),((32,33),34),38)))));

Tree I1, northern lowland clade not including *P. axillaris*, and viviparous/Tibet clade as basal (clades L and M), length 5712 steps—

(1,((2,(3,4)),((((5,6),(((7,8),9),(10,11))),((12,13),(14,15)),((16,17),18))),((19,(20,(21,22))),((23,24),25)),((26,27),(28,29))),((30,31),((32,33),34),38)),(35,(36,37))),((39,(40,41)),(42,((43,46),45),44))))));

Tree J1, northern lowland clade including *P. axillaris*, and viviparous/Tibet clade as basal (clades H, L and M), length 5714 steps—

(1,((2,(3,4)),((((5,6),(((7,8),9),(10,11))),((12,13),(14,15)),((16,17),18))),((23,24)),((19,(20,(21,22))),((26,27),(28,29))),((25,((39,(40,41)),(42,((43,46),45),44))))),((30,31),((32,33),34),38)),(35,(36,37))))));

APPENDIX 5

Samples measured for snout-vent length (SVL) and tail-length (TL) are presented below in phylogenetic order based on results presented in figure 8, and following table 6. In some cases we refer to literature which is presented after novel data are shown from specimens at the following museums: The California Academy of Sciences, San Francisco (CAS:Herp), the Museum of Vertebrate Zoology, University of California, Berkeley (MVZ:Herp), and the ZISP Zoological Institute, St. Petersburg. An attempt to provide as much information is included, but there is difficulty with sexually dimorphic forms and new data presentation did not sex specimens to avoid major invasive procedures with valuable specimens. In the case of *P. longicaudatus* only a single individual is available from Oman, so we measured 10 individuals from Saudi Arabia as noted.

(Sample 25) *L. caucasia*, N=10; CAS:Herp:184556-58, 60-66. (Sample 45) *B. laungwalaensis* (Sharma 1978), SVL male 29-69 mm, TL male 15-42, SVL female 31-54 mm, TL female 18-32 mm. (Sample 46) *T. persicus* (Anderson 1999), largest SVL male 97 mm, TL male 147 mm, SVL female 78 mm, TL female 113 mm (based on Iranian samples). (Sample 26) *T. sanguinolentus*, N=10; CAS:Herp:179759, 65-67, 69, 179850, 52, 79, 179917, 39. (Sample 39) *P. scutellatus*-1, N=6; MVZ:Herp:243893-95, 898-900. (Sample 40) *P. scutellatus*-2, N=10; CAS:Herp:141192-93, 209-10, 228684-89. (Sample 27) *P. arabicus*-1, N=17; CAS:Herp:84295, 377, 379, 382-85, 387, 479, 484-85, 18368-69, 72-75. (Sample 28) *P. arabicus*-2, N=5; CAS:Herp:251008, 22-23, 255704, 255713. (Sample 31) *P. longicaudatus*, N=1/11; Oman CAS:Herp:251100; Saudi Arabia CAS:Herp:84442-49, 52, 55, 84511. (Sample 34) *P. maculatus*-1, N=8; MVZ:Herp:231869, 236911, 243677, 245936, 250470, 72-73, 75. (Sample 35) *P. maculatus*-1, N=1; MVZ:Herp:243677. (Sample 29) *P. clarkorum*, N=15; MVZ:Herp:236886-88, CAS:Herp:97989, 103787, 120225, 27-34, 36. (Sample 37) *P. ornatus*, N=10; MVZ:Herp:236915-24. (Sample 32) *P. luteoguttatus*-1, N=10; MVZ:Herp:235901-10. (Sample 33) *P. luteoguttatus*-2, N=2; CAS:Herp:232112, 22. (Sample 8) *P. interscapularis*, N=10; CAS:Herp:179151, 56, 59, 61, 72, 75-76, 82, 88-89. (Sample 20) *P. sogdianus*, N=10; CAS:Herp:182980-89. (Sample 42) *P. vindumi*, N=9; CAS:Herp:228786-94. (Sample 38) *P. persicus*, N=5; CAS:Herp:140824, 217448, MVZ:Herp:236927-29. (Sample 5) *P. golubewii*, N=4; CAS:Herp:185159-185162; Shammakov (1981) reported SVL males (N=68) 48-67 mm, TL males 60-87 mm, SVL females (N=82) 48-62 mm, TL females 53-77 mm; samples in ZISP (N=21) maximal SVL 63 mm, maximal TL 77 mm. (Sample 7) *P. helioscopus*, N=11; CAS:Herp:183043-46, 183380-86. (Sample 22) *P. turcomanus*, N=10; CAS:Herp:184795-797, 799, 801-802, 804-805, 807-808. (Sample 9) *P. mystaceus*-1, N=11; CAS:Herp:179754, 818-19, 876, 890-93, 936-38. (Sample 36) *P. mystaceus*-2, N=10; CAS:Herp:228612-16, 19-20, 30, 32-33. (Sample 1) *P. axillaris*, N=10; MVZ:Herp:208887-96. (Sample 2) *P. bannikovi*, N=10; CAS:Herp:184584-585, 587, 595-596, 607, 609, 612, 615, 617. (Sample 14) *P. raddei*, N=10; CAS:Herp:179770-76, 79-81. (Sample 17) *P. rossikowi*, N=18; CAS:Herp:179641-48, 83-87, 89-92, 94. (Sample 41) *P. trauchi*, N=6; samples in ZISP (N=6) maximal SVL 55 mm, TL 82

mm; Sattarov (1993) reported SVL males 41-50, TL males 67-82, SVL females 39-49, TL females 56-72. (Sample 3) *P. forsythii*-1, N=2; CAS:Herp:196903, 197127. (Sample 4) *P. forsythii*-2, N=7; CAS:Herp:167820-26. (Sample 15) *P. roborowskii*-1, MVZ:Herp:211571-72, 74-75, 77, 79, 81, 83, 85-86. (Sample 16) *P. roborowskii*-2, N=8; CAS:Herp:167503-10. (Sample 30) *P. hongyuanensis*, N=14; MVZ:Herp:211418-23, 216683-90. (Sample 24) *P. vlangalii*-1, N=10; MVZ:Herp:211525-26, 35-36, 39-41, 46-47, 55. (Sample 43) *P. vlangalii*-2, N=5; MVZ:Herp:272842-46 (male MVZ:Herp:272845). (Sample 44) *P. vlangalii*-3, N=4; MVZ:Herp:272830-32, 49 (male). (Sample 21) *P. theobaldi*, N=10; CAS:Herp:171730-33, 35, 37-39, 41-42. (Sample 6) *P. guttatus* (N=10; MVZ:Herp:216020-26, 28-30. (Sample 18) *P. salenskyi*-1 (N=10; CAS:Herp:171596, 601-602, 610, 626, 630-631, 646, 649, 651. (Sample 19) *P. salenskyi*-2, N=5; CAS:Herp:183389-93. (Sample 23) *P. versicolor*, N=10; CAS:Herp:170914-18, 21-22, 36-38. (Sample 10) *P. przewalskii*-1, N=10; CAS:Herp:166770-71, 76, 79, 82, 88, 90-91, 96-97. (Sample 11) *P. przewalskii*-2, N=10; CAS:Herp:166963-65, 68-69, 70, 72, 76, 87-88. (Sample 12) *P. przewalskii*-3, CAS:Herp:166820-23, 26-28, 39-40, 44. (Sample 13) *P. przewalskii*-4, N=10; CAS:Herp:167164-65, 167-68, 171, 177, 183, 196, 201, 225.